Naval Research Laboratory
Washington, DC 20375-5320

NRL/MR/8140--95-7654

As of Tropospheric Propagation Characteristics Based on Regional Meteorological Data

JUNHO CHOI
MARA MELTON

Command Contol Communication Computer and Intelligence
Spacecraft Engineering Division

JOHN DONOHUE
ALBERT FRYLAND

Allied Signal Technical Services Corporation
Alenandria, VA 3402-22303

February 14, 1995

Approved for public release; distribution unlimited.

REPORT DOCUMENTATION PAGE

Form Approved
OMB No. 0704-0188

1. AGENCY USE ONLY (*Leave Blank*)	2. REPORT DATE	3. REPORT TYPE AND DATES COVERED
	February 14, 1995	11-94

4. TITLE AND SUBTITLE

Analysis of Tropospheric Propagation Characteristics Based on Regional Meteorological Data

5. FUNDING NUMBERS

6. AUTHOR(S)

Junho Choi, Mara Melton, John Donohue,* and Albert Frydland*

7. PERFORMING ORGANIZATION NAME(S) AND ADDRESS(ES)

Space Systems Development Department
Naval Center for Space Technology

8. PERFORMING ORGANIZATION REPORT NUMBER

NRL/MR/8140--95-7654

9. SPONSORING/MONITORING AGENCY NAME(S) AND ADDRESS(ES)

SPAWAR 40 E
Washington, D.C. 20375-5320

10. SPONSORING/MONITORING AGENCY REPORT NUMBER

11. SUPPLEMENTARY NOTES

*Allied Signal Technical Services Corporation
5904 Richmond Highway, Alexandria, VA 3402-22303

12a. DISTRIBUTION/AVAILABILITY STATEMENT

Approved for public release; distribution unlimited.

12b. DISTRIBUTION CODE

13. ABSTRACT (*Maximum 200 words*)

Meteorological data has been processed to investigate RF propagation effects of the tropospheric region from ground to 28 KM in space. A data base has been developed to provide enough information for analyzing many different phenomena of the tropophere in terms of lapse rate, refractivity, range error, angle error, slant range, and interrelationships among these parameters. Based on preliminary analysis, the results are very distinguishable from the values arrived at through the application of conventional data for analysis of RF propagation patterns. This implies that the seasonal average value provides better indications of the current atmospheric variation than the annual global average value which most users have adopted for convenience.

14. SUBJECT TERMS

RF propagation	Troposphere	Time delay	Global	Dry height
Ray tracing	Lapse rate	Range error	Database	Wet height
Ray bending	Refractivity	Angle error	Marsden square	

15. NUMBER OF PAGES

100

16. PRICE CODE

17. SECURITY CLASSIFICATION OF REPORT	18. SECURITY CLASSIFICATION OF THIS PAGE	19. SECURITY CLASSIFICATION OF ABSTRACT	20. LIMITATION OF ABSTRACT
UNCLASSIFIED	UNCLASSIFIED	UNCLASSIFIED	UL

NSN 7540-01-280-5500

Standard Form 298 (Rev. 2-89)
Prescribed by ANSI Std 239-18
298-102

CONTENTS

ANALYSIS OF TROPOSPHERIC PROPAGATION CHARACTERISTICS BASED ON REGIONAL METEOROLOGICAL DATA

I. INTRODUCTION

I-1. BACKGROUND

It is now well known over a half century that, at frequencies in the VHF band and above, radio wave propagation over paths extending well beyond the radio horizon is not consistent with classical diffraction theory, received field strength being persistently much higher than that theory predicts. This is true even when the refractive index/height profile is known to be that appropriate to a well-mixed standard atmosphere, so that trapping of the radio wave in ducts, and partial reflection from elevated subsidence inversion layers, are excluded. Thus another propagation mechanism must be involved. The suggestion that this mechanism might be one of scattering from irregularities of refractive index in the atmosphere was first made by Pekeris [1]. Such irregularities arise from the fluctuations of pressure, temperature and water vapor content caused by atmospheric turbulence, which both observation and theory suggest is always present to some degree throughout the troposphere and lower stratosphere. Experimental confirmation of the existence of these refractive index variations is provided by the well-known phenomenon of the twinkling or scintillation of stars [2].

Theoretical investigations into the possibility of beyond-the-horizon scatter propagation were first made by Megaw [3] and Booker and Gordon [4], and since then numerous other contributions to the theory of the subject (1950 - 1965) have been published. The scientists developed models based on parameters such as the turbulence scale, the size of reflective layers, the fluctuation spectrum of the refractive index etc. However, since these factors are difficult to deduce from standard meteorological measurements, the resulting models were not effective for predicting propagation characteristics. Such theoretical studies were progressively abandoned over the following 15 years and replaced by empirical or semi-empirical methods. These latter revealed the laws of the propagation mechanism, providing sufficiently accurate predicting tools so that so called transhorizon links could be planned.

The leading early contributors in this studies in the 1960s-1970s are H. S. Hopfield [5,6,7,8,9], Saxton [10], Bean and Dutton [11], Smith and Weintraub [12], Blake [13], Campen and Cole [14], Rowden et al [15], Millman [16], and Crain and Deam [17]. Contributors in mid 1970s to present Ippolito [18], Fang and Chen [19], Oguchi [20], Crane [21,22,23], Liebe [24], Hitney et al [25], Davis and Norbury [26], Goad [27], Boithias and Battesti [28], Smith [29], Hall [30], Allnut [31] and many other excellent papers and books.

A variety of explanations of tropospheric propagational problems has been offered based on model-based or empirical measurements in terms of frequencies and climatic regions over the years. However, important details relating to the properties of the received signal are generally less certain; such details might be signal amplitude, delay times between different paths, and individual angles of arrival under multipath conditions. Meteorological uncertainties severely limit the usefulness of models of existing microwave propagation specifically in the presence of precipitation, and many of the propagational problems on line-of-sight links arise from the occurrence of anomalous departures in the vertical gradient in the refractive index from the normal almost steady value.

This value itself will vary slowly with season, time of day, and location, the standard gradient in refractivity often being quoted as -40 N-unit/km corresponding to a 4/3 Earth [32]. Departures from this linear variation with height often take the form of changes of a few tens of N-unit over a short height interval. When such change is

Manuscript approved November 23, 1994.

negative and elevated, so-called "ducts" may be formed which can lead to multipath propagation. The development of such anomalies is discussed by many authors, notably Bean and Dutton [11] and Hitney et al [25].

I-2. OBJECTIVES AND SCOPES

The main objective of this study is to determine time delays and range errors between ground-space link due to RF propagation through the troposphere and the stratosphere for low elevation angles. To meet this requirement, both the model-based approach and empirical experimental approach has been evaluated to improve the understanding of tropospheric propagation effects based on real-time and archival meteorological data colllected from various sources [33,34,35,36]. As pointed out in the previous section, the refractive index is determined by pressure, humidity, and temperature. Since all three parameters vary with height there arises a curvature in the propagation path of RF energy leading to a radio horizon which is different from the geometrical horizon.

It is variation of these parameters with meteorological conditions which leads to variability of microwave propagation. These effects are generally more pronounced in the maritime environment. Three sets of meteorological data, real-time global data from the FNMOC, Monterey, C.A., ten year monthly average data from the ETAC of the Air Force Weather Forecast, Scott Air Force Base, IL., and maritime annual average data from the NCDC of Asheville, NC., have been studied for the mid and north Eastern Region of the United States of America with respect to height variations of all three parameters including range and angle errors. Coastal and land-based areas of Washington D.C. vicinity also have been evaluated to compare effects of maritime and continental atmosphere for low elevation angle propagation in section V. The current status of database development for annual as well as monthly global meteorological mean and standard deviation is presented in section III and the present status of the task in section IV. Finally, conclusions and recommendations are in section VI with references in section VII.

II. THEORETICAL CONSIDERATIONS OF ATMOSPHERIC RF PROPAGATION

For all microwave systems that use unguided transmission, propagation phenomena are of the highest importance. Indeed the most fundamental system parameter, namely, the operating frequency, is generally chosen on the basis of propagation factors. The majority of many commercial and military systems have to be able to function under extreme conditions as well as under average conditions, and hence knowledge of variability of propagation effects is very important. Depending particularly upon the frequency and elevation angle of the transmission, the clear atmosphere has propagation characteristics which can vary from those of a virtually transparent medium to one which is almost completely opaque. Areas which suffer these effects are: primary radar, navigation aids, secondary surveillance radar, microwave identification systems, communications, telemetry, command links, radiometers, countermeasure emitters, and electronic warfare support measures. Two examples, therefore, of the paramount importance of propagation effects would be extended communications range and a radar coverage hole [37].

There are a number of other significant system implications. Operations of those systems are required to know the current propagation conditions in order to optimize its employment. It would no doubt be convenient if good propagation estimates could be available in the near real-time from readily available measurements. An approach toward this ideal is the goal of this study and has been pursued in recent years by way of computer-based prediction models utilizing radiosonde data from meteorological stations in many Institutes throughout the world. A high level of technical and scientific discussion regarding propagation characteristics will not be presented here. A brief review of issues concerning RF propagation in the lower atmosphere is presented in this report.

II-1. PROPAGATION MECHANISM THROUGH IONOSPHERE

The ionosphere, consisting of several ionized layers at altitudes between 70 and 300 km, can produce strong reflection, and also absorption, of radio waves. The reflecting properties of the ionosphere are utilized to provide communication links over long distances and are a dominant influence on terrestrial radiowave interactions with the tropospheric constituents 30 MHz. These effects diminish with increasing frequency up to about 70 MHz when the ionosphere becomes effectively transparent. However, for space-to-Earth or Earth-to-space transmissions, ionospheric effects persist, mainly in the form of induced signal scintillation, radiowave group delay and rotation of the plane polarization (i.e., Faraday rotation) up to frequencies of several GHz [38].

Although transmissions greater than 70 MHz generally pass through the ionosphere, without being absorbed significantly, the effect of the ionosphere can be detected at considerably higher frequencies. As with the troposphere, small variations in the effective refractive index of the ionosphere (caused by variations in the electron content) produce a variety of effects which extend through VHF and UHF into the microwave parts of the spectrum. Scintillations (i.e. rapid variation of signal strengths) are one of the pronounced effects. The frequency dependence for relatively weak scintillation (< few dB) can be approximated by a $1/f^{1.5}$ law where f is the transmission frequency. Their character is determined by global position and local time[39]. In general, equatorial scintillations occur at night time and exhibit large fluctuations, e.g., several dB at 4 GHz. At midlatitudes, the occurrence of scintillation varies on a daily, monthly, seasonal, locational and epoch of sunspot cycle basis. In the polar region scintillations are strongly correlated with aurora.

Faraday rotation causes significant effects for Earth-space communications. Linearly polarized electromagnetic waves, when traversing the ionosphere, split into two independent elliptically polarized components. These two waves travel inside the ionized region at different velocities. Hence, on recombination, the plane of polarization is changed. At 100 MHz, for example, the linearly polarized transmission vector could rotate 30 times during its passage through the ionosphere, whereas at 6 GHz a maximum of only a few degrees would be expected [38, 46].

Clearly, if frequency reuse is to be employed, any significant rotation of the polarization vector causes unwanted crosstalk in the adjacent channel. Radio waves are refracted in their passage through the ionosphere due to the non uniform vertical structure of electron content. The effect is relatively small and of the order of a few tenths of a degree at low elevation angles (5^0) at 10 MHz. The effects decrease with increasing elevation and transmission frequency. In general, ionospheric effects such as Faraday rotation, delay, refraction and absorption follow an inverse squared law with respect to

frequency ($1/f^2$). The frequency dependence of scintillation is more complex and depends on the amplitude, whereas dispersion exhibits a ($1/f^3$) dependence [40].

II-2. PROPAGATION MECHANISM THROUGH TROPOSPHERE

The frequency dependent radiowave interactions with the tropospheric constituents occurring in the altitude range about 0 to 20 km need to be taken into account at frequencies greater than 1 GHz. It extends from ground level to an altitude of about 9 km at the Earth's poles and 17 km at the equator. The height of the upper boundary also varies with atmospheric conditions: for instance, at the middle latitudes it may reach about 13 km in anticyclones and decline to less than 7 km in depressions. It is in the troposphere that changes of temperature, pressure and humidity, as well as clouds and rain, influence the way in which radiowaves propagate from one point to another. At frequencies above 30 MHz:

(a) localized refractive index fluctuations in the troposphere can scatter radio energy,
(b) horizontally-stratified abrupt changes in refractive index can cause reflection and
(c) extended negative gradients can cause ducting.

All these mechanisms can carry energy far beyond the normal horizon and so give rise to interference between one radio path and another. Reflection most affects frequencies between about 30 MHz and 1 GHz and ducting most affects frequencies above about 1 GHz. Fortunately the latter occur very infrequently over land, although ducts often exist over sea. However, forward scattering of radio energy is sufficiently dependable that it may be used as a mechanism for long-distance communications, especially at frequencies of about 0.3 to 10 GHz [29].

In addition, large-scale changes of refractive index with height cause refraction (ray bending) of radiowaves that can be quite significant at all frequencies at low elevation angles, especially in effectively extending the radio horizon distance beyond that of the optical horizon. Apart from these refractive index effects, radio propagation may be strongly influenced at frequencies above 3 GHz by the presence of heavy rain, and above 15 GHz the attenuation caused by oxygen and water vapor in the air may be important, depending on the application. The absorption by rain and atmospheric gases also will have an associated thermal noise emission. At frequencies greater than 30 MHz, the presence and shape of hills (terrain) has an important influence on the field strength of energy propagating beyond the horizon. At yet higher frequencies, buildings and other obstacles have a marked effect by diffraction, scatter and specular reflection mechanisms, when the wavelength is small compared with the dimensions of the obstacles [41].

The fluctuations in elevation angle are about an order of magnitude greater than those that occur in the azimuth angle. The fluctuations are higher in the summer, consistent with the increase in surface refractivity that normally occurs in this period. Angle of arrival fluctuations, like ray-bending in general, are independent of frequency between 1 and 100 GHz. Angle of arrival fluctuations can be considered to be a single ray that is being deviated from its normal path. In some situations, however, several possible paths can exist simultaneously through the atmosphere between the transmitter and receiver.

The rays traveling the various paths arrive at the receiver with different amplitudes and phases, and interference results. This phenomenon is called multipath. On

terrestrial paths, multipath is the most common propagation outage in the frequency range 1 to 10 GHz owing to the proximity of a reflecting surface, the ground in most cases, to the ray path. On satellite-to-ground paths above an elevation angle of 10^0, multipath is virtually non-existent. If the elevation angle is low enough or the beamwidth of the Earth station antenna is wide enough, destructive interference due to reflections from the ground can occur [30].

Without referring to any specific theory or model, it can be reasonably considered that up to an altitude of several kilometers above the ground the refractive index of air shows, in addition to its large-scale variations, slight irregularities (several N-units) resulting primarily from temperature and humidity irregularities. Therefore equal index surfaces are not perfect spheres concentric to the Earth, but may take a variety of forms. Some may even constitute closed surfaces in which the internal refractive index may be slightly higher (or lower) than external values. Considering the general characteristics of the lower atmosphere, these refractive index irregularities necessarily feature a very flat shape, much larger horizontally than vertically. In addition, the number of irregularities, as well as the amplitude of their index discontinuities, drop in average value as altitude increases and disappear entirely at very high altitudes. With this structure in mind it can be expected that a radiowave propagating in an almost horizontal direction will give rise to a number of secondary waves making up multipaths which deviate slightly from the main path.

On a line-of-sight link, these various secondary waves interfere with the direct wave at the receiver, causing deep and rapid fadings. On a transhorizon link, however, there is no direct wave; the secondary waves alone carry the signals toward the receiving antenna. The refractive index inhomogeneities, existing in the common volume of the antenna beams, scatter a part of the energy sent by the transmitter antenna in all directions, and, in particular, toward the receiving antenna. It can then be inferred that the received level permanently undergoes rapid fluctuations, since the relative phases of each wave vary with atmospheric movements. Such rapid fluctuations are characteristic in this propagation mechanism [28].

III. STATUS OF DATABASE DEVELOPMENT

III-1. DATABASE STATUS

There are currently three working databases of processed information that is collected from the following Agencies:

Climatological Data from the National Climatological Data Center (NCDC) in Asheville, North Carolina
Climatological Data from the Fleet Numerical, Meteorological & Oceanographic Command (FNMOC) in Monterey, California.
European Center for Medium-Range Weather Forecast (ECMWF) data from the Environmental Technical Applications Center (ETAC), Scott Air Force Base, Illinois.
Additional data from the SSM/T1&T2 satellite has been started receiving from the Remote Sensing Division, Code 7211 originated by DMSP Office..

III-1.1. DATABASE ACCURACY

III-1.1.1. NCDC ACCURACY

The database from the NCDC, contains upper air observations from stations operated by the National Weather Service, the U.S. Navy and certain South American Stations whose data receive quality control at the National Climatic Data Center. The data contains mandatory, standard and significant pressure levels of data through the upper air. Where there was missing data for a particular level, the corresponding data was discarded during processing. Observations were taken at several times around the clock in the data. For the Marine upper air data set, data falling within the time 1200 to 2300 range were grouped as afternoon or PM data. Data falling within the time 0000 to 1200 were grouped as morning or AM data. The CD-ROM data was extracted for 0000 and 1200 time only. Only mandatory and significant levels were extracted for the CD-ROM data. US. data processed by the NCDC are subjected to extensive quality control procedures. Suspicious data are returned to the originator for the verification through manual correction.

III-1.1.2. FNMOC ACCURACY

The database from the FNMOC, contains near global data observations for surface and upper air data. Data is encoded by the information gatherer in WMO (World Meteorological Observation) format. Data is recorded at 0000 GMT and 1200 GMT. The encoder is available to anyone who requests it. Data is occasionally missing for a given day at a site or AOI (area of interest).

III-1.1.3. ECMWF ACCURACY

The ECMWF database contains monthly modeled upper air and surface air data for the entire globe. The database consists of means and standard deviations for temperature, dew point, air density and geopotential height for each of 14 pressure levels per 2.5 by 2.5 degree land area. (The original database provided 17 pressure levels but missing data points resulted in an effective 14 pressure levels). The monthly mean or average is based on varying numbers of observations (generally between 280 to 610 observations) obtained over a ten-year period.

III-1.2. PERIODS COVERED

III-1-2.1. NCDC

The period covered by the Marine data observations was January 1980 to June 30 1993. The CD-ROM data period extracted from the disks was January 1981 to December 1992. CD-ROM data only was available up until December 1992. The year 1980 was missing from the CD-ROM database for certain North American regions.

III-1.2.2. FNMOC
The period covered by the FNMOC data is January 30, 1994 -July 13, 1994 without height data and July 13, 1994 to the present with height data.

III-1.2.3. ECMWF

The ECMWF modeled data is based on data obtained over a ten-year period from the year 1980 to 1991.

III-1.3. REGIONS COVERED

III-1.3.1. NCDC

The data received on tape was strictly radio soundings from shipborn (Marine) sounders. Therefore only ocean and coastline data was available on a global scale. Land based soundings for North America were obtained on CD-ROM disk. Every grid point is not covered by the CD-ROM database over the land because of no station being available to take soundings in certain locations. Other land masses were not included. Seven Regions of interest were grouped as a preliminary measure in the database in order for the convenience and storage utilization purposes as follows and will expand to the global area later. Tables 1 through 3 show grids for the DC , Eastern US, and Western US Regions.

DC - Washington DC area, EUS - Eastern US, WUS - Western US, ALSK - Alaska, EUR - Europe
MEST - Middle East, FEST - Far East

III-1.3.2. FNMOC

The data received is from any weather station, domestic or foreign, that is able to send their data in WMO format. Five Regions of interest give rise to five sets of databases.

DC - Washington DC area, USA - USA and Alaska, EUR - Europe, MIE - Middle East
ASIA - Far East

III-1.3.3. ECMWF

The ECMWF database contains one mean and standard deviation (per each of four variables) for each of 14 pressure layers per 2.5 by 2.5 degree grid area.
Seven regions of interest are identified as follows, with the remaining data available in separate files.

DC - Washington DC area, EUS - Eastern US, WUS - Western US, ALSK - Alaska, EUR - Europe
MEST - Middle East, FEST - Far East

III-1.4. DATABASE STORAGE CAPACITIES

III-1.4.1. NCDC

The NCDC database currently is housed on the ACCESS software on a PC486. It contains approximately 250 MB of information. This is stored on an optical disk drive peripheral connected to the PC486. Although ACCESS claims a maximum size of 1 GB, the NCDC database often suffers corruption problems while being manipulated or while importing data. This may be due to its size or bit error problems with the optical drive. It would seem the solution would be to keep the database in smaller pieces as in regions of interest for example. This way the integrity of the database could be ensured and still be kept in an organized fashion. However, the PC486's throughput may not be enough when it comes to processing large volumes of data even on a regional basis. It may be better to move this data to a SUN workstation and develop our own data handling program. This idea is also currently under study.

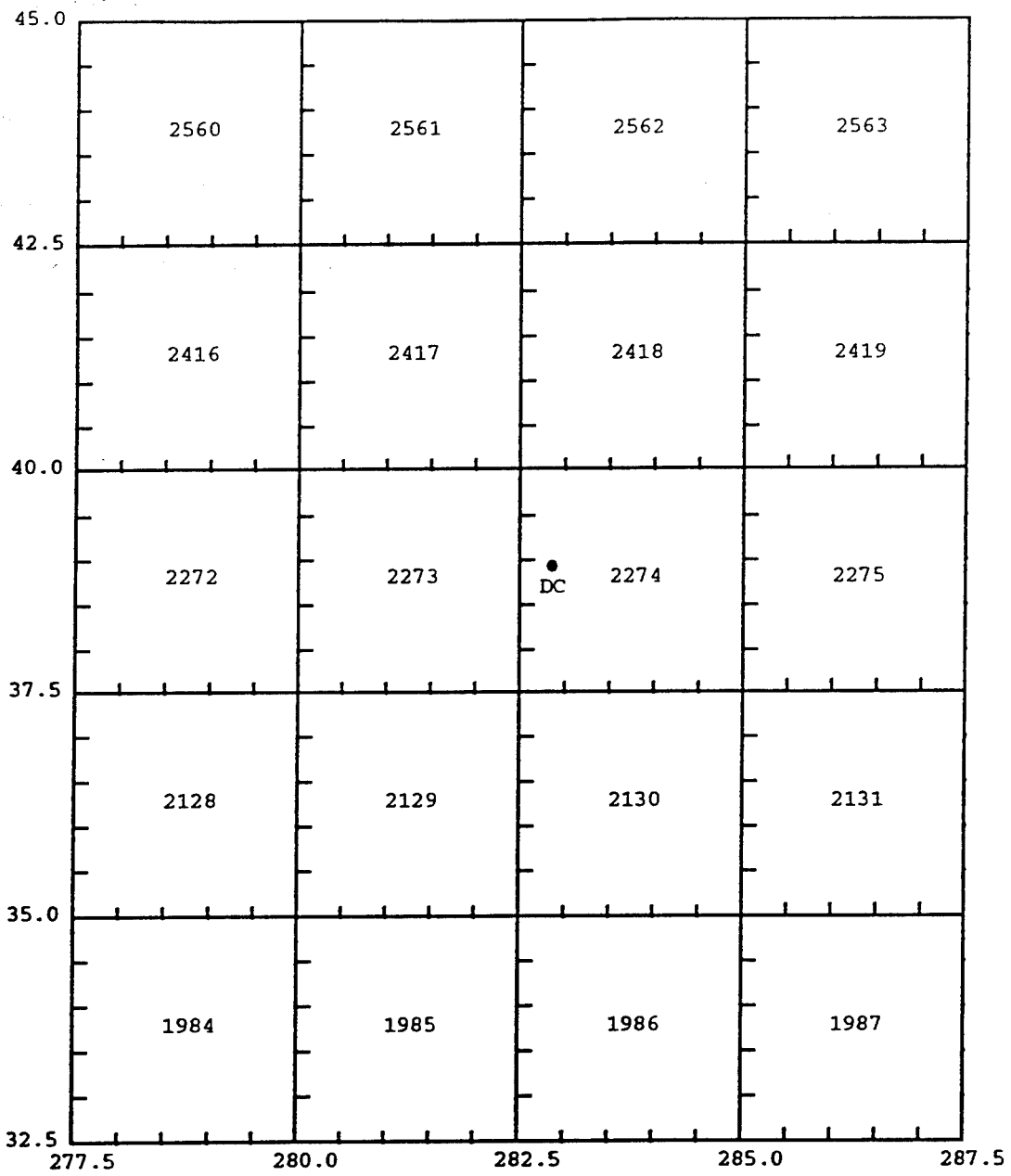

TABLE 1 – DC Region Grid Squares
(DC is at 38 deg 49 min N Latitude,
282 deg 58 min East Longitude)

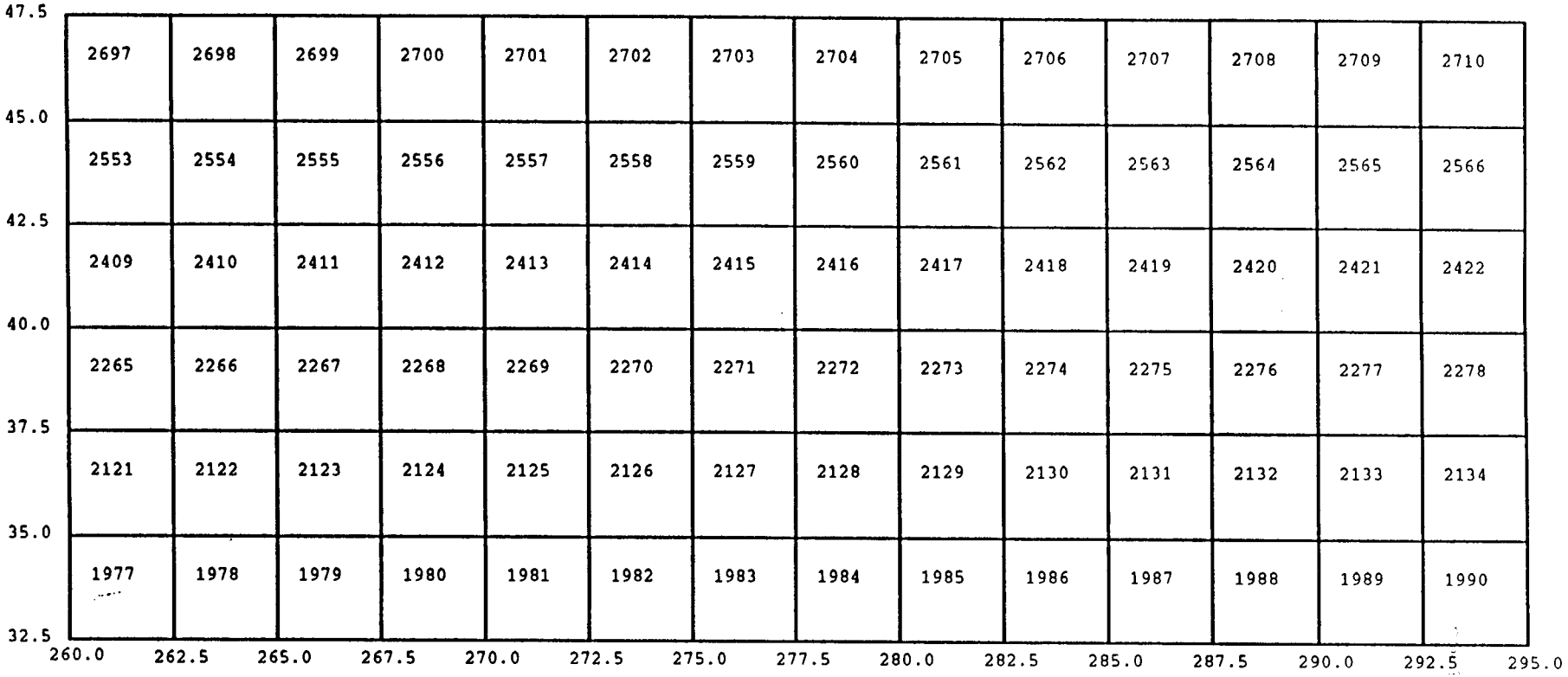

TABLE 2 -- Eastern US Region Grid Squares

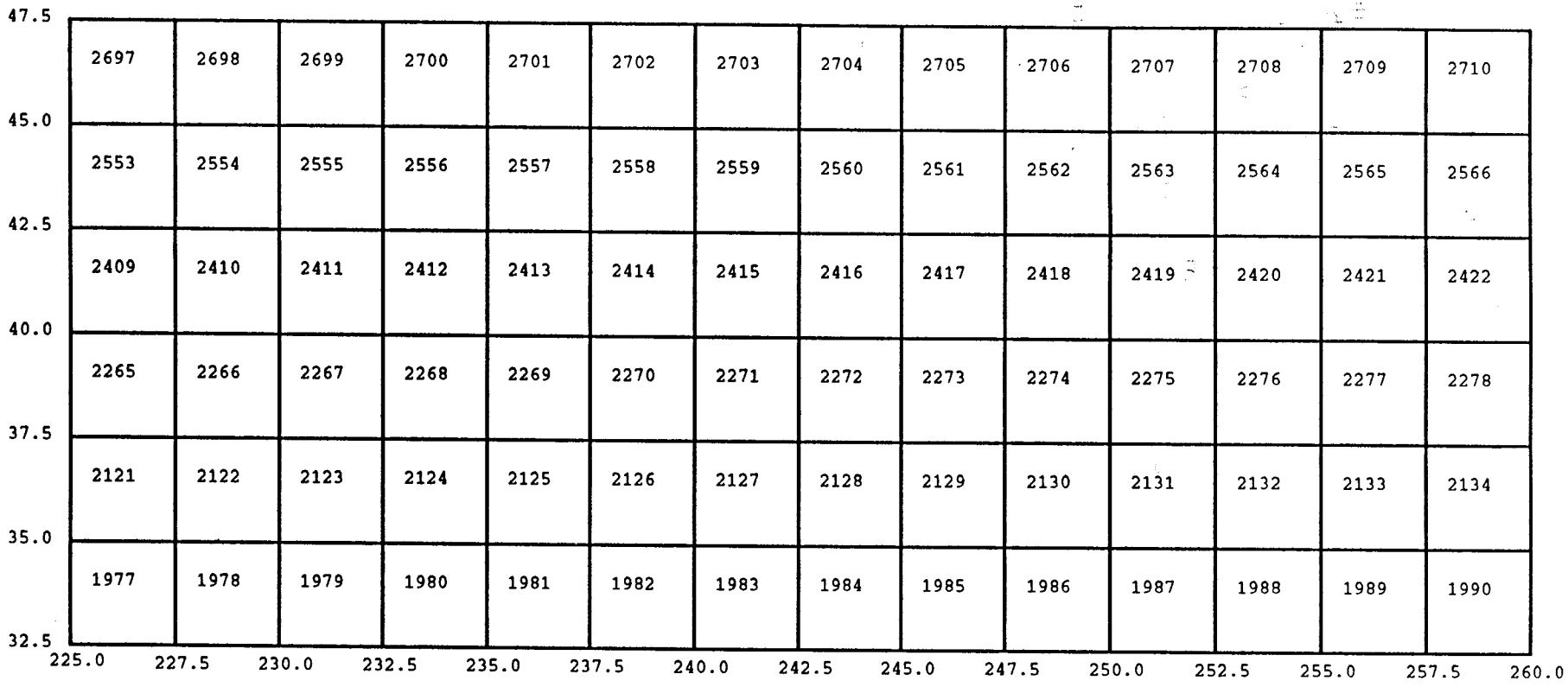

TABLE 3 -- Western US Region Grid Squares

III-1.4.2. FNMOC

The database is currently housed on the ACCESS software on a PC486. The databases themselves are stored on optical disk drives. The databases are divided by data without height data (pre August 1, 1994 data) and data with height data (post July 13, 1994).

III-1.4.3. ECMWF

The ECMWF database is housed on NRLVAX. The original data files contain 162MB of information. The processed global database is divided into two sections (Table 1 and Table 2 files) of size 4.4MB and 217MB, respectively. The organization of these primary, monthly files is such to facilitate imported data into ACCESS on the PC486 as well as ongoing processing on the VAX. As mentioned above, because of difficulties encountered with ACCESS when handling large quantities of data and problems with the optical disk drive attachment, the ECMWF database has not been imported.

III-1.5. PROGRAMS USED TO PROCESS THE DATA

III-1.5.1. NCDC

Several Fortran programs were written to process the data from NCDC. One program was written to actually extract data from the tape containing marine data (DATAREAD.FOR & DATACHECK.FOR). Another was written to extract data from the CD-ROM data (CDREAD.FOR) once it had been placed into a text file by the CDROM software. Both of these programs would then manipulate the data by placing them into data tables which is explained in a section to follow. These tables, containing upper air data, are designed for easy importation into the Microsoft ACCESS database software or manipulation within other Fortran data processing programs.

III-1.5.2. FNMOC

The raw FNMOC data in a binary form is stored on a Sun file server and is in the process of being decoded and imported to Microsoft ACCESS. It is unpacked on a Sun computer, data extracted for an AOI, and transferred via File Transfer Protocol (FTP) to Microsoft ACCESS.

Raw data with heights requires a separate and different processing algorithm on the Sun computer and have a different database structure on ACCESS. Data is unpacked with a Fortran program named unpkgrb1.x. Data without heights are processed using a variation of a program such as readlatusa.x, readlatdc.x, readlateur.x, readlatmie.x, or readlatasia.x, one for each of the AOI's, the USA and ALASKA, the DC region, the European region, the Middle East region, or the Asia region, respectively. Data with heights are processed using a variation of a program such as readallusa.x, readalldc.x, readalleur.x, readallmie.x, or readallasia.x.

III-1.5.3. ECMWF

The original ECMWF data were provided on 8 mm tape in ASCII format in 512 Byte blocks. Two Fortran programs (WRITE1Z and WRITE75Z) were written to massage the data into readable and manageable files. The data were read one byte at a time to extract embedded excess bits and rewritten into appropriate size units.

The Fortran programs GRID, CONTBL, and REMMISS were written to remove missing data records, convert to standard units of measure, calculate variables (such as relative humidity based on dew point) and to write the processed information into monthly files. The primary monthly files are in two sections. Table 1 files contain grid square information (i.e., latitude and longitude), while Table 2 monthly files contain the means and standard deviations of variables of interest.
The Fortran program AOITB1 reads Table 1 and Table 2 files and extracts information based on the seven areas of interest previously identified. The output files produced by REMMISS and AOITB1 are used in the Ray Trace and Graph programs.

The Fortran program MULTI was written to allow a user to create geometric mean files based on more than one grid square. For example, MULTI was used with the DC area-of-interest in order to calculate mean Land-based and Sea-based parameters for use in the Ray Trace and Graph programs.

III-1.6. WHERE EACH DATABASE IS CURRENTLY HOUSED AND ITS STATUS

III-1.6.1. NCDC

All Marine upper air data is currently housed on an optical disk drive in an ACCESS database file, complete with tables for six regions of interest. Data can be extracted fairly easily into text files for processing by the ray tracing program or graphing programs. The CD-ROM data is still currently in text files that need to be imported into a different ACCESS database file that will include the Marine data. After the CD ROM data is imported and processed, this database will be considered complete. The Eastern United States AOI is completed.

NOTE: ACCESS has been somewhat unreliable in its use with the optical disk drive. The Marine upper air data is available in its present form, but only in an exportation capacity. Further manipulation of this data could put it at risk in this form. All data processing should be done on the main hard drive from now on.

III-1.6.2. FNMOC

The FNMOC database on ACCESS containing data with height for the DC region is up-to-date. The FNMOC database on ACCESS containing data without heights for the DC region contains data from May 1994 to August 1994. Previous months of data are in the process of being decoded and added to the database. Decoding is accomplished on only one Sun computer for raw data with heights due to the large size of the unpacked binary data. A typical unpacked binary file containing worldwide data with heights is about 11 Mbytes; a typical unpacked binary file containing worldwide data without heights is about 8 Mbytes. The CCF Sun computers have a total limit of 10 MBytes and are used to decode the data without heights; the Tomahawk Sun computer has a limit of 32 Mbytes and is used to decode the data with heights. The group is in the process of significantly increasing our computer capabilities with the expected addition of FORTRAN software for a SPARC 1 and the expected addition of the use of a SPARC 5 with Fortran.

The FNMOC database on ACCESS containing data with height for the USA continental region and Alaska is up-to-date. The FNMOC database on ACCESS containing data without heights for the USA continental region and Alaska contains data for January and February 1994 and is in the process of being updated. The FNMOC database on ACCESS

containing data with height for the Europe AOI contains data from 7/13/94 to 8/7/94 and 8/21/94 - 8/28/94 . The FNMOC database on ACCESS containing data without heights for the Europe AOI is 7/13/94 - 8/21/94 with the exception of the week of 8/1/94 - 8/7/94. This week as well as the other weeks not listed will shortly be added.

The databases for the AOI's of the Middle East and Asia contain data without heights for 6/13/94 - 7/10/94. The FNMOC database produces an output file that is identical to the output file for the NCDC database with the exception of that the Marsden Square is not included for files where averages of data over a region that includes many grid squares are calculated; the grid square number or equivalent must be manually entered into the text file for when combined squares are calculated. This ACCESS Table is easily exported to the disk drive using an ACCESS export routine and transferred to the VAX using the file transfer protocol (FTP). If only a particular grid square is desired, or a listing by grid squares, a separate group of queries is used. This produces an output file similar to the NCDC output file with the exception that the average temperature is not included. The second output file contains the average temperatures in Kelvin. The second file is printed out and the typical seven values of temperature for the seven pressure levels are manually added to the near complete first file. A new query will be made so that this will automatically produce a complete file. The temperature standard deviation is not yet included but is easily implemented and will be included in this new query.

III-1.6.3. ECMWF

All ECMWF data are housed on NRLVAX. A dual strategy was used in establishing and maintaining these data. Primary data files were created in keeping with the formats of the NCDC and FNMOC ACCESS databases. The primary ECMWF files were originally established for export to the PC. Because of problems encountered with large blocks of data, these files will be broken down by areas-of-interest and, eventually, exported to ACCESS. These files consist of two sections (Table1 and Table2) where each table contains 12 monthly datasets. These files are complete and ready for export.

At the same time, subsets of the primary files were created for use on the VAX in order to run the Fortran programs mentioned above. Again, due to the quantity of data, the larger files are broken down into AOI files by month and are tailored for efficient processing by the Fortran programs. Currently, very detailed files and subfiles exist for the DC AOI. The DC AOI data is easily accessed and manipulated on the VAX. It is anticipated that similarly detailed files will be generated for the remaining AOIs. This is an ongoing effort. The Eastern United States AOI is currently complete for all 12 months.

III-1.7. TABLE DESIGNS

Database Design and Final Output Tables for Exportation

III-1.7.1. NCDC

The NCDC database starts out with two basic tables of data as shown below. The two main tables are:

Table 1 Combined	Table 2 Combined
Record Number 1 (Primary Key)	Record Number 1
Grid Square Number	Pressure
Latitude	Temperature
Longitude	Relative Humidity
Number of Levels	Height
Date	
Time	

FIGURE III.1 -- Table 1 and 2 Structures NCDC Database

The relationship is set up with fields Record Number 1. These two tables are then processed by a set of queries to produce the final output table as follows. From Table 1 Combined a Make Table Query was designed to compute the Dry Height. Thus the query appears as follows:

Field	Record Number 1	Latitude	Dry Height: 43.13-5.206*(sin([Latitude]*3.14/180))^2
Sort:			
Show:	x	x	x
Criteria:			

FIGURE III.2 -- Dry Height Make Table Query NCDC Database

The goal of the next query was to compute the averages and standard deviations of the Temperature, Relative Humidity, Height, and Dry Height. The avg. and stdev. were found for all points in each grid square at each pressure level.

The select query uses the previously mentioned three tables, joined by Record Number 1. The query is shown in figure III.3. It is broken up into two parts due to the limited page width.

Field:	Grid Square #	Pressure	Temperature	Temperature
Total:	Group By	Group By	Avg	StDev
Sort:				
Show:	x	x	x	x
Criteria:				

Field:	Date	Time	Latitude	Longitude
Total:	Where	Where	Where	Where
Sort:				
Show:				
Criteria:	Like [Enter month:] & "/*/*"	Between 1 and 12	Between x and y	Between x and y

FIGURE III.3 -- Average and Standard Deviation Query NCDC Database

The final output table which is produced by a Make Table query is shown in figure III.4. The average/standard deviation query shown above is the input to the final output table query shown below.

Field:	Grid Square #	Pressure	Avg Height: ...	Nd: ...
Sort:				
Show:	x	x	x	x
Criteria:				

Field:	Nw: ...	[Nd]+[Nw]	Avg Dry Height: ...	Avg Temperature
Sort:				
Show:	x	x	x	
Criteria:				

FIGURE III.4 -- Final Output Table for NCDC Marine Database

This final output table can then be exported to a text file to be used for data analysis in the ray tracing program. The CDROM data is being placed into a database with a slightly different format. The final output table with this data will contain the following: Grid square, latitutude, longitude, pressure, dry refraction, wet refraction, total refraction , total refraction (stdev), average dry height (Hopfield), dry height (Goad), and wet height (Goad), average temperature, average relative humidity, avg height, std deviation of temperature, std deviation of relative humidity, and std deviation of height. The final table will contain all 17 parameters.

III-1.7.2. FNMOC Design on Access/VAX and Final Output Table

The four main tables appear in Figure III.5. No relationships between the tables are needed since they are all keyed on date and time.These first table is processed by a set of queries to produce a final output table as follows for groups of grid squares. From Table 1 of Figure III.5 a Make Table Query was designed to compute the Dry Height. Thus the query appears as in Figure III.6.

The goal of the next query was to compute the averages of the N dry, N wet, N total, and Dry Height, and Average Temperature. The averages were found for all points for given grid squares at each pressure level. This produces an intermediate Table called 3x3 Intermediate.
Then another query groups by pressure and produces an output with all the parameters needed named 3x3 Final. The equations are identical to the equations used in NCDC.

If a single grid square or a group of individual grid squares is needed for an AM query, a query named N values with H/am and a second query Temp Values/AM is used. Similarly for PM values a query named N values with H/pm and a second query Temp Values/PM is used. This final output table can then be exported to a text file to be used for data analysis in the ray tracing program.

Table 1	
Date	Latitude
Grid Square Number	
Time (GMT)	
Pressure (mb)	
Height (m)	
Temperature (C)	
Relative Humidity (%)	

Table 2	
Grid Square Number	
Date	
Time (GMT)	
Surface Pressure (mb)	

Table 3	
Grid Square Number	
Date	
Time (GMT)	
Surface Temperature (C)	

Table 4	
Grid Square Number	
Date	
Time (GMT)	
Precipitation (12 hours after)kg/m2	

FIGURE III.5 -- Table 1,2,3, and 4 Structures FNMOC Database

Field: Record Number 1	Latitude	Dry Height: 43.13-5.206*(sin([Latitude]*3.14/180))^2
Sort:		
Show: x	x	x
Criteria:		

FIGURE III.6 -- Dry Height Make Table Query FNMOC Database

III-1.7.3. ECMWF Design on VAX (and later ACCESS) and Final Output Table

III-1.7.3.1. VAX FILES:
The VAX ECMWF database contains two primary sets of monthly files. For example, JANTB1.DAT through DECTB1.DAT and JANTB2.DAT through .DECTB2.DAT, as follows:

JANTB1.DAT	JANTB2.DAT
Record #	Record #
Latitude	Pressure (mb) (μ & σ)*
Longitude	Temperature (C) (μ & σ)
Grid square	Geopotential Height (m) (μ & σ)
	Dew Point (μ & σ)
	Density (μ & σ)
	Number of Observations
	Relative Humidity
	Percent Relative Humidity

FIGURE III.7 -- Data Structure of ECMWF Primary Files Located on NRLVAX

In order to facilitate processing the Ray Trace and Graph programs, a set of AOI_TB1.DAT, AOIMONTHR.DAT, and AVERAGED.DAT files were created. There are seven sets of AOI_TB1.DAT files: DC_TB1.DAT, EUS_TB1.DAT, WUS_TB1.DAT, ME_TB1.DAT, FE_TB1.DAT, EUR_TB1.DAT, and AK_TB1.DAT. These files contain the latitudes and longitudes of the regions of interest. For example, DC_TB1.DAT contains the Record#, Latitude, Longitude and grid square for the DC area of interest (Lats N35.0 to N42.5 and Lons E277.5 to E287.5).

There will be seven sets of twelve AOIMONTHR.DAT. Currently DCJANR.DAT through DCDECR.DAT files are complete and are used as input to the Ray Trace and Graph programs. These files contain the following:

DCJANR.DAT
Grid Square
Pressure Level
Geopotential Height
Dry Refractivity
Wet Refractivity
Total Refractivity
Dry Height
Temperature (deg K)

FIGURE III.8 -- Data Structure of ECMWF Area of Interest Monthly Data Files Located on NRLVAX

In addition, AVERAGED.DAT files are created as required. For instance, the DC Land-based and DC Sea-based files. These files are entitled DC_AUG_AVGCode_Function.OUT. These files have the same format as the DCAUGR.DAT files mentioned above. The AOI_TB1.DAT, AOIMONTHR.DAT, and AVERAGED.DAT files are used in the Ray Trace and Graph programs to produce several output files which are described in Section III.1.7.3.1. The following table are samples of the Ray Trace and Graph program final output files that exist for the DC area.

DC_AUG_1079_ELANGVRE.OUT;2	DC_AUG_1059_ELANGVRE.OUT;1
DC_AUG_1079_F4OP1.OUT;3	DC_AUG_1059_F4OP1.OUT;2
DC_AUG_1079_F4OP2.OUT;3	DC_AUG_1059_F4OP2.OUT;2
DC_AUG_1079_F4OP3.OUT;3	DC_AUG_1059_F4OP3.OUT;2
DC_AUG_1079_F4OP4.OUT;3	DC_AUG_1059_F4OP4.OUT;2
DC_AUG_1079_FILE1.OUT;1	DC_AUG_1059_FILE1.OUT;1
DC_AUG_1079_FILE2.OUT;1	DC_AUG_1059_FILE2.OUT;1
DC_AUG_1079_FILE3.OUT;1	DC_AUG_1059_FILE3.OUT;2
DC_AUG_1079_FILE4.OUT;1	DC_AUG_1059_FILE4.OUT;1
DC_AUG_1079_HTVDEL_ANG10.OUT;1	DC_AUG_1059_HTVDEL_ANG10.OUT;1
DC_AUG_1079_HTVDEL_ANG15.OUT;1	DC_AUG_1059_HTVDEL_ANG15.OUT;1
DC_AUG_1079_HTVDEL_ANG20.OUT;1	DC_AUG_1059_HTVDEL_ANG20.OUT;1
DC_AUG_1079_HTVDEL_ANG25.OUT;1	DC_AUG_1059_HTVDEL_ANG25.OUT;1
DC_AUG_1079_HTVDEL_ANG30.OUT;1	DC_AUG_1059_HTVDEL_ANG30.OUT;1
DC_AUG_1079_HTVDEL_ANG35.OUT;1	DC_AUG_1059_HTVDEL_ANG35.OUT;1
DC_AUG_1079_HTVDEL_ANG40.OUT;1	DC_AUG_1059_HTVDEL_ANG40.OUT;1
DC_AUG_1079_HTVDEL_ANG45.OUT;1	DC_AUG_1059_HTVDEL_ANG45.OUT;1
DC_AUG_1079_HTVDEL_ANG50.OUT;1	DC_AUG_1059_HTVDEL_ANG50.OUT;1
DC_AUG_1079_HTVDEL_ANG55.OUT;1	DC_AUG_1059_HTVDEL_ANG55.OUT;1
DC_AUG_1079_HTVELANGERR.OUT;2	DC_AUG_1059_HTVELANGERR.OUT;1
DC_AUG_1079_HTVRE.OUT;1	DC_AUG_1059_HTVRE.OUT;1
DC_AUG_1079_MILLRAY.DAT;1	DC_AUG_1059_MILLRAY.DAT;1
DC_AUG_1079_NVHT.OUT;1	DC_AUG_1059_NVHT.OUT;1
DC_AUG_1079_TVHT.OUT;1	DC_AUG_1059_TVHT.OUT;1

FIGURE III.9 -- DC Area of Interest Final Output Files
Generated by Ray Trace and Graph Programs
Located on NRLVAX

III-1.7.3.2. Planned ACCESS Files:
The ECMWF database will be imported into ACCESS. The structure for the database has been established. The two main tables will contain:

Table 1 Combined	**Table 2 Combined**
Record Number 1 (Primary Key)	Record Number 1
Grid Square Number	Pressure (μ & σ)*
Latitude	Temperature (μ & σ)
Longitude	Height (μ & σ)
	Dewpoint (μ & σ)
	Density (μ & σ)
	Number of Observations

FIGURE III.10 -- Planned Table 1 and 2 ACCESS Structures for ECMWF Database
* Monthly mean and standard deviations over 10-year period

The relationship will be set up with fields Record Number 1and keyed on REC#, LAT and LON. Since the ECMWF database has its own statistics, no further single grid averaging will occur. However, seasonal as well as multi grid averages and standard deviations will be calculated. Subtables will be exported from the VAX such as described above. For example, the seven sets of twelve AOIMONTHR.DAT will be established as follows:

DCJANR.DAT
Grid Square
Pressure Level
Geopotential Height
Dry Refractivity
Wet Refractivity
Total Refractivity
Dry Height
Temperature (deg K)

FIGURE III.11. – Planned Area of Interest ACCESS Structures for ECMWF Database

The seven sets of AOI_TB1.DAT files: DC_TB1DAT, EUS_TB1.DAT, WUS_TB1, ME_TB1.DAT, FE_TB1.DAT, EUR_TB1.DAT, and AK_TB1.DAT which contain the latitudes and longitudes of the regions of interest will be established also. These tables will be available for processing by a set of queries similar to those used with the NCDC and FMNOC datasets. Any specified output table can be exported to a text file to be used for data analysis.

III-1.7.3.3. How The Tables Are Used In The Ray Tracing Program

The final output table shown in section III.1.7.1.1 is used as the input data file to the ray tracing program called RAYSCONT7.FOR. These data are then used along with a few other user entries to trace the ray through this observed atmosphere. The index of refraction, height and elevation angle are the key variables in tracing the ray. Dry height is used to indicate where the tropopause most likely ends. In almost all instances, this height is never exceeded by the data. The grid square number is also included in this data file to indicate which grid the ray trace is in. All heights are geopotential heights and are converted to geometric heights within the program. Dry and Wet refraction are included for other graphing programs. The total refractivity number (N) is converted to the index of refraction (n) within the program in order to perform a ray trace. Average temperature is also included for another graphing program to graphically show temperature lapse rate. Five output files are produced from this data by the program. They are Millray.dat, file1.out, file2.out, file3.out and file4.out. The four *.OUT files contain data that can be used for graphical analysis and will be explained in the next section.

III-1.7.3.4. How These Results Are Used In Graphical Analysis

As mentioned in the previous section, there are four output data files produced by the ray tracing program used in the graphical analysis.

File1.out, File2.out, FIle3.out, and File4.out

Each file carries a header with the data. The header will indicate what each column of data contains, the grid square location, the input data filename and what output file it is, i.e. FILE1.OUT, for example. In FILE1.OUT, the first column contains the elevation angle in degrees in either half degree increments from 1 to 5.5 degrees or full degree increments from 1 to 10 degrees. Column two contains the range error for each of these elevation angles in meters. Column three contains the corresponding propagation delay in nano-seconds found by dividing by the speed of light.

In FILE2.OUT, the first column contains the angle error in degrees. The second column contains the geometric height in meters. The third column contains the elevation angle for each iteration through the ray program and the fourth column contains the apparent angle for each corresponding elevation angle and height. There is no angle error until the first layer is crossed into the second layer. That is why the angle error is 0 at the beginning of each iteration of elevation angles.

In FILE3.OUT, the first column contain the range error that corresponds to the present height and elevation angle. The second column is the geometric height for ith layer and the third column is the elevation angle for that iteration.

In FILE4.OUT, the first column contains the apparent range in meters computed using Millman's stratified layer method. Column two is the straight line slant range or true range in meters. Column three is a numerically integrated range value using Gauss Quadrature Integration computed from an integral for range given in Millman's papers. Column four is also a numerical integration of the same equation except that it uses Simpson's rule. Column five contains the geometric height of each layer in meters. Column six is the input elevation angle.

The final output table which is exported from the database is also used in producing graphical information. Four programs have been developed to produce graphical analysis. They are the following:

GRAPH3.FOR
REFRACTC.FOR
MONTHREF.FOR
LAPSE.FOR

Figure III.12 illustrates each graph program's capabilities and data files used.

X AXIS	Y AXIS	DATA INPUT FILE	GRAPH PROGRAM USED	VARIABLES INCLUDED
Delta (slant rng - true rng)	Height	FILE4.OUT	GRAPH3.FOR	Elevation Ang Grid Sq. Lat & Long Month Region AM or PM
Height	Total Refraction Dry Refract. Wet Refract.	Final Output Table from Database	REFRACTC.FOR	Grid Sq. Lat & Long Month Region AM or PM
Range Error	Elevation Ang	FILE1.OUT	GRAPH3.FOR	Grid Sq. Lat & Long Month Region AM or PM
Angle Error	Height	FILE2.OUT	GRAPH3.FOR	Elevation Ang Grid Sq. Lat & Long Month Region AM or PM
Range Error	Height	FILE3.OUT	GRAPH3.FOR	Elevation Ang Grid Sq. Lat & Long Month Region AM or PM
Slant Range	Height	FILE4.OUT	GRAPH3.FOR	Elevation Ang Grid Sq. Lat & Long Month Region AM or PM
HEIGHT	REFRACTIVITY	Final Output Table from Database	MONTHREF.FOR	Months) Grid Sq. Lat & Long Region AM or PM
HEIGHT	Temperature	Final Output Table from Database	LAPSE.FOR	Grid Sq. Lat & Long Month Region AM or PM

FIGURE III.12 – Capabilities of Graph Programs
(The above graphs can be produced for any grid square from the three databases)

III-2. RAY PROGRAM STATUS

III-2.1. INPUT FORMAT

The RAYSCONT7.FOR program can accept three data formats. Originally, the program was designed to accept raw climatological data that needed to be processed within the program. This format is as follows: Pressure (Mean and Std Dev in mb), Temperature (Mean and Std Dev in Celsius), Dew Point (Mean and Std Dev in Celsius), and Geopotential Height(Mean and Std Dev in meters).

Temperature had to be converted to degrees in Kelvin. Dew point needed to be converted to relative humidity using temperature and the dew point. Geopotential height was converted to geometric height. These quantities would then be used to produce refractivity for each atmospheric layer.

The output table format in the database shown below was used as the input format used in the program. It is as follows: Grid Square, Pressure, Geopotential Height, Dry Refraction, Wet Refraction, Total Refraction, Dry Height, and Average Temperature

This format allows for immediate ray tracing for a given location. Only the geopotential height must be converted to geometric height. Finally, a 17 element output table will be incorporated as the input file into the program with the following format : Grid Square, Pressure, Latitude, Longitude, Dry Refraction, Wet Refraction, Avg Total Refraction, Stdev Total Refraction, Avg Dry Height(Hopfield), Avg Dry Height(Goad), Avg Wet Height (Goad), Avg temperature, Avg Rel. Humidity, Avg Height, Stdev temperature, Stdev Rel. Humidity, and Stdev Height.

III-2.2. OUTPUT FORMAT

The following variables are outputted:

Grid Square number
Refractivity index n
Radius of the earth at this location
Input data filename
Radii of each layer from the center of the Earth
Elevation angle of each layer
True distance traveled through each layer
Geometric height above the Earth (relative to mean sea level)
Incident angle on each layer
Central angle subtended over the Earth's surface for each layer
Apparent elevation angle for each layer
True Range for each layer
Apparent range (stratified layer method)
Apparent range (numerical integration method, Gauss quadrature) for each layer
Apparent range total for Gauss quadrature
Total time traveled through all layers
Time delayed by troposphere
Range delay
Angle refraction error
True elevation angle

Straight line distance total
Total central angle subtended over the Earth
Apparent range (numerical integration method, Simpson's Rule) for each layer
Apparent range total (Simpson's rule)

III-2.3. OUTPUT FILES AND PROGRAM CAPABILITIES

The Rayscont7 program produces five output files. Four of these files are data files used in the graph programs. These four files are explained in the database section. The fifth file is called millray.dat. This file contains useful information about the ray trace for the user. At the top of the file, the grid square number, the input data filename and the initial elevation angle are indicated as the Earth's radius (RLZERO) and the radius of the first layer R(1) or RL(1).

The next data set indicates the stratified layer method ray trace results.
The first column indicates the refractive index n for each layer. Column two indicates the height of each layer as measured from the center of the Earth.
Column three indicates the elevation angle (ALPHA) as the ray traverses each atmospheric layer. The next column is headed by RX(M). This is the straight line or true distance through each layer. The fourth column indicates the geometric height above the Earth's surface which has been corrected from geopotential height. Column five is the incident angle on the following layer, i.e. the angle of the ray relative to the horizontal of the next layer. The final column in this set contains the central angle subtended over the Earth's surface called PHI. It is essentially the measured angle from the starting position of the ray to the ray's destination over the surface of the Earth relative to the Earth's center.

The next data set to follow has five columns. The first column indicates the apparent elevation angle for each layer. Column 2 indicates the straight line distance total as each layer is traversed. The third column is the apparent range for each layer as calculated by the stratified layer method. The fourth column is the apparent range of each layer as calculated by the numerical integration method called Gauss-quadrature. The last column is the running total of the range value using the Gauss quadrature method. The total time traveled in seconds is then indicated. This is followed by the time delay computed using a value of c which corresponds to the RF speed of light. Both of these are indicated in seconds. The range delay is then shown in meters. The value called SUM is the total apparent slant range as calculated by the stratified layer method. Next, the total angle refraction error is given in degrees. This is followed by the true elevation angle from the station to the top layer in degrees. The straight line distance or total true range is listed next in meters. Finally the central angle subtended over the Earth's surface is given in degrees. The last data set is the Simpson's rule apparent range calculation. The first column indicates the apparent range for each layer. Column two indicates the total slant range as each layer is traversed.

The program will be able to produce these values stated above for one angle or for several angles. One option will produce results for angles from 1 to 5.5 degrees in .5 degree increments. Another option will produce results for angles from 6 to 15 degrees in 1 degree increment. A ray trace can be produced using the two quartic Hopfield model if desired or using actual data as described previously.

III-2.4. PROGRAM DEVELOPMENT PROBLEMS AND SOLUTIONS

Several developmental steps are still required to be added to the ray trace program. Currently, the program assumes a spheroidal Earth. When computing slant range at low angles, the curvature of the Earth becomes significant. The program already calculates the Earth's radius for a given transmitter location (this radius includes the Earth's oblateness). This value is then used in a law of cosines formula to compute the slant range. The aforementioned formula needs to be altered to include the effects of the curvature of the Earth as the ray travels down range. This effort is in process.

Another developmental problem is that of the geoidal undulation. This is the separation between the geoid and the ellipsoid Earth models. All tropospheric data that is currently being processed is relative to the geoid or the mean sea level. Since the transmitter locations are computed relative to the ellipsoid as is the satellite Ephermeris, the tropospheric height data must be converted to match the ellipsoid altitude. This becomes critical in computing slant range. The project team has obtained a geoid undulation program from Arthur Holt of Code 8114. This program originally comes from the Defense Mapping Agency. It is a model of the geoidal separation for every 30 minutes of a degree around the globe. After some manipulation, the program was converted from PC Fortran to a working VAX Fortran program. This program eventually will need to be incorporated as a subroutine to the ray tracing program.

Currently, the ray tracing program is a two dimensional vertical ray trace program. Eventually, the program should be converted to a three dimensional program taking azimuthal angle into account. As the ray traces through the atmosphere in the azimuthal direction, it is possible for the ray to cross into a new 2.5 X 2.5 degree grid square grid which possesses different refractive properties than the one before it. In fact 2 or 3 squares could be traversed before reaching its destination. The ray program will be altered in such a manner as to compute the square numbers for the latitude and longitude locations when it is traversing the troposphere. This will be based on a ground range calculation along with the slant range. The program will be designed to go outside the program and fetch the appropriate grid square tables from an exported database file. Having obtained the correct data, the appropriate refractivity constants can be used to perform the ray trace. It should be duly noted that this is not a trivial program alteration. There are several operations that must be done in parallel and/or iteratively to achieve this.

The ray trace program can produce a range and time delay for any grid area. There was some question as to how to match this delay with the true range calculation from a station location and a satellite Ephemeris. It is assumed that the true range values used will be used as a rough order of magnitude in characterizing the Hopfield model correction versus this ray program's correction value.

IV. PRESENT STATUS AND FUTURE PLANS

This report is intended to present the overall direction toward the development of a global atmospheric database which was originally tasked for better understanding of RF propagations from ground to space. As pointed out in section III, the development of a global database requires acquisition of huge computational facilities and accompanying software development efforts for processing collected data from various Agencies. These processed data are then transformed into the new database (in this case, ACCESS) to run the ray-tracing algorithms for investigations of time-delays, range errors, RF speed in

space, and other interesting atmospheric characteristics. The final product of this task will be presented in the format of a 2.5 degree by 2.5 degree grid for the entire globe with 17 layers of pressure levels from the ground and 17 parameters of the final output of the ACCESS database as shown in the Figure IV.1.

The computational facilities currently depend heavily on the PC 486 and NRL VAX computers. Since these are not enough to support current and future requirements, two additional PC 586s (Pentium) and a SPARC 5 Sun Workstation will be added to speed up the data processing and analysis efforts in this fiscal year with other required accessories and related softwares. The data processing (including handling and transforming of the original data) of the Eastern United States, from 32.5 degree to 47.5 degree North latitude and 260 degree to 295 degree East longitude, is complete. The effort will be continued to include the rest of the North America, then be extended to the Northern Hemisphere, and, finally, extended to the Southern Hemisphere. After these global databases are completed, the ray-tracing and other data analysis efforts will continue until the atmospheric characteristics are understood better in the sense of time delays and range error corrections of RF propagations in space. The ultimate goal of this task may be the development of a real-time or near real-time database which can deliver the information in real-time to potential users to correct any errors or discrepancies of time-delays and other errors. This goal may be achieved without any difficulties in the near future if the computational and funding supports are available.

V. DATA PROCESSING AND ANALYSIS RESULTS

Elementary physics introduces the concept of representing the direction of energy flow of light in terms of rays, and the use of Snell's law to compute changes in the ray direction as light crosses the boundary surface between two media of differing refractive indices. The application of such techniques to a medium in which the refractive index changes continuously is, perhaps, slightly less well known, but not because the idea is new. The use of ray-tracing is generally confined to conditions contained within the limitations imposed on geometrical optics; however, there are at least two special conditions in which ray-tracing procedures can be shown to give acceptable results, even when geometrical optics is not properly applicable. Both the limitations on geometrical optics and the special cases when ray-tracing can be performed outside these limitations have been studied [42].

It is common in ray-tracing studies to assume that the refractive index of the atmosphere is spherically stratified with respect to the surface of the Earth. Thus, the effect of refractive index changes in the horizontal direction is normally not considered. Neglecting the effect of horizontal gradients seems quite reasonable in the troposphere because of the relatively slow horizontal change of refractive index in contrast to the rapid decrease with height. Although the assumption of small horizontal changes of the refractive index appears to be true in the average or climatic sense, there are many special cases such as variations occurring in frontal zones and land-sea breeze effects where one would expect the refractive index change abruptly within the horizontal distance traversed by a tangential ray passing through the first kilometer in height [43].

In the fields of atmospheric link, ray-tracing constitutes a useful means for investigating the influence of the structure of the medium, including ground reflection and diffraction, on the propagation path. Furthermore, ray-tracing is important from

DATABASE: ECMWF Data
REGION: Eastern US
NLAT:32.5-47.5 ELON:260.0-295.0
DATE: August (1980-1991 average)
TIME: N/A

NOTE: "-11" indicates missing value

Grid#	Lat (deg)	Lon (deg)	Press (mb)	Ndry (N)	Nwet (N)	Ntot(m) (N)	Ntot(s) (N)	Hdry(H) (km)	Hdry(G) (km)	Hwet(G) (km)	TK(m) (k)	%RH(m) (%)	Ht(m) (m)	TK(s) (k)	%RH(s) (%)	Ht(s) (m)
2272	37.50	277.50	20.	6.8932	0.0000	6.8932	-11.	41.2007	33.0326	0.0000	225.15	0.00	26951.0	2.0	-11.	37.0
2272	37.50	277.50	30.	10.5268	0.0000	10.5268	-11.	41.2007	32.4458	0.0000	221.15	0.00	24277.0	1.0	-11.	56.0
2272	37.50	277.50	50.	18.2031	0.0000	18.2031	-11.	41.2007	31.2721	0.0000	213.15	0.00	21025.0	2.0	-11.	45.0
2272	37.50	277.50	70.	26.2225	0.0000	26.2225	-11.	41.2007	30.3918	0.0000	207.15	0.00	18963.0	2.0	-11.	50.0
2272	37.50	277.50	100.	37.8260	0.0000	37.8260	-11.	41.2007	30.0984	0.0000	205.15	0.00	16822.0	3.0	-11.	59.0
2272	37.50	277.50	150.	54.1018	0.0000	54.1018	-11.	41.2007	31.5655	0.0000	215.15	0.00	14343.0	2.0	-11.	68.0
2272	37.50	277.50	200.	68.6270	0.0000	68.6270	-11.	41.2007	33.1794	0.0000	226.15	0.00	12482.0	1.0	-11.	68.0
2272	37.50	277.50	250.	82.1512	0.0000	82.1512	-11.	41.2007	34.6465	0.0000	236.15	0.00	10967.0	2.0	-11.	64.0
2272	37.50	277.50	300.	95.3512	1.6135	96.9647	-11.	41.2007	35.8202	9.4369	244.15	43.17	9681.0	2.0	-11.	56.0
2272	37.50	277.50	400.	120.7078	5.2188	125.9265	-11.	41.2007	37.7275	9.9445	257.15	51.72	7570.0	2.0	-11.	41.0
2272	37.50	277.50	500.	144.6951	10.3356	155.0307	-11.	41.2007	39.3413	10.3744	268.15	47.12	5851.0	2.0	-11.	31.0
2272	37.50	277.50	700.	189.1694	27.3858	216.5552	-11.	41.2007	42.1289	11.1178	287.15	37.50	3111.0	3.0	-11.	24.0
2272	37.50	277.50	850.	221.9754	45.6057	267.5811	-11.	41.2007	43.5960	11.5095	297.15	35.60	1454.0	5.0	-11.	33.0
2272	37.50	277.50	1000.	255.9789	65.5122	321.4911	-11.	41.2007	44.4763	11.7447	303.15	37.37	65.0	6.0	-11.	43.0
2273	37.50	280.00	20.	6.8932	0.0000	6.8932	-11.	41.2007	33.0326	0.0000	225.15	0.00	26951.0	2.0	-11.	36.0
2273	37.50	280.00	30.	10.5268	0.0000	10.5268	-11.	41.2007	32.4458	0.0000	221.15	0.00	24277.0	1.0	-11.	57.0
2273	37.50	280.00	50.	18.2031	0.0000	18.2031	-11.	41.2007	31.2721	0.0000	213.15	0.00	21026.0	2.0	-11.	46.0
2273	37.50	280.00	70.	26.0966	0.0000	26.0966	-11.	41.2007	30.5385	0.0000	208.15	0.00	18964.0	2.0	-11.	52.0
2273	37.50	280.00	100.	37.8260	0.0000	37.8260	-11.	41.2007	30.0984	0.0000	205.15	0.00	16822.0	3.0	-11.	62.0
2273	37.50	280.00	150.	54.1018	0.0000	54.1018	-11.	41.2007	31.5655	0.0000	215.15	0.00	14342.0	2.0	-11.	73.0
2273	37.50	280.00	200.	68.6270	0.0000	68.6270	-11.	41.2007	33.1794	0.0000	226.15	0.00	12481.0	1.0	-11.	74.0
2273	37.50	280.00	250.	82.1512	0.0000	82.1512	-11.	41.2007	34.6465	0.0000	236.15	0.00	10965.0	2.0	-11.	70.0
2273	37.50	280.00	300.	95.3512	1.6135	96.9647	-11.	41.2007	35.8202	9.4369	244.15	43.17	9679.0	2.0	-11.	62.0
2273	37.50	280.00	400.	120.7078	5.2188	125.9265	-11.	41.2007	37.7275	9.9445	257.15	51.72	7569.0	3.0	-11.	44.0
2273	37.50	280.00	500.	144.6951	11.1775	155.8726	-11.	41.2007	39.3413	10.3744	268.15	50.96	5850.0	2.0	-11.	32.0
2273	37.50	280.00	700.	189.8305	31.5237	221.3542	-11.	41.2007	41.9822	11.0787	286.15	45.79	3113.0	3.0	-11.	23.0
2273	37.50	280.00	850.	223.4796	55.6246	279.1041	-11.	41.2007	43.3026	11.4311	295.15	48.40	1462.0	5.0	-11.	30.0
2273	37.50	280.00	1000.	256.8261	78.9694	335.7955	-11.	41.2007	44.3296	11.7055	302.15	47.41	75.0	6.0	-11.	39.0
2274	37.50	282.50	20.	6.8932	0.0000	6.8932	-11.	41.2007	33.0326	0.0000	225.15	0.00	26952.0	2.0	-11.	36.0
2274	37.50	282.50	30.	10.5268	0.0000	10.5268	-11.	41.2007	32.4458	0.0000	221.15	0.00	24275.0	1.0	-11.	55.0
2274	37.50	282.50	50.	18.2031	0.0000	18.2031	-11.	41.2007	31.2721	0.0000	213.15	0.00	21026.0	2.0	-11.	46.0
2274	37.50	282.50	70.	26.2225	0.0000	26.2225	-11.	41.2007	30.3918	0.0000	207.15	0.00	18962.0	2.0	-11.	53.0
2274	37.50	282.50	100.	37.8260	0.0000	37.8260	-11.	41.2007	30.0984	0.0000	205.15	0.00	16822.0	3.0	-11.	65.0
2274	37.50	282.50	150.	54.1018	0.0000	54.1018	-11.	41.2007	31.5655	0.0000	215.15	0.00	14341.0	2.0	-11.	79.0
2274	37.50	282.50	200.	68.6270	0.0000	68.6270	-11.	41.2007	33.1794	0.0000	226.15	0.00	12477.0	1.0	-11.	82.0
2274	37.50	282.50	250.	82.1512	0.0000	82.1512	-11.	41.2007	34.6465	0.0000	236.15	0.00	10962.0	2.0	-11.	77.0
2274	37.50	282.50	300.	95.3512	1.3269	96.6781	-11.	41.2007	35.8202	9.4369	244.15	35.50	9677.0	3.0	-11.	67.0
2274	37.50	282.50	400.	120.7078	5.2188	125.9265	-11.	41.2007	37.7275	9.9445	257.15	51.72	7565.0	3.0	-11.	47.0
2274	37.50	282.50	500.	144.6951	13.0452	157.7403	-11.	41.2007	39.3413	10.3744	268.15	59.47	5848.0	3.0	-11.	33.0
2274	37.50	282.50	700.	190.4962	38.7124	229.2086	-11.	41.2007	41.8355	11.0395	285.15	59.67	3113.0	3.0	-11.	23.0
2274	37.50	282.50	850.	225.7744	59.7590	285.5334	-11.	41.2007	42.8625	11.3136	292.15	61.41	1482.0	3.0	-11.	29.0
2274	37.50	282.50	1000.	260.2717	79.9550	340.2267	-11.	41.2007	43.7428	11.5487	298.15	59.16	111.0	4.0	-11.	33.0

FIGURE IV.1 -- Final Output Format of the Tropospheric Research Database

the point of view of the inverse problem for obtaining information on the structure of the crossed medium from the analysis of the characteristics of the received signals. Ray-tracing has been discussed in a number of works using either simplified or general methods. When simple models are used, analytical solutions are generally searched, and for more complete systems numerical integration of the propagation equations are used.

One of the most commonly used analytic forms for representing ray-tracing is the second-order or parabolic approximation. Some advantages of the parabola over other methods are immediately apparent. It is an improvement over simpler virtual path techniques because its finite thickness allows for penetration into the layer as frequency is increased and also permits the calculation of the often important high ray as well as the normal ray. The principal advantage of the second order approximation, however is the simplicity of the ray-path equations in and through this model. Herein lies the chief advantage of the parabola over more exact but always more complicated methods of ray-path calculation. Several methods have been developed for calculating the characteristics of a ray path propagating in or reflecting from a parabolic layer. There are many different models used to calculate ray bending: the exponential model [42], linear or effective Earth's radius model, Schulkin's model, initial gradient correction model, bi-exponential model, partial differential equation model, parabolic equation model, Hitney and Richter model (IREP) [44], Goad model [26], etc. These models are also further classified by different numerical approaches applied to the model.

There are many variables which may influence Earth-space propagation. They fit into the broad categories of frequency, space such as elevation angle, climate and microscale (i.e., siting), and time as diurnal, monthly, seasonal, annual, year-to-year variability and time-series signal behavior. Propagation effects depend on all these variables. The data processing and analysis efforts should include as many of these variables as possible for better understanding of relationships among the variables. Several different ray-tracing algorithms have been developed for relative performance comparison. Some results are presented in this section for nine different categories, investigating interrelationships and characteristics in the DC region as a test case of functional relations and performance.

V-1. HEIGHT vs. TEMPERATURE

Temperature profiles have been plotted for the ECMWF data in Figure V-1-1 for July, August, September monthly average during 1980-1991 period, grid 2273 and 2274 in Table1. For the FNMOC data the Figure V-1-2 is for both AM and PM of September 1994, for the area of grid # 2273 and 2274, and Figures V-1-3 and V-1-4 for July, August and September of 1994 for grid # 2273 and 2274 respectively. The NCDC data in Figures V-1-5, both AM and PM of July, August, and September during 1980-1993 for the 2274 grid only. The NCDC data was not available in the land-based area at the time of this report prepared.

It is noticed that the lapse rate for the ECMWF data is approximately 6.67^0C/km from Figure V-1-1, 5.8^0C/km for the FNMOC of Figure V-1-2 and 5.0^0C/km for the FNMOC of Figure V-1-3 while 5.6^0C/km for Figure V-1-4, and 6.4^0C/km for the NCDC data in the Figure V-1-5. It is interesting to find out that the lapse rate of past ten-year average data is generally higher than that of the near real-time monthly average data value. The lapse rate currently applied is 6.8^0C/km throughout the country in the past ten years. Another important fact is that the lapse rate does not behave linearly above 15 km in space from the ground. Most models developed until today have assumed that the lapse

rate decreased linearly with height up to 40 km and beyond in space. This fact should be carefully examined and redeveloped or adjusted based on this new finding after further data evaluation and more statistics throughout the globe.

V-2. HEIGHT vs. REFRACTIVITY

The gaseous constituents of the atmosphere also influence the propagation of radio waves by varying the refractive index in time and space, causing refraction, reflection, and guiding or scattering of the waves. The radio refractivity, N, which is generally used to describe the spatial and temporal variations of the refractive index, n, is defined as

$$N = (n-1) \times 10^6 \qquad \text{(v-1)}$$

At radio frequencies the refractivity may be approximated by [11] as

$$N = 77.6 \times (P/T) + 3.73 \times 10^5 (e/T^2) \qquad \text{(v-2)}$$

where

P atmospheric pressure, mbar;
T absolute temperature, ^{0}K;
e water vapor pressure, mbar.

The first term in equation (v-2) is usually referred to as the dry component, and the second term as the wet component. The refractivity at a point in space thus varies primarily because of variations in temperature and water vapor concentration. The variations may occur on a short-term scale (i.e., a time scale up to the order of minutes) as small-scale irregularities or turbulent fluctuations or on a longer time scale, for example, diurnal or seasonal variations. The vertical variation of refractivity for an average standard atmosphere can to a first approximation be described by an exponential decrease with height [45]. Owing to the vertical variation in refractive index, the radio waves do not propagate in straight lines. For a vertical gradient of refractive index of dn/dh the rays are bent toward the region of higher refractive index. This makes the vertical gradient an important parameter for the estimation of propagation conditions.

In order to emphasize the importance of the vertical refractivity variations, the height versus refractivity has been plotted for the month of August for all three databases in the vicinity of Washington, D.C. area including grid 2273 and 2274 in Table 1. Total refractivity averages are presented for comparisons of each component of the equation (v-2). Both ECMWF data and NCDC data were plotted as a monthly average only as in Figures V-2-1 and V-2-2 respectively. The FNMOC data was plotted for both AM and PM average of the month of both July, August and September 1994 as shown in Figures V-2-3 and V-2-4. The refractivity of dry component and wet component with total refractivity is shown in Figures V-2-5 and V-2-6 for the NCDC and ECMWF data respectively. Figures V-2-7 through V-2-10 show the refractivity of both dry and wet component along with total component for 6:00 o'clock in the morning and 6:00 o'clock in the afternoon of the FNMOC data. As can be seen from the graphs, refractivity variations are dominant in the tropospheric regions from the ground to about 20 km in space for the dry component while the wet component varies below 5 km in space. Note also that the wet component consists of more than 20 % of the total refractivity from the ground to about 3 km high

in the space. This contrasts with the conventional argument where the wet component is generally less than 10 % of the total refractivity. Figures V-2-11 and V-2-12 present monthly variations of refractivity for past ten years in Washington, DC area. It also shows that the refractivity is generally constant above 5 km in space, and during June through September the refractivity is higher than the rest of the year.

V-3. RANGE ERROR VS. ELEVATION ANGLE

Significant increases in radio propagation coverage can be obtained from a given geostationary orbit location or from the ground if acceptable performance can be achieved at elevation angles below the current standard of 10^0 at K_u-band. Lowering the elevation angle of a link to a site, however, will lengthen the path through the troposphere, the region of the atmosphere where, at frequencies below 3 GHz, most signal impairments occur. A longer path translates into more attenuation; a correspondingly higher incidence of depolarization and tropospheric scintillation will also result. All three impairments will cause the quality of the link to degrade below acceptable availability and performance standards unless sufficient margins are built into the link or adequate signal restoration capability can be provided. As the path length increases, the amplitude of the high ray declines while its delay decreases. Conversely, the stronger anomalous ray shows a mild increase in amplitude and delay time; the fact that the delay time is not linearly related to path length will be noted and, in fact, the delay may decrease with increasing path length. As the path length is decreased, and the limit of the multipath support approached, the two rays approach each other and coalesce into one ray at the limit.
Other sources of the range error can be induced through the transformation process such as geoid undulation, ellipsoid, and ground range from the collected data.

Because of graphical limitations and technical concerns below 5^0 of the elevation angle, the elevation angle from the ground to 10^0 for all three data sources has been presented against the range error as shown in Figures V-3-1 through V-3-4. If the elevation angle is lower than 3^0, the resulting range error reaches more than 30 meters which implies almost 100 nsec time delay below that elevation angle. The range errors at 5^0 are larger than 20 meters which is equivalent to more than 60 nsec time delay. It is a serious matter for the task objective to maintain below 10 nsec time delay. Therefore, it is a major challenge to reduce or compensate this error by developing tools to reduce error as much as possible.

V-4. HEIGHT VS. ELEVATION ANGLE ERROR

Because of the non isotropic characteristics of the troposphere and the ionosphere, radio waves on their passage through the atmosphere experience angular deviation. Calculations of the predictable bias errors based on assumed static atmospheric models are presented together with the unpredictable angular errors. The latter are basically due to the non stationary inhomogeneities which are present along the path traversed by the waves. In calculating the average or bias refractive errors, the stratified layer method has been employed. The elevation angle error due to refraction is the angle between the apparent path direction and the direct line-of-sight path. The computations of the refraction errors are based on a 17 layer stratification. Layer thicknesses are not uniformly distributed from the ground to an altitude of 28 km.

The deviations in the refraction angle error due to meteorological observations supplied by several Agencies were shown in Figures V-4-1 through
from the elevation angles of 1^0 to 10^0. It is noticed that the angle errors at 1^0 elevation angle are six times larger than those of 10^0 at an altitude of 24 km or above, and the angle errors at 6^0 elevation angle are also more than four times of those at 10^0. The angle errors at 6^0 are three times larger than those at 10^0 elevation angle. For the low elevation angles from one degree to 5.5^0, the ECMWF data was plotted from the ground to an altitude of 28 km for the month of August during last 10 year period in Figures V-4-9 and V-4-10. The angle errors of 1^0 at 27 km altitude are almost four times larger than those of elevation angle of 5.5^0. These results indicate that the propagation in the lower elevation angle is much more serious than expected in the real environment.

V-5. HEIGHTS VS. RANGE ERROR

Range errors are always inherent in radar target measurements. This effect is present primarily because the velocity of electromagnetic propagation in the atmosphere is slightly less than the free space velocity. An additional source of error is the increase in path-length brought about by the refractive bending of the propagated ray. Range errors are shown in Figures V-5-1 through V-5-8 for each data source from 1^0 to 10^0 in the vicinity of the Washington, D.C. with direct neighborhood comparison such as grid 2273 and 2274. For the sources of NCDC and FNMOC, both morning and afternoon range errors are plotted to show any distinctive differences.

Note that the range errors at 1^0 elevation angle are more than five times larger than those of 10^0 elevation angle. Even at 6^0 elevation angle the range errors are almost four times larger than those of 10^0 elevation angle at the altitude of 24 km or above. For the low elevation angles from one degree to 5.5^0, the ECMWF data was plotted from the ground to an altitude of 28 km for the month of August during last 10 year period in Figures V-5-9 and V-5-10. The range errors of 1^0 at 27 km altitude are almost three times larger than those of elevation angle of 5.5^0. These results indicate that the propagation in the lower elevation angle is much more serious than expected in the model-based results.

V-6. HEIGHTS VS. SLANT RANGE ERROR

Slant range errors are plotted for four different approaches- stratified model method, Simpson's method, Gaussian approximation method, and straight line method. The statistical comparison study among these different numerical methods has not been presented in this report and will be included in the following report with the recommendations of the better choice. There is no clear difference found among these methods at the present time. Figures V-6-1 through V-6-6 show slant range errors vs. height plots for each data source. Slant range errors are presented for each different elevation angle from 1^0 to 2^0 and 5^0 elevation angles for the month of August. Each graph for all three data sources presents error propagation from the ground up to 15 km for the FNMOC and 25 km and 28 km for the ECMWF and NCDC data in space.

Comparing Figures V-6-1 and V-6-2, for example, the slant range errors at 1^0 and 2^0 elevation angle are more than four times larger than those of 5^0 elevation angle. Even at 5^0 elevation angle, the slant range errors are about 24 meters at the altitude of 27 km in space. This implies the time delays are more than 70 nsec if we convert this into time. As pointed out in section V-4 for the range errors, intensive research efforts are required to bring these errors down to the level of less than 10 nsec time delays.

V-7. LAND-BASED WIDE AREA

As pointed out earlier, all variables of the previous seven sections are tested in this particular area to find any peculiar distinction between mountain (or land-based) and bay (or coastal-based) area meteorological behavior. In addition, the land-based grids (grid numbers, 2416-2418, 2272-2274. 2128-2130 in Table 1) are plotted to study any significant differences in atmospheric behavior. Figure V-7-1 shows the plot of temperature lapse rate aginst the altitude up to 27 km for both land-based and sea-based area for ECMWF data. Temperature of September for both land- and sea-based areas is around 5^0 less than that of July and August in the average. Figures V-7-2 and V-7-3 show plots of lapse rate for the land-base area of FNMOC and NCDC data respectively.

Figure V-7-4 presents the graph of the refractivity vs. height for both land- and sea-based area of the ten year average value of the August from ECMWF data. As can seen from the Figure, there is no difference in the average sense for the 10-year meteorological data. Figures V-7-5 and V-7-6 are the graphs of refractivity vs. height for NCDC and FNMOC data respectively. The refractivity of September is slightly lower than those of July and August as presented in Figures V-7-5 and V-7-6.

V-8. COASTAL-BASE WIDE AREA

As can be seen in Table 1, the east area of the 282.5 longitude East is considered to be mainly influenced by ocean front meteorological characteristics. Again, several ray-tracing graphs are included for reference to compare with the land-based ray-tracings. In addition, the ray-tracings for the maritime-based area (grid numbers, 2417-2419, 2273-2275, 2129-2131 as shown in Table 1) are presented in Figures V-8-1 and V-8-2 for the lapse rate from the ground to 22 km for FNMOC and 24 km for NCDC data respectively. Figures V-8-3 to V-8-5 are refractivity vs. height for the ECMWF, NCDC and FNMOC data. Figures V-8-6 through V-8-11 present elevation angle vs. range error plots for all three datasets. The refractivity value of the land-based area is slightly higher than that of the sea-based area in the average sense for the period of July to September during the last 10 years. This result will be studied for a wider area to verify whether ocean area refractivity is lower than that of the land or mountain areas.

VI. CONCLUSIONS

The meteorological data has been processed to investigate RF propagation effects of the tropospheric region from ground to 28 km in space. This task handles a huge volume of data as specified in section III. This report presents a current status of database development and a capability of analyzing those data in the form of ray tracing plots through several packages of modeling software, which have been developed for this

task. The approaches presented in this report are the frame work for the global database buildup and real-time processing development. Since the volume of data is very large, the efforts for analysis are limited to the smaller DC region to present current status and capability with future directions for the task.

The objective of data processing is to develop a database which can provide enough information for analyzing many different phenomena of the atmosphere in terms of lapse rate, refractivity, range, elevation angle, slant range and interrelationships among those parameters. These results will provide details of atmospheric effects on RF propagation to deduce time delays, range errors, time of arrival, and other important intelligent information.

A total of 60 graphs are included for those parameter relations in the vertical directional variation only. The analysis tool for the horizontal variations has been developed for the application, but it is not applied in this report. As a preliminary observation, the results are very distinguishable from the values arrived at through the application of conventional data for analysis of RF propagation patterns. This implies that the diurnal or seasonal average value provides better indications of the current atmospheric variation than the annual global average value which most users have adopted for convenience. The final database output format is shown in tabular form in Figure IV.1.

VII. REFERENCES

1. Pekeris, C.L.: "Wave Theoretical Interpretation of Propagation of 10 cm and 3 cm Waves in Low-Level Ocean Ducts", Proceedings of the Institute of Radio Engineers, Vol. 35, PP453, 1947

2. Johnson, M.A.: "A Review of Tropospheric Scatter Propagation Theory and Its Application to Experiment", Proc. of IEE, paper # 2534R, pp165-176, January 1958.

3. Megaw, E.C.S.: "Experimental Studies of the Propagation of Very Short Waves", J. of IEE, Vol. 93, Part IIIA, pp79, 1946.

4. Booker, H.G. and W.E. Gordon: "A Theory of Radio Scattering in the Troposphere", Proc. of IRE, Vol. 38, pp401, 1950.

5. Hopfield, H.S.: "The Effect of Tropospheric Refraction on the Doppler Shift of a Satellite Signal", J. of Geophysical Research, Vol. 68, No. 18, September 15, 1963.

6. Hopfield, H.S.: "Two Quartic Tropospheric Refractivity Profile for Correcting Satellite Data", J. of Geophysical Research, Vol. 74, No. 18, August 20 1969.

7. Hopfield, H.S.: "Tropospheric Effect on Electromagnetically Measured Range: Prediction from Surface Weather Data", Radio Science, Vol. 6, No. 3, pp357-367, March 1971.

8. Hopfield, H.S.: "Tropospheric Range Error Parameters: Further Studies", The Johns Hopkins University, Space Systems, Technical Report APL/JHU CP-015, June 1972.

9. Hopfield, H.S.: "Tropospheric Effects on Signals at Very Low Elevation Angles", Technical Memorandum APL/JHU #TG-1291, The Johns Hopkins University, March 1976.

10. Saxton, J.A.: Edited, "Advances in Radio Research", Academic Press, Vol. 1, 1964.

11. Bean, B.R. and E.J. Dutton: "Radio Meteorology", Dover Publications, New York, 1966

12. Smith, E.K., Jr. and S. Weintraub: "The Constants in the Equation for Atmospheric Refraction Index at Radio Frequencies", Proc. of IRE, Vol. 41, pp1035-1037, 1953.

13. Blake, L.V.: "Ray Height Computation for a Continuous Nonlinear Atmospheric Refractive-Index Profile", Radio Science, Vol. 3, No. 1, pp85-92, January 1968.

14. Campen, C.F. and A.E. Cole, "Tropospheric Variations of Refractive Index at Microwave Frequencies", Geophysical Res. Directorate, Air Force Surveys in Geophysics, NO. 79, October 1955.

15. Rowden, R.A. and J.W. Stark : "Long-Distance Propagation of a Very High Frequency (94.35 MHz) over the North Sea", Proc. of IEE, Paper No. 2345R, May 1957.

16. Millman, G.H. : "A Survey of Tropospheric, Ionospheric and Extraterrestrial Effects on Radio Propagation between the Earth and Space Vehicles"., AGARD Conference Proc. No.3 (Propagation Factors in Space Communication), pp3-55, Techivision, 1967.

17. Crain, C.M. and A.P. Deam : "Measurements of Tropospheric Index of Refraction Profiles", Proc. of IRE, Vol. 41, No. 2, pp284-289, 1953.

18. Ippolito, L.J.: "Radio Propagation for Space Communications Systems", Proc. of IEEE, Vol. 69, No. 6, pp697-727, June 1981.

19. Fang, D.J. and C.H. Chen: "Propagation of Centimeter/Millimeter waves along a Slant Path through Precipitation", Radio Science, Vol. 17, pp989-1005, 1982.

20. Oguch, T.: "Scattering from Hydrometers: A Survey", Radio Science, Vol.16, pp691-730, 1981.

21. Crane, R.K.: "Propagation Phenomena Affecting Satellite Communication Systems Operating in the Centimeter and Millimeter Wavelength Bands", Proc. of IEEE, Vol. 59, No. 2, pp173-188, February 1971.

22. Crane, R.K.: "Fundamental Limitation caused by RF Propagation", Proc. of IEEE, Vol. 69, No. 2, pp196-209, February 1981.

23. Crane, R.K.: "Prediction of Attenuation by Rain", IEEE Transactions on Communications, Vol. COM-28, No. 9, pp1717-1733, September 1980.

24. Liebe, H.J.: "Modelling Attenuation and Phase of Radio Waves in Air at Frequencies below 1000 GHz", Radio Science, Vol. 16, pp1183-1199, 1981.

25. Hitney, H.V., J.H. Richter, R.A. Pappert, K.D. Anderson, and G.B. Baumgartner: "Tropospheric Radio Propagation Assessment", Proc. of IEEE, Vol. 73, No. 2, pp265-283, February 1985.

26. Davies, P.G. and J.R. Norbury: "Review of Slant Path Propagation Mechanisms and Their Relevance to System Performance", Proc. of IEE, Vol. 130, Part F, pp665-678, December 1983.

27. Goad, C.C. and Lt. L. Goodman: "A Modified Hopfield Tropospheric Refraction Correction Model", Proc. of the Fall Annual Meeting, American Geophysical Union, San Francisco, CA, December 12-17, 1974.

28. Boithias, L. and J. Battesti: "Propagation due to Tropospheric Inhomogeneities", Proc. of IEE, Vol. 130, Part F, No. 7, pp657-664, December 1983.

29. Smith, E.K.: "Centimeter and Millimeter Wave Attenuation and Brightness Temperature due to Atmospheric Oxygen and Water Vapor", Radio Science, Vol. 17, No. 6, pp1455-1464, Nov.-Dec. 1982.

30. Hall, M.P.M.: "Effects of The Troposphere on Radio Communication", Peter Peregrinus, Ltd., The Institute of Electrical Engineers, London/New York, 1979.

31. Allnut, J.E.: "Satellite-to-Ground Radiowave Propagation: Theory, Practice and System Impact at Frequencies Above 1 GHz", Peter Peregrinus Ltd., The Institute of Electrical Engineers, London/New York, 1989.

32. Webster, A.R.: "Angles-of-Arrival and Delay Times on Terrestrial Line-of-Sight Microwave Links", IEEE transactions on Antennas and Propagation, Vol. AP-31, No. 1, pp12-17, January 1983.

33. ECMWF (European Center for Medium-Range Weather Forecast) data from the U.S.Air Force Environmental Technical Applications Center (AWS), Scott Air Force Base, Illinois 62225-5116.

34. Climatological Data from the Fleet Numerical, Meteorological and Oceanographic Command (FNMOC), Monterey, California and the Naval Oceanography Command Detachment at NCDC, Asheville, North Carolina.

35. Climatological Data from the National Climatological Data Center (NCDC), Asheville, North Carolina.

36. Special Sensor Microwave/Imager (SSM/I) Data from the Defense Meteorological Satellite Program (DMSP) via NRL Remote Sensing Division, Code 7211, Washington, D.C., 20375.

37. Almod, T, Flt Lt. and J. Clarke: "Consideration of the Usefulness of Microwave Propagation Prediction Methods on Air-to-Ground Paths", Proc. of IEE, Vol. 130, Part F, No. 7, pp649-656, December 1983.

38. CCIR Report 263-5: "Ionospheric Effects upon Earth-space Propagation". Vol. VI-Propagation in Ionised Media. XVth Plenary Assembly. International Telecommunication Union, Geneva 1982.

39. Aarons, J.: "Equatorial Scintillations-A Review", IEEE Transactions on Antennas and Propagation, Vol. AP-26, pp729-736, 1978.

40. Snyder, W.F. and C.L. Bragaw: "Achievement in Radio: Seventy Years of Radio Science, Technology, Standards, and Measurement at the National Bureau of Standards", Chapter XII, National Bureau of Standards, Boulder, CO 80303, 1986.

41. Millman, G.H.: "A Survey of Tropospheric, Ionospheric and Extraterrestrial Effects on Radio Propagation between Earth and Space Vehicles.", Propagation Factors in Space Communications AGARD Conference Proceedings No. 3, paper No. 3-3-55, 1967.

42. Kelso, J.M.: "Ray Tracing in the Ionosphere", Radio Science, Vol. 3, No. 1, pp1-12, January 1968.

43. Bean, B.R.: "Tropospheric Refraction", Advances in Radio Research, Vol. 1, edited by J.A. Saxton, pp53-119, 1964.

44. Hitney, H.V. and J.H. Richter: "Integrated Refractive Effects Prediction Systems (IREPS)", Naval Engineers Journal, Vol. 88, pp257-262, 1976.

45. CCIR: "Radiometeorological Data", Report #563-1, Vol. V, "Propagation in Non-Ionized Media", Recommendations and Reports of the CCIR, pp97-102, Geneva, 1978.

46. The Handbook of Digital Communications, Microwave System News, Vol. 9, NO. 11, pp79, 1979.

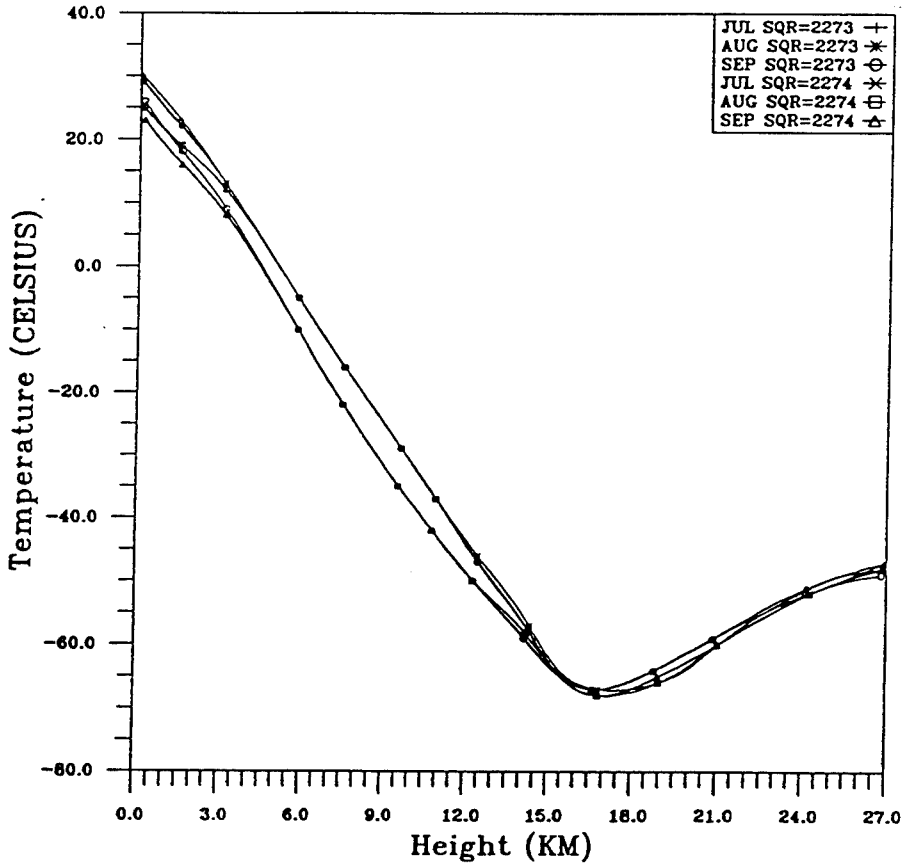

TEMPERATURE (C) VS HEIGHT (KM)
DC JULY, AUGUST, SEPTEMBER
ECMWF Data
SQR=2273 NLAT=37.5-40.0 ELON=280.0-282.5
SQR=2274 NLAT=37.5-40.0 ELON=282.5-285.0
10-Year Average

Figure V-1-1. Lapse Rate for Washington DC Vicinity for Average Temperature Variations of July, August, and September during 1980-1991 from ECMWF Database.

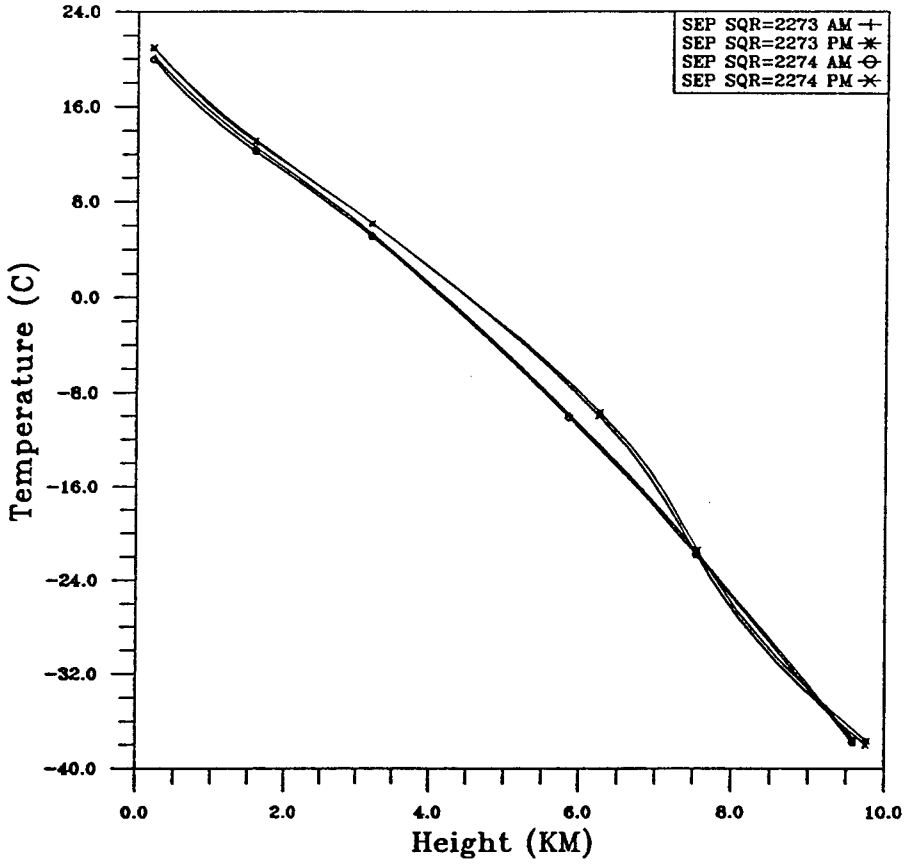

TEMPERATURE VS HEIGHT
DC LAND REGION COMPARISON
FNMOC
SQUARE = 2273 NLAT=37.5-40 ELON=280-282.5
SQUARE = 2274 NLAT=37.5-40 ELON=282.5-285
SEPTEMBER 1994 (AM & PM)

Figure V-1-2. Lapse Rate for Washington DC Vicinity for Average AM and PM Temperature Variations of September, 1994 from FNMOC Database.

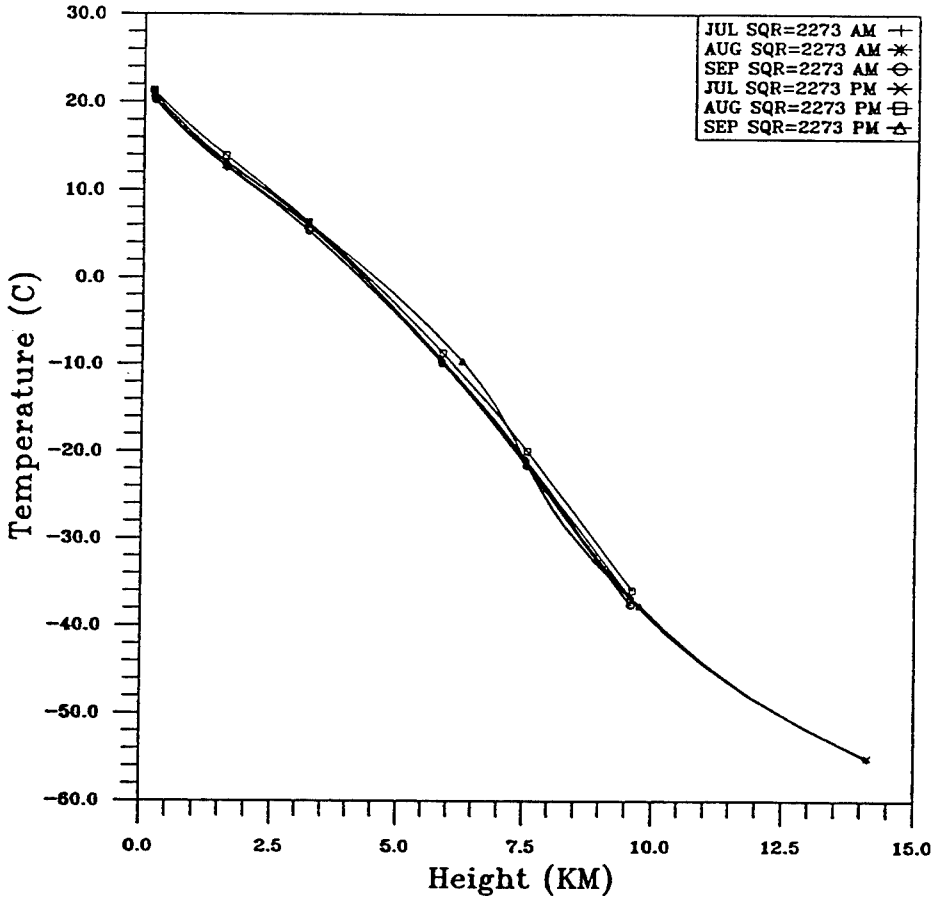

TEMPERATURE VS HEIGHT
DC LAND REGION
FNMOC
SQUARE = 2273 NLAT=37.5-40 ELON=280-282.5
JULY, AUGUST, SEPTEMBER 1994 (AM & PM)

Figure V-1-3. Lapse Rate for In-land Region of Washington DC Vicinity for Average AM and PM Temperature Variations for July, August, and September of 1994 from FNMOC Database.

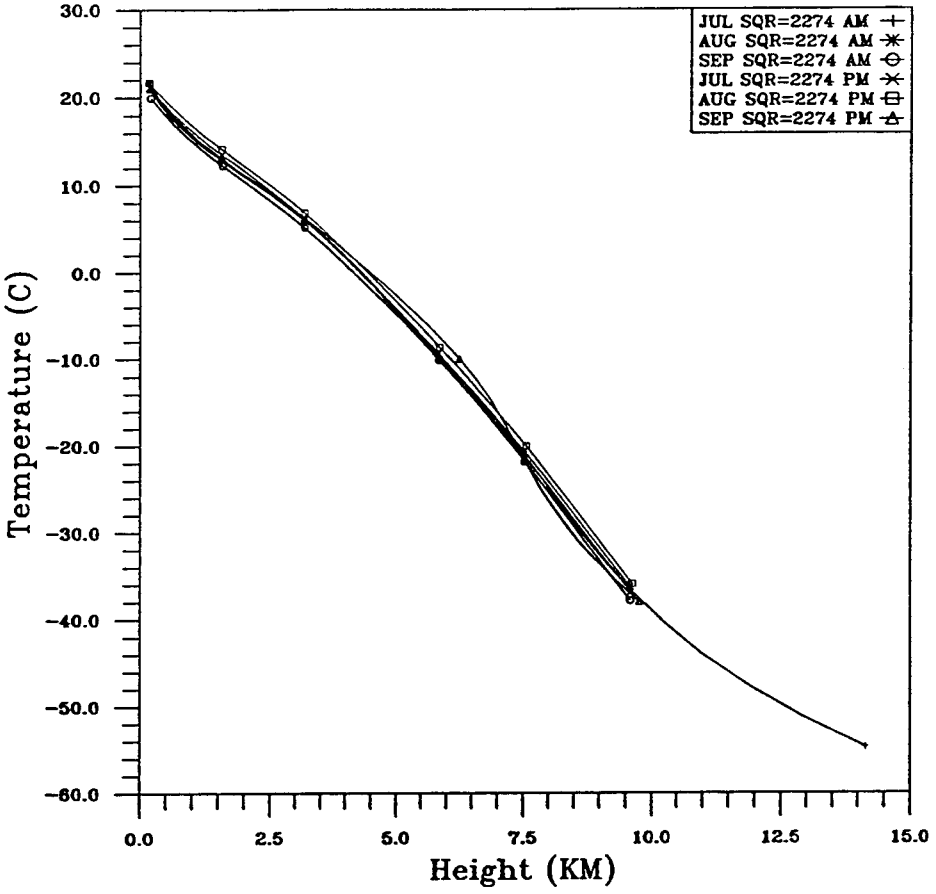

TEMPERATURE VS HEIGHT
DC LAND REGION
FNMOC
SQUARE = 2274 NLAT=37.5-40 ELON=282.5-285
JULY, AUGUST, SEPTEMBER 1994 (AM & PM)

Figure V-1-4. Lapse Rate for Bay Area of Washington DC Vicinity for Average AM and PM Temperature Variations for July, August, and September of 1994 from FNMOC Database.

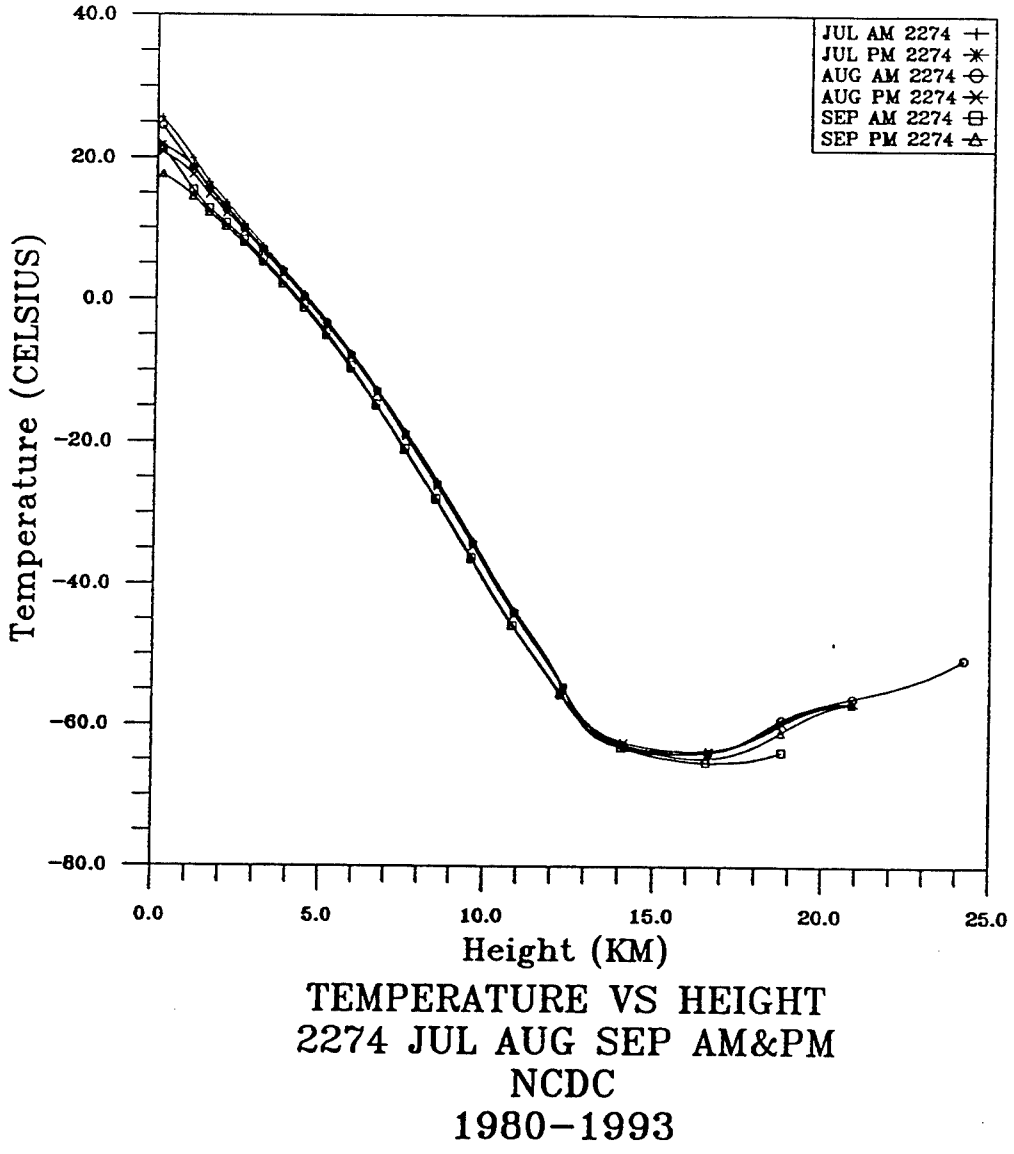

Figure V-1-5. Lapse Rate for Bay Area Only of Washington DC Vicinity for Average AM and PM Temperature Variations for July, August, and September during 1980-1993 from NCDC Database.

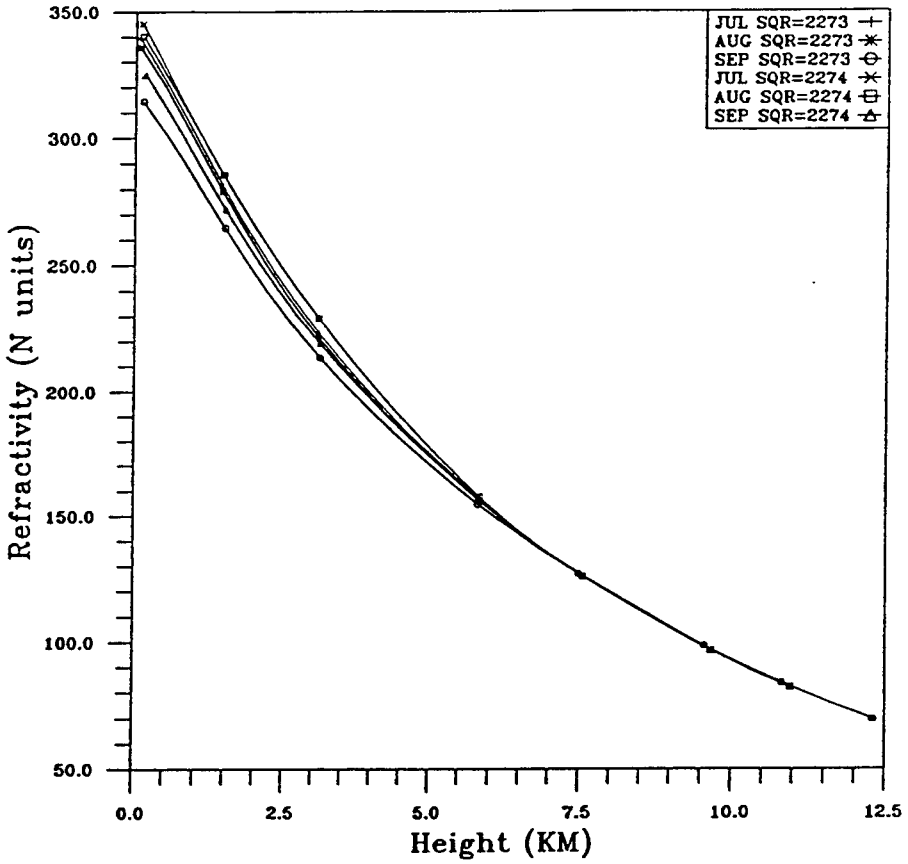

REFRACTIVITY (N) VS HEIGHT (KM)
DC JULY, AUGUST, SEPTEMBER
ECMWF Data
SQR=2273 NLAT=37.5-40.0 ELON=280.0-282.5
SQR=2274 NLAT=37.5-40.0 ELON=282.5-285.0
10-Year Average

Figure V-2-1. Average Refractivity Variations in Washington DC Vicinity for July, August, and September during 1980-1991 from ECMWF Database.

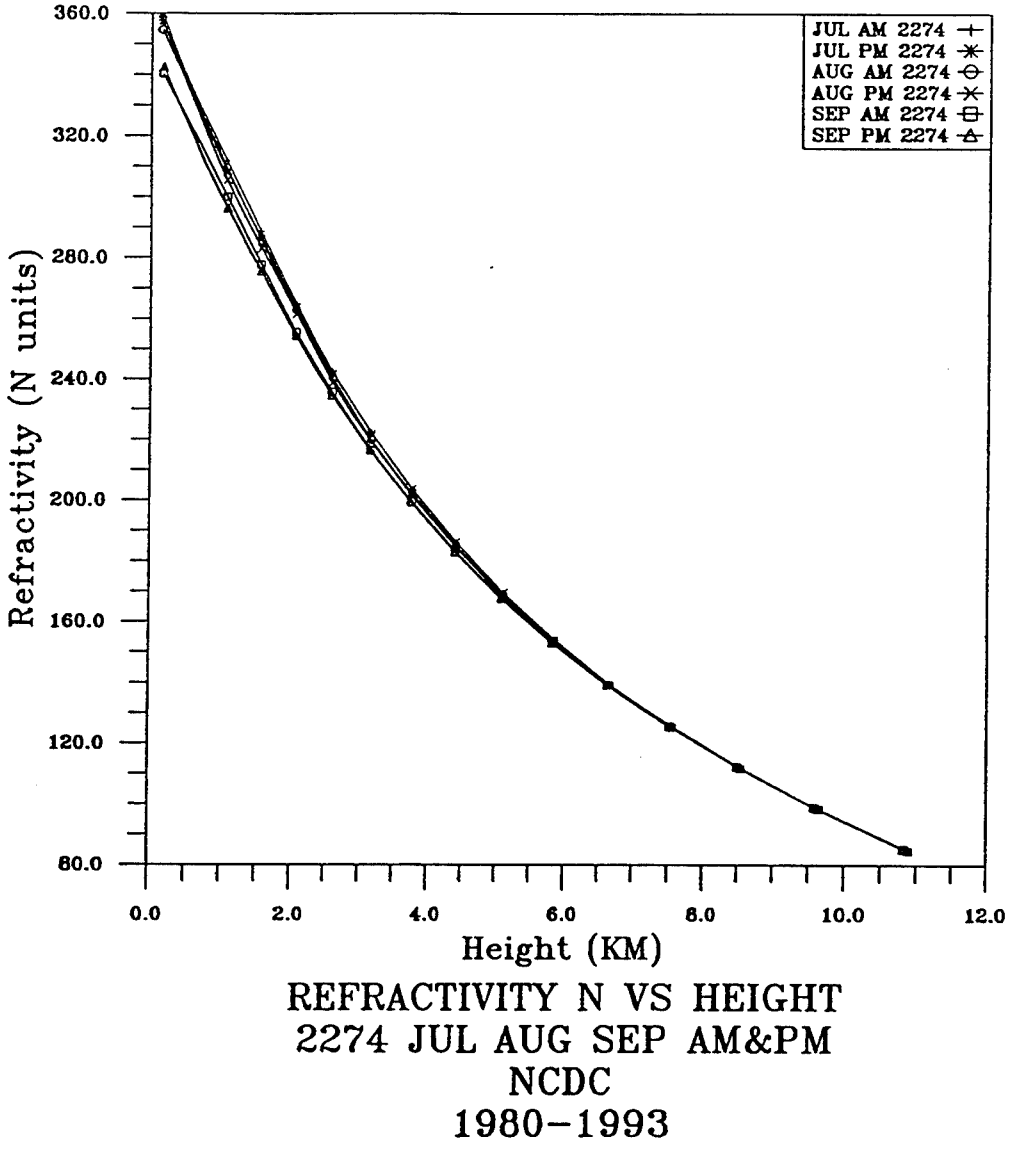

Figure V-2-2. Average Refractivity Variations in Bay Area of Washington DC Vicinity for AM and PM of July, August, and September during 1980-1993 from NCDC Database.

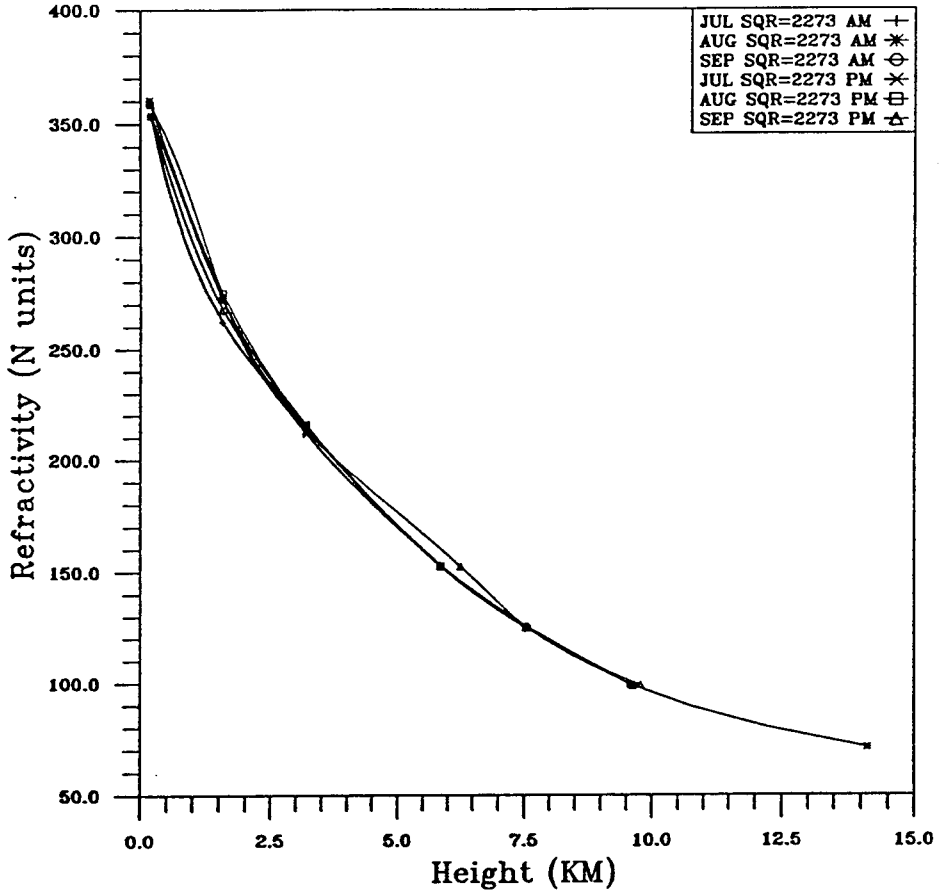

REFRACTIVITY N VS HEIGHT
DC LAND REGION COMPARISON
FNMOC
SQUARE = 2273 NLAT=37.5-40 ELON=280-282.5
JULY, AUGUST, SEPTEMBER 1994

Figure V-2-3. Average Refractivity Variations in In-land Area of Washington DC Vicinity for AM and PM of July, August, and September of 1980-1991 from FNMOC Database.

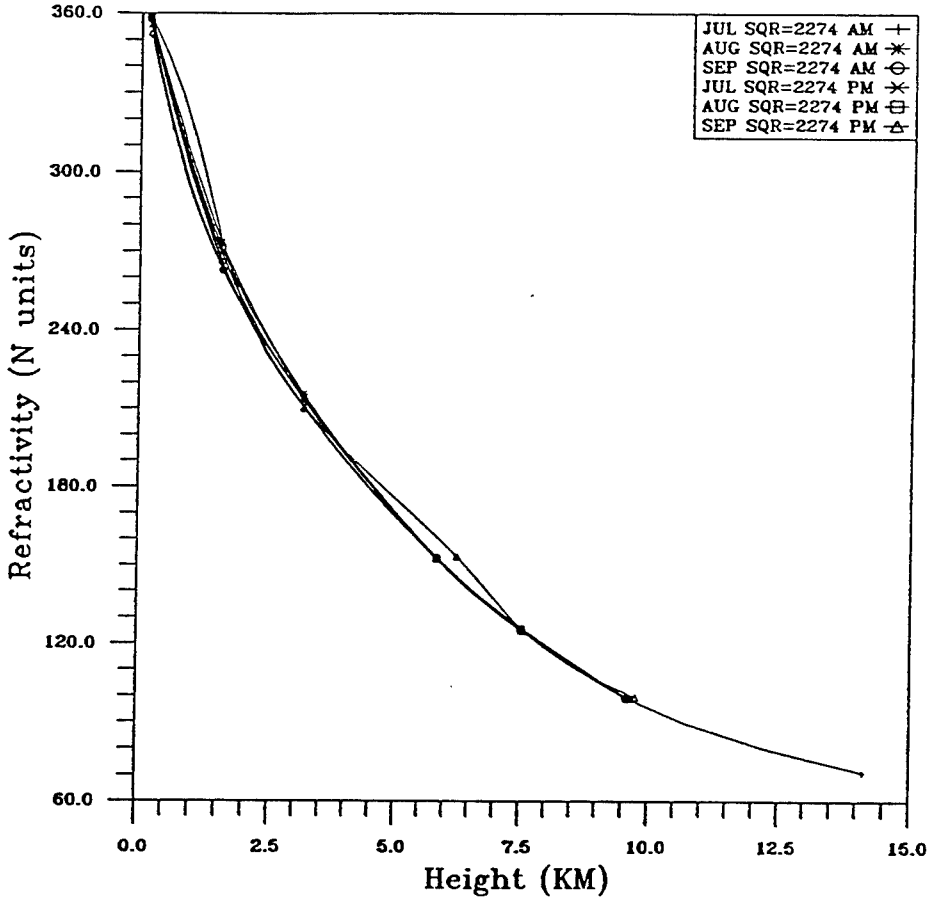

REFRACTIVITY N VS HEIGHT
DC LAND REGION
FNMOC
SQUARE = 2274 NLAT=37.5-40 ELON=282.5-285
JULY, AUGUST, SEPTEMBER 1994 (AM & PM)

Figure V-2-4. Average Refractivity Variations in Bay Area of Washington DC Vicinity for AM and PM of July, August, and September of 1994 from FNMOC Database.

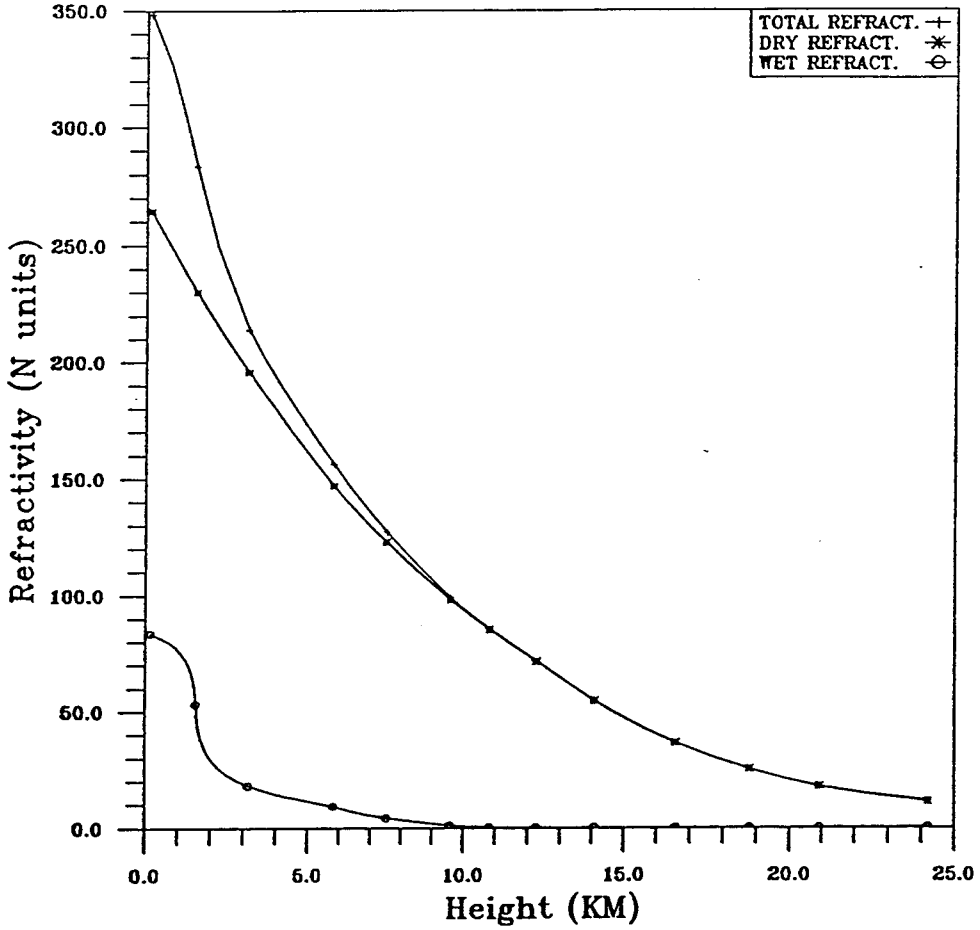

Figure V-2-5. Average Refractivity Variations separated with Dry, Wet and Total Refractivity for In-land Area of Washington DC Vicinity for AM of August during 1980-1993 from NCDC Database.

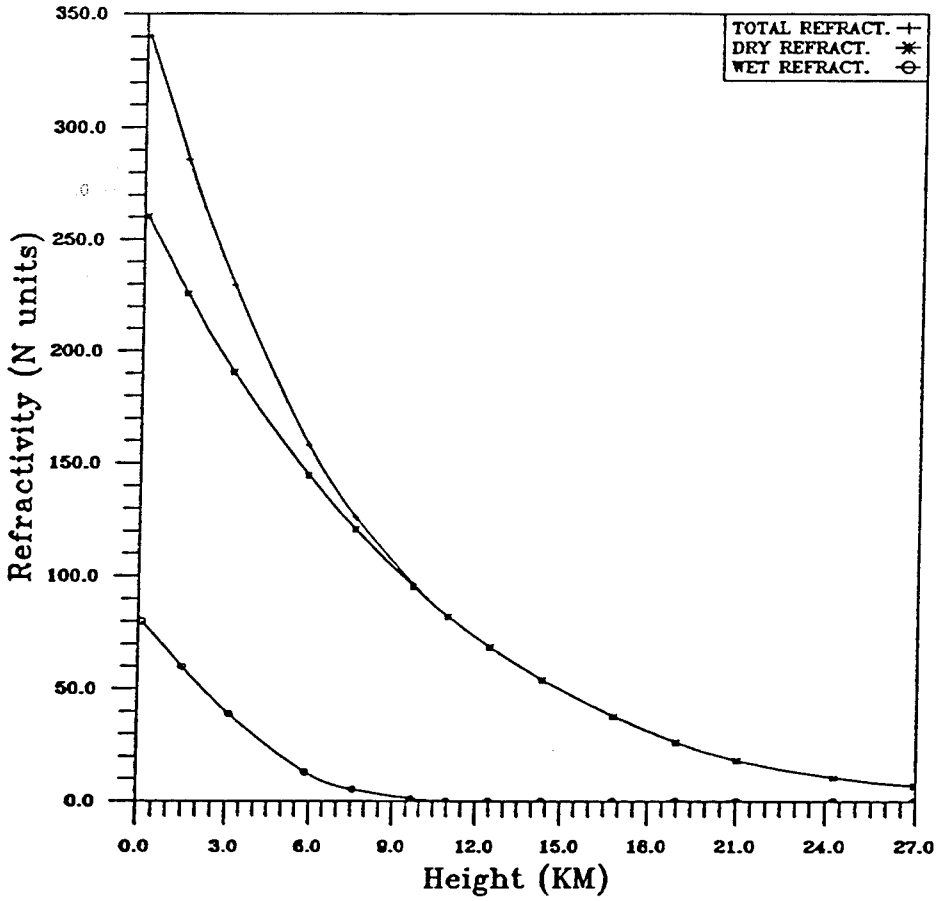

REFRACTIVITY (N) VS HEIGHT
DC AUGUST
ECMWF Data
SQR=2273 NLAT=37.5-40.0 ELON=280.0-282.5
10-Year Average

Figure V-2-6. Average Refractivity Variations separated with Dry, Wet, and Total Refractivity for In-land Area of Washington DC Vicinity for August 1980-1991 from ECMWF Database.

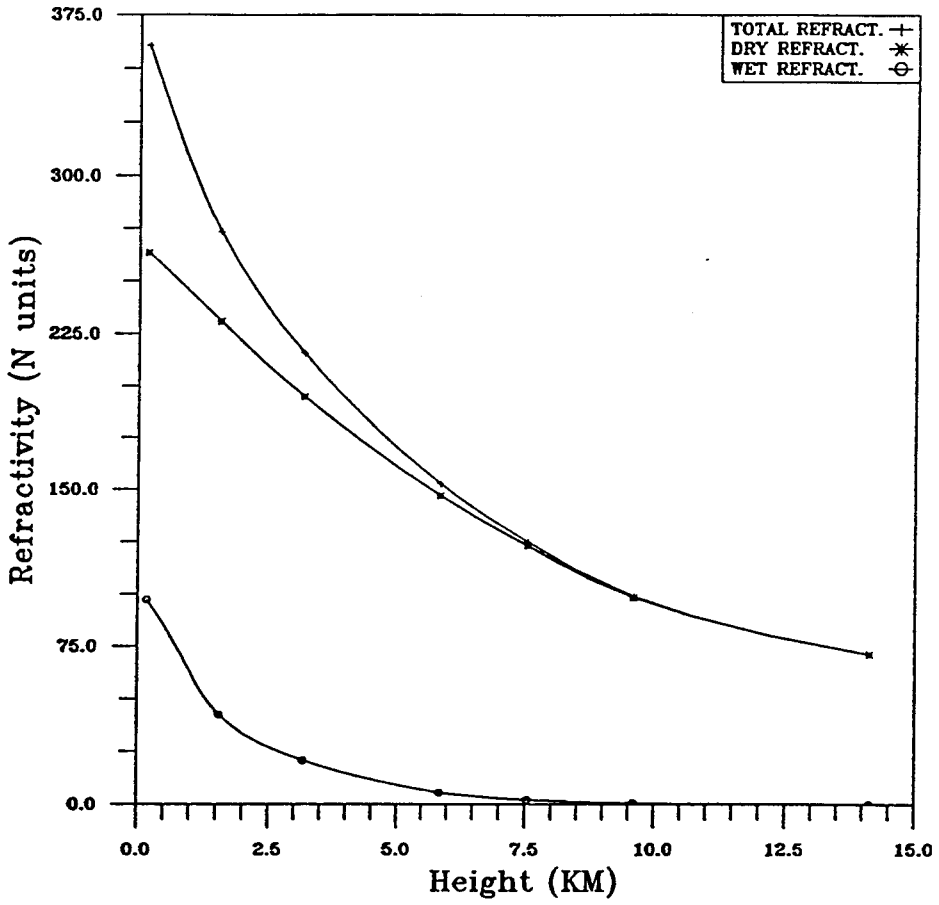

REFRACTIVITY N VS HEIGHT
DC AUGUST AM AVG
FNMOC
SQR=2273 NLAT=37.5-40 ELON=280-282.5
1994

Figure V-2-7. Average Refractivity Variations separated with Dry, Wet, and Total Refractivity for In-land Area of Washington DC for AM of August 1994 from FNMOC Database.

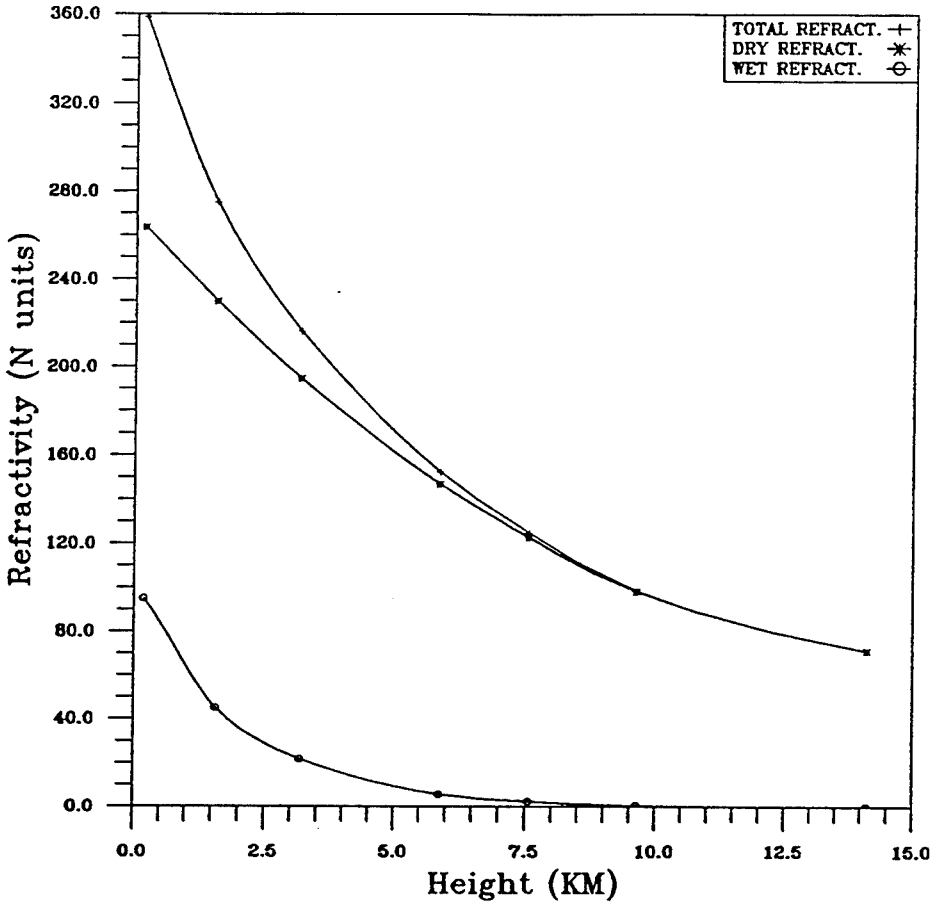

REFRACTIVITY N VS HEIGHT
DC AUGUST PM AVG
FNMOC
SQR=2273 NLAT=37.5-40 ELON=280-282.5
1994

Figure V-2-8. Average Refractivity Variations separated with Dry, Wet, and Total Refractivity for In-land Area of Washington DC for PM of August 1994 from FNMOC Database.

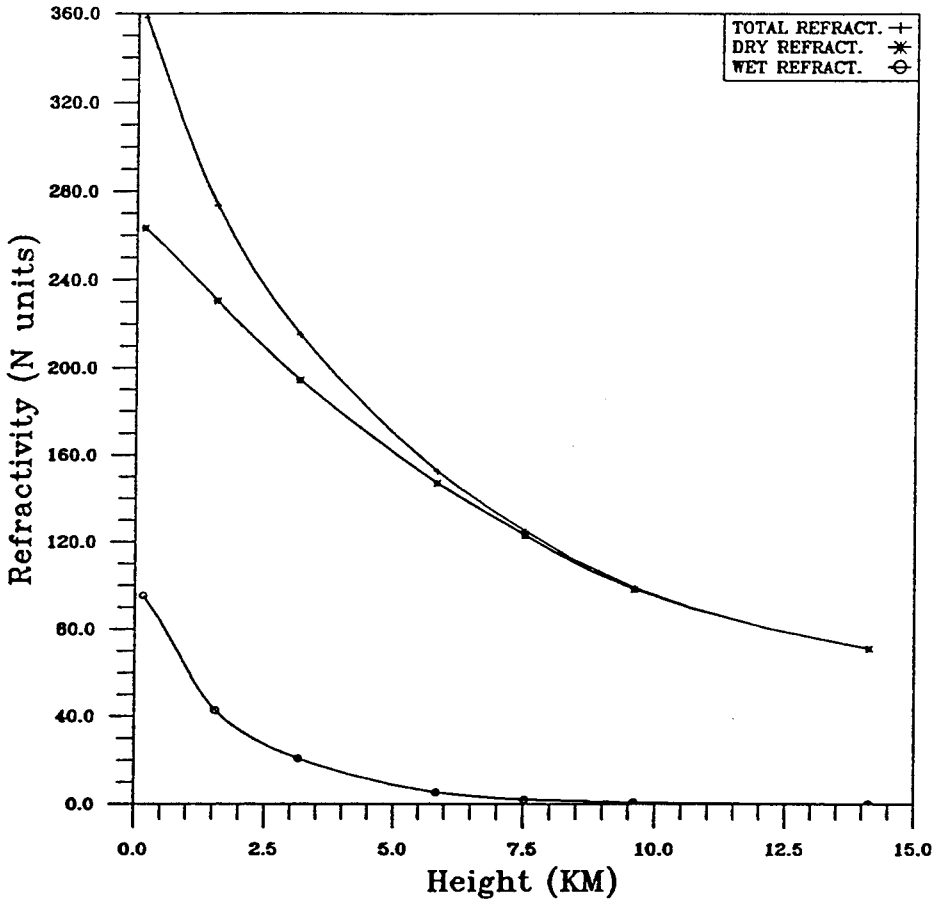

REFRACTIVITY N VS HEIGHT
DC AUGUST AM AVG
FNMOC
SQR=2274 NLAT=37.5–40 ELON=282.5–285
1994

Figure V-2-9. Average Refractivity Variations separated with Dry, Wet, and Total Refractivity for Bay Area of Washington DC for AM of August 1994 from FNMOC Database.

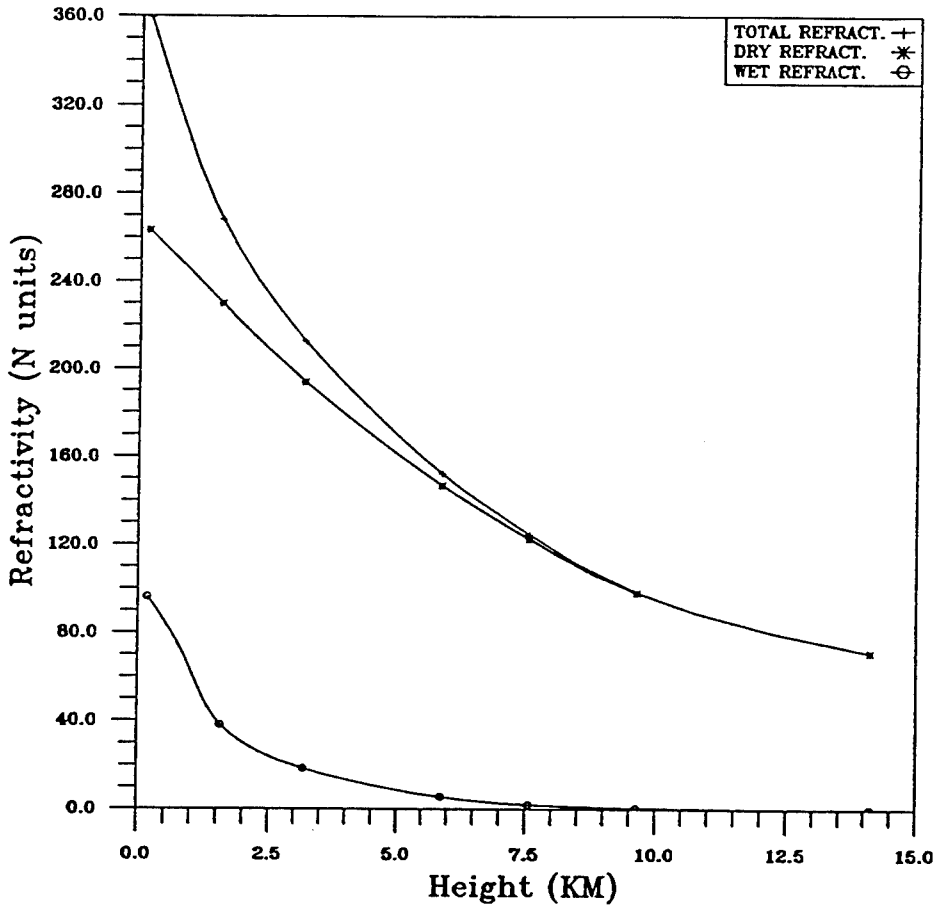

REFRACTIVITY N VS HEIGHT
DC AUGUST PM AVG
FNMOC
SQR=2274 NLAT=37.5-40 ELON=282.5-285
1994

Figure V-2-10. Average Refractivity Variations separated with Dry, Wet, and Total Refractivity for Bay Area of Washington DC for PM of August 1994 from FNMOC Database.

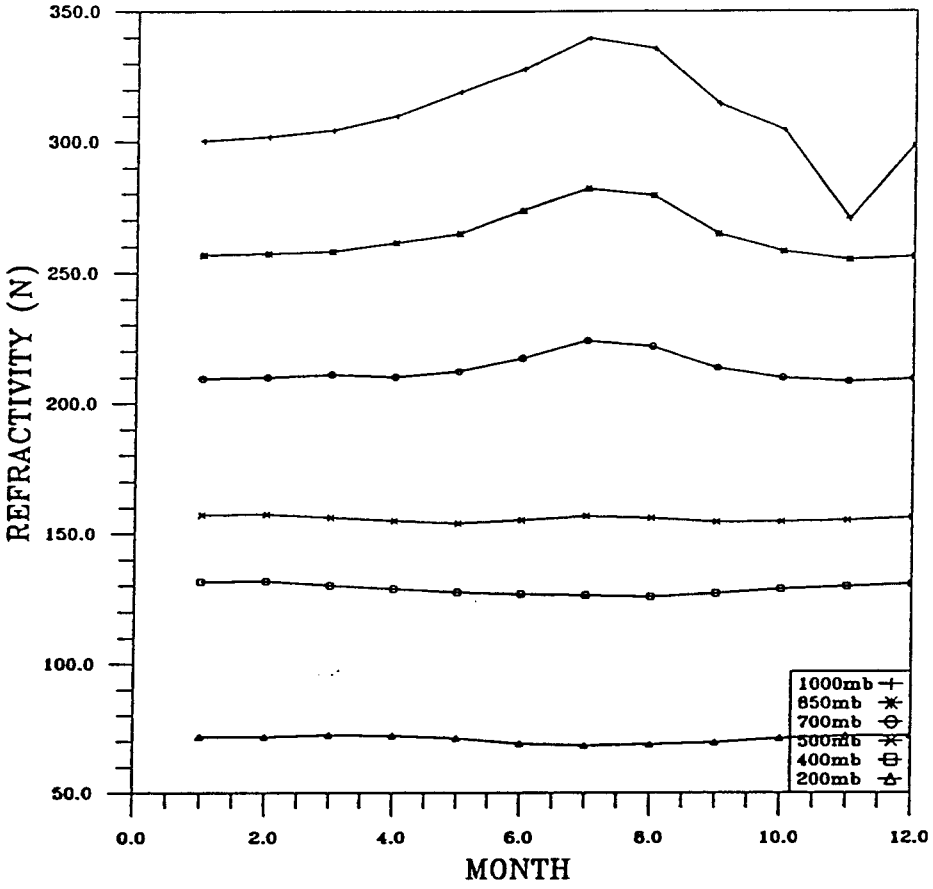

REFRACTIVITY (N) VS MONTH
DC
ECMWF Data
SQR=2273 NLAT=37.5-40.0 ELON=280.0-282.5
10-Year Average

Figure V-2-11. Monthly Average Refractivity Variations from Surface to 12.5 km in Space for In-land Area of Washington DC Neighbor for 1980-1991 from ECMWF Database.

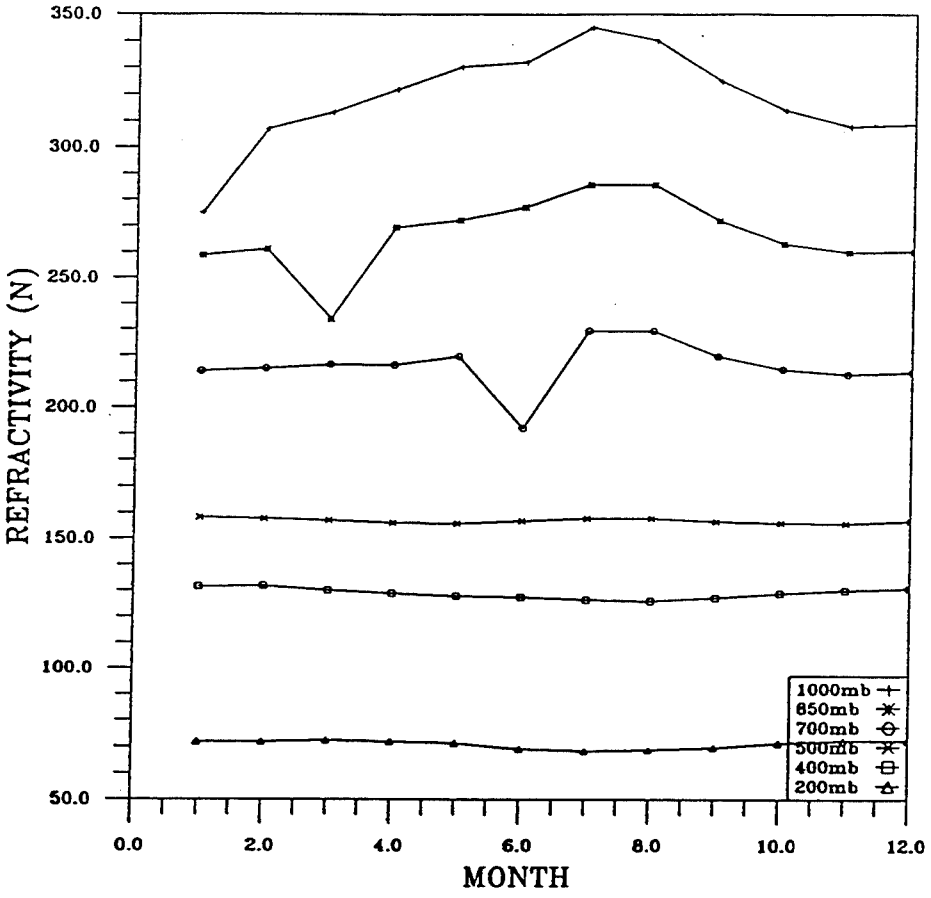

Figure V-2-12. Monthly Average Refractivity Variations from Surface to 12.5 km in Space for Bay Area of Washington DC Vicinity for 1980-1991 from ECMWF Database.

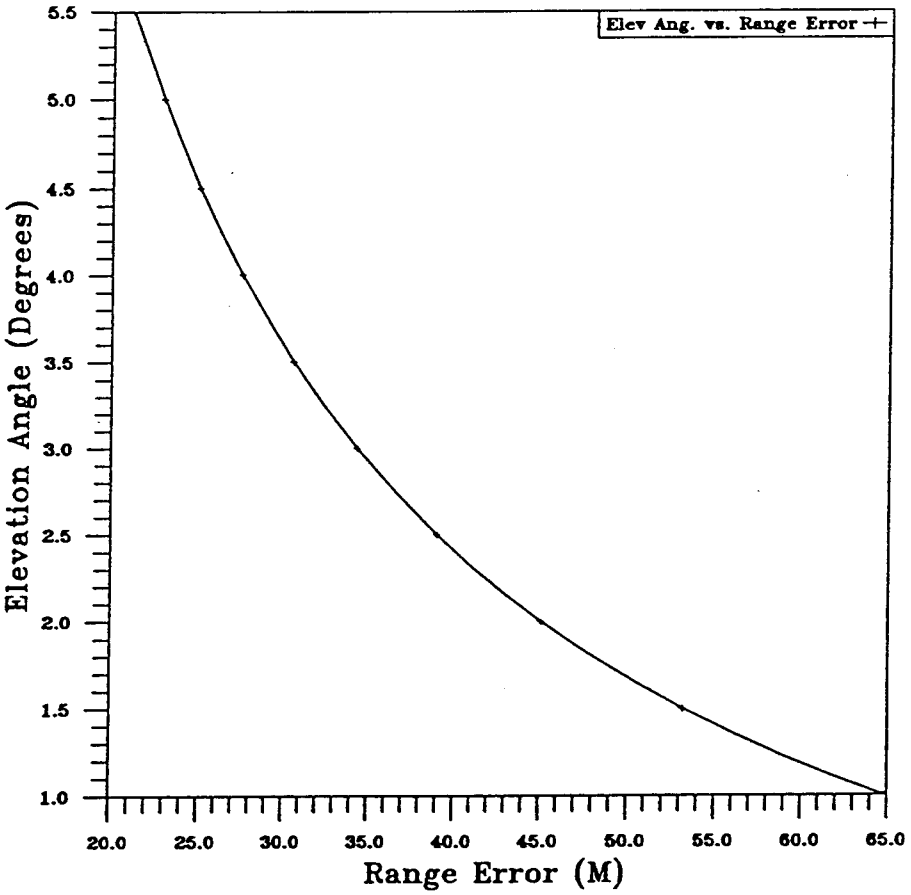

ELEVATION ANGLE VS RANGE ERROR
DC AUGUST
ECMWF Data
SQR=2273 NLAT=37.5-40.0 ELON=280.0-282.5
10-Year Average

Figure V-3-1. Range Error Variations based on Elevation Angle Changes for In-land Area of Washington DC Vicinity for 1980-1991 from ECMWF Database.

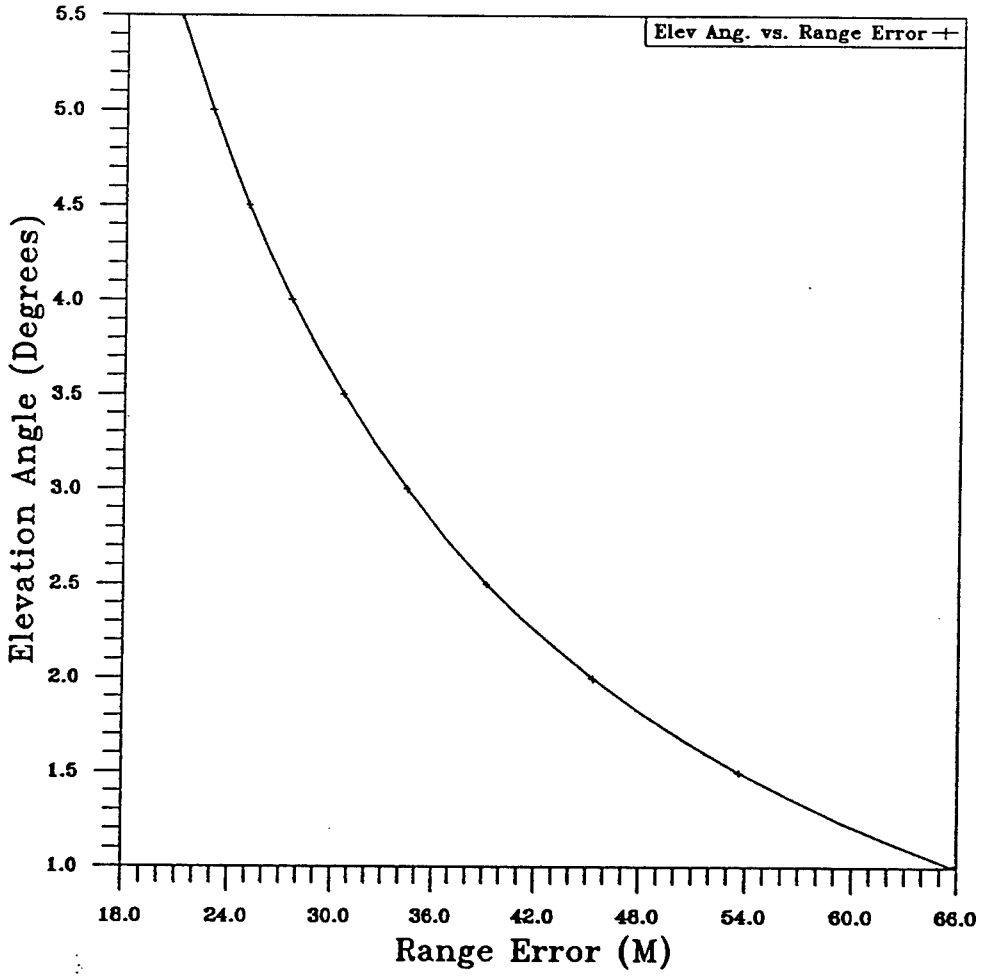

Figure V-3-2. Range Error Variations based on Elevation Angle Changes for Bay Area of Washington DC Vicinity for 1980-1993 from NCDC Database.

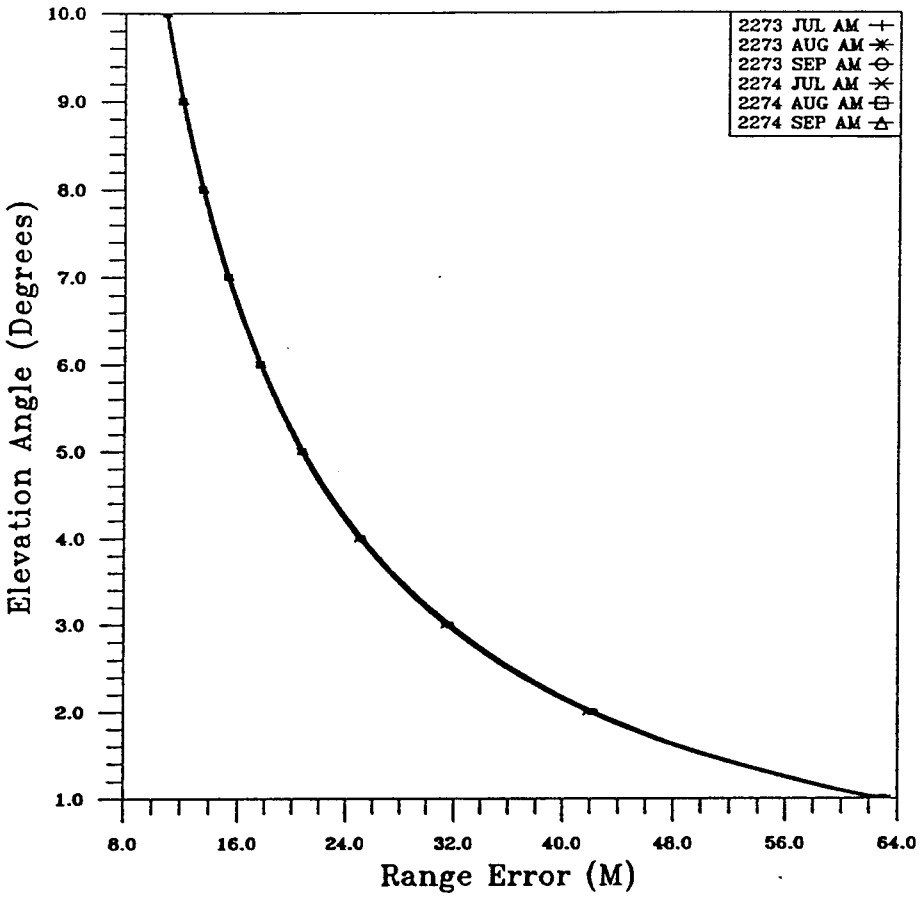

Elevation Angle VS Range Error
FNMOC
SQUARE=2273 NLAT=37.5-40 ELON=280-282.5
SQUARE=2274 NLAT=37.5-40 ELON=282.5-285
JULY, AUGUST, SEPTEMBER AM 1994

Figure V-3-3. Range Error Variations based on Elevation Angle Changes for Washington DC Vicinity for AM of July, August, and September of 1994 from FNMOC Database.

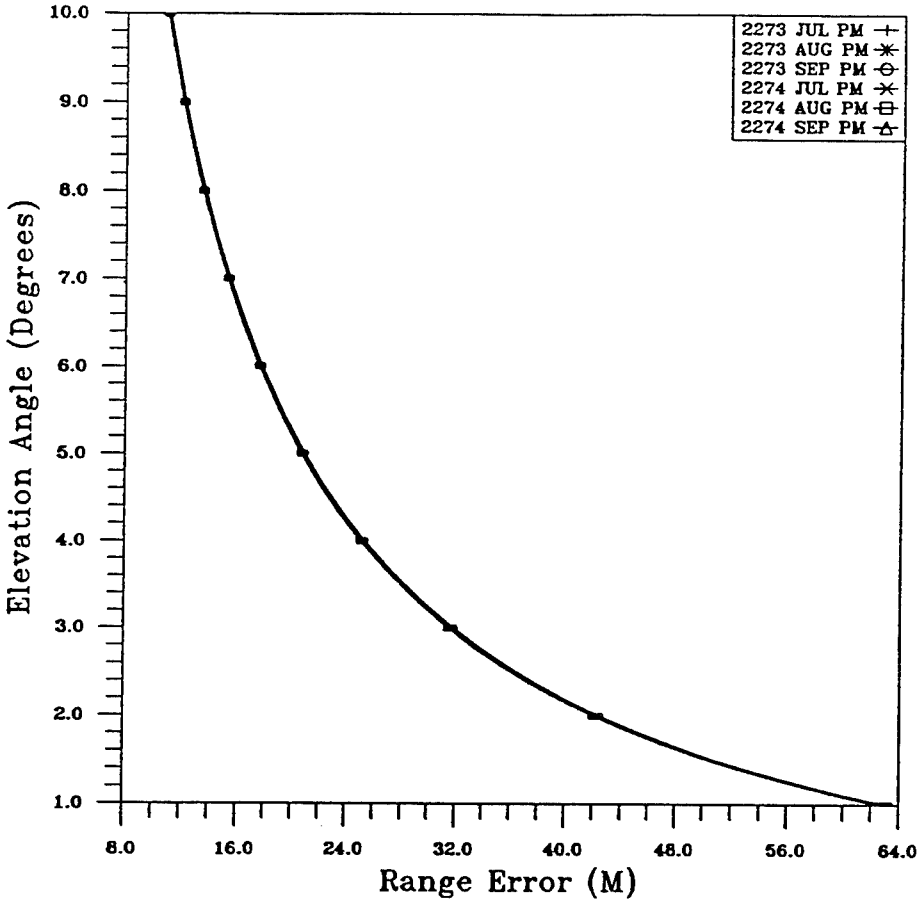

Elevation Angle VS Range Error
FNMOC
SQUARE=2273 NLAT=37.5–40 ELON=280–282.5
SQUARE=2274 NLAT=37.5–40 ELON=282.5–285
JULY, AUGUST, SEPTEMBER PM 1994

Figure V-3-4. Range Error Variations based on Elevation Angle Changes for Washington DC Vicinity for PM of July, August, and September of 1994 from FNMOC Database.

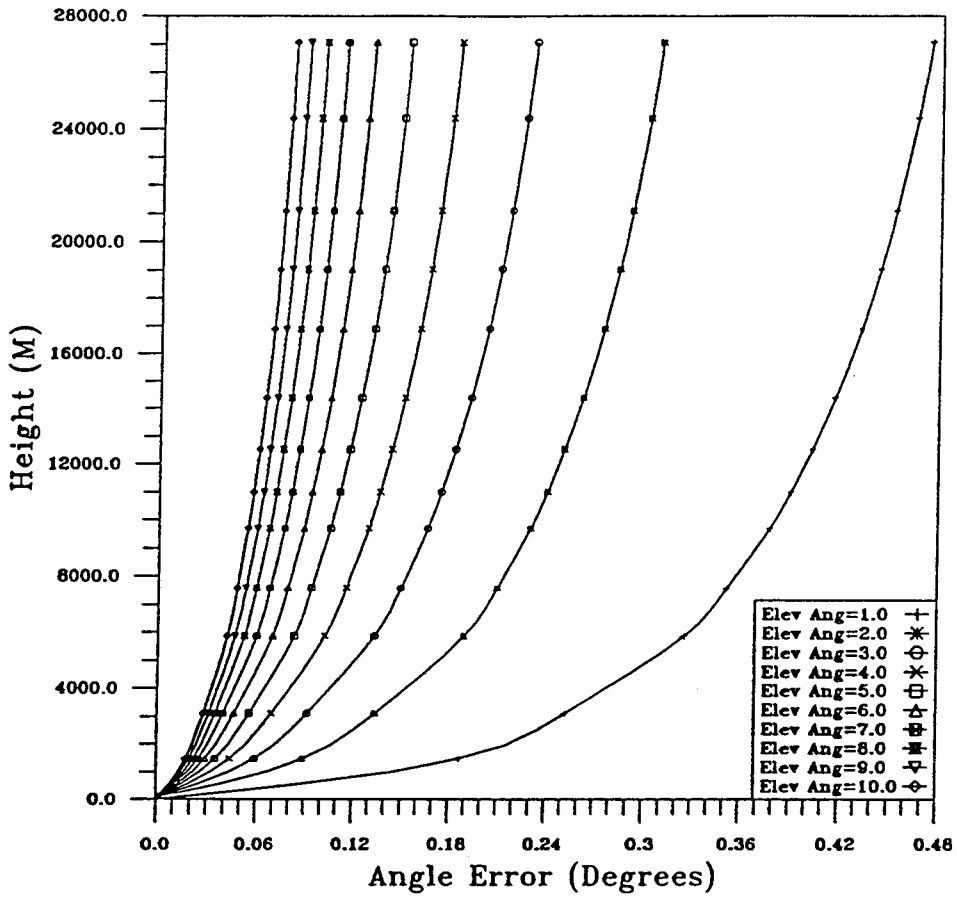

HEIGHT VS ANGLE ERROR
DC AUGUST
ECMWF Data
SQR=2273 NLAT=37.5-40.0 ELON=280.0-282.5
10-Year Average

Figure V-4-1. Elevation Angle Error for Each One Degree Interval for ECMWF Database from One to Ten Degree Elevation Angles for In-land Area of Washington DC Vicinity During 1980-1991.

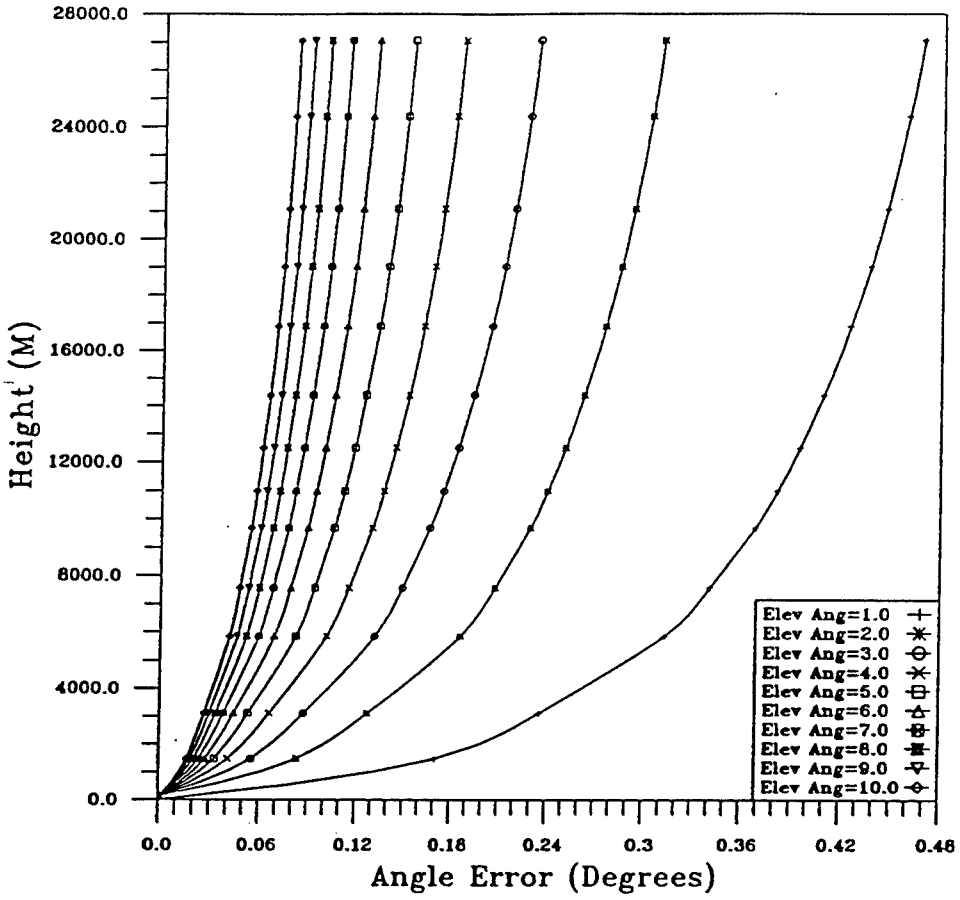

Figure V-4-2. Elevation Angle Error for Each One Degree Interval for ECMWF Database from One to Ten Degree Elevation Angles for Bay Area of Washington DC Vicinity During 1980-1991.

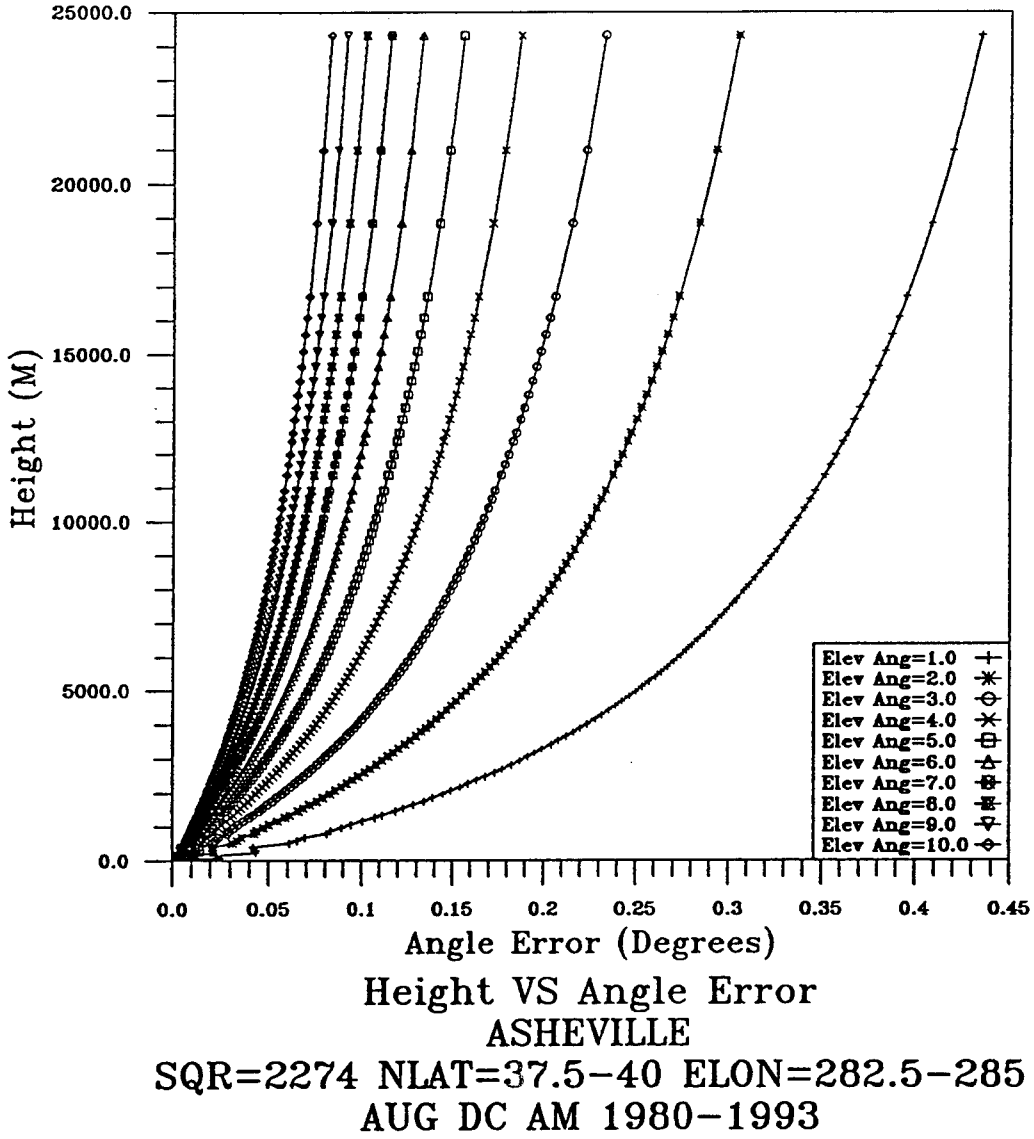

Figure V-4-3. Elevation Angle Error for Each One Degree Interval for NCDC Database from One to Ten Degree Elevation Angles for Bay Area of Washington DC Vicinity for AM of August during 1980-1991.

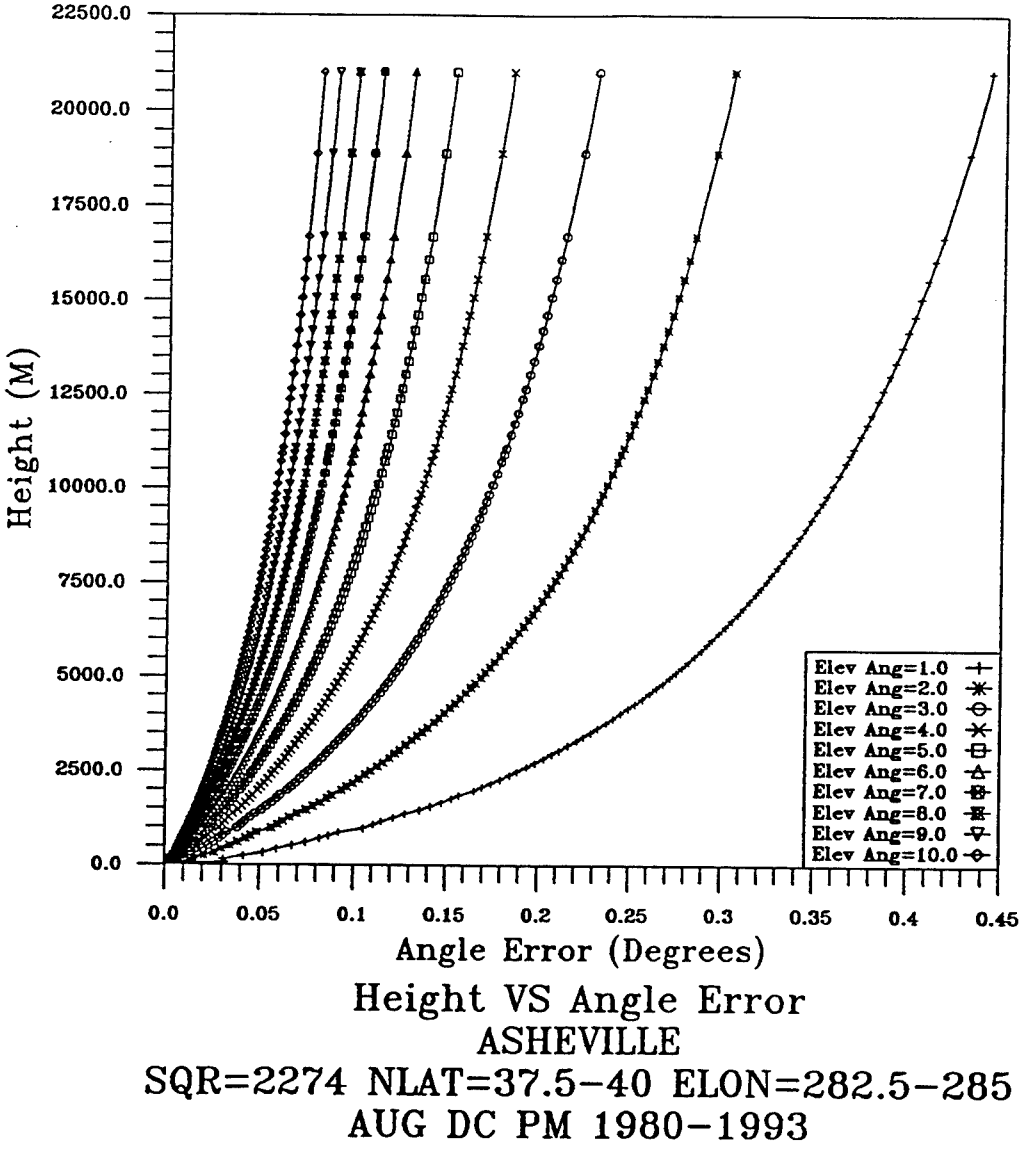

Figure V-4-4. Elevation Angle Error for Each One Degree Interval for NCDC Databasse from One to Ten Degree Elevation Angles for Bay Area of Washington DC Vicinity for PM of August during 1980-1991.

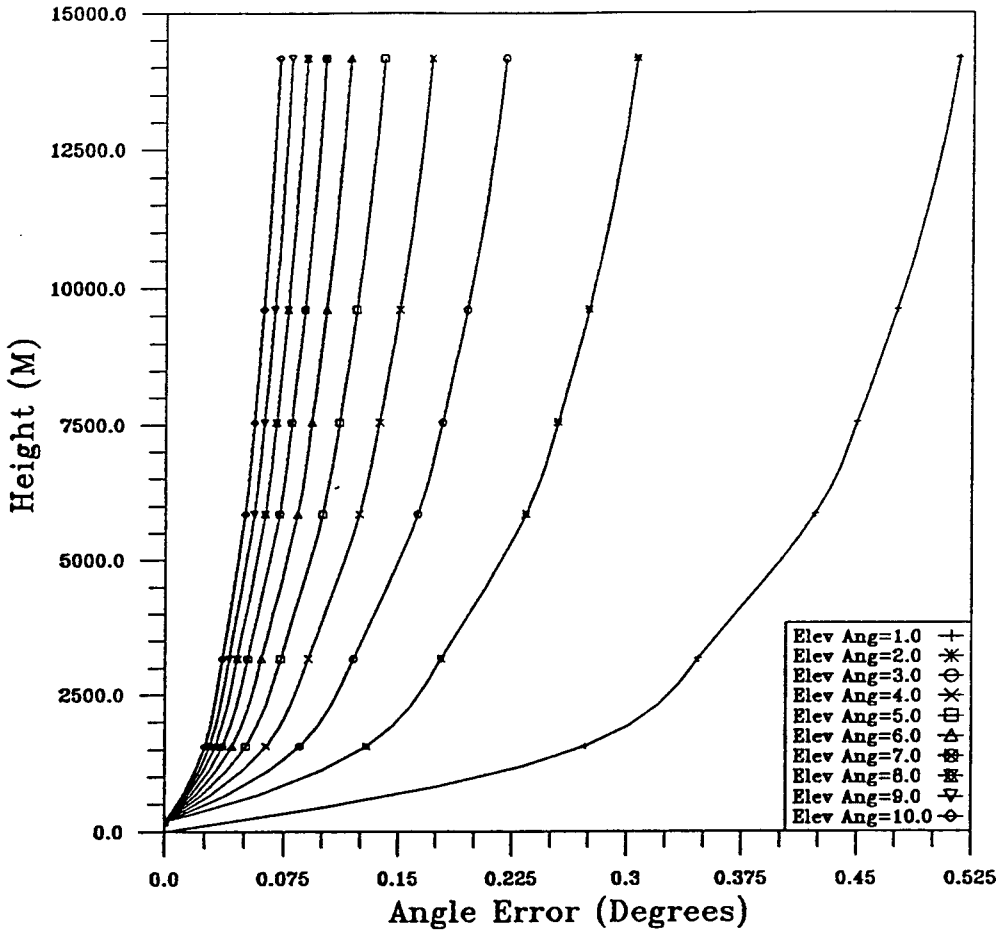

Height VS Angle Error
FNMOC
SQUARE=2273 NLAT=37.5-40 ELON=280-282.5
AUGUST DC REGION AM 1994

Figure V-4-5. Elevation Angle Error for Each One Degree Interval for FNMOC Database from One to Ten Degree Elevation Angles for In-land Area of Washington DC Vicinity for AM of August during 1994.

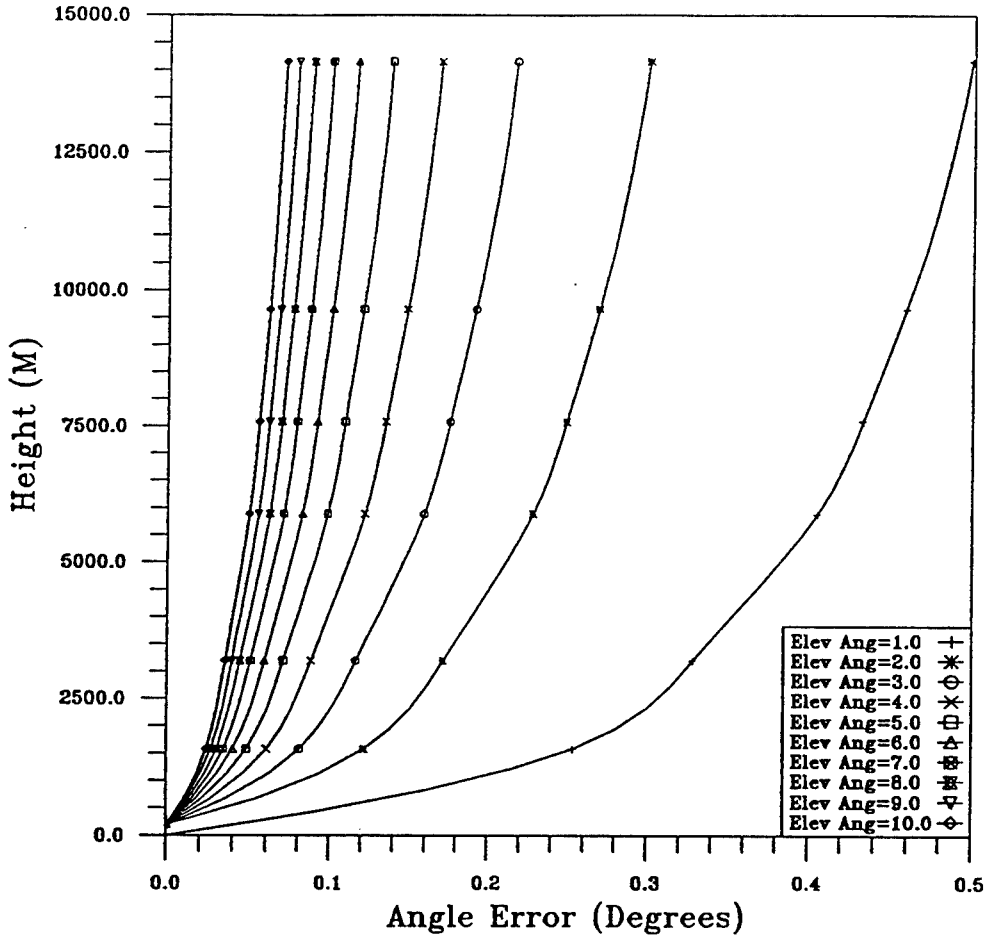

Height VS Angle Error
FNMOC
SQUARE=2273 NLAT=37.5-40 ELON=280-282.5
AUGUST DC REGION PM 1994

Figure V-4-6. Elevation Angle Error for Each One Degree Interval for FNMOC Database from One to Ten Degree Elevation Angles for In-land Area of Washington DC Vicinity for PM of August during 1994.

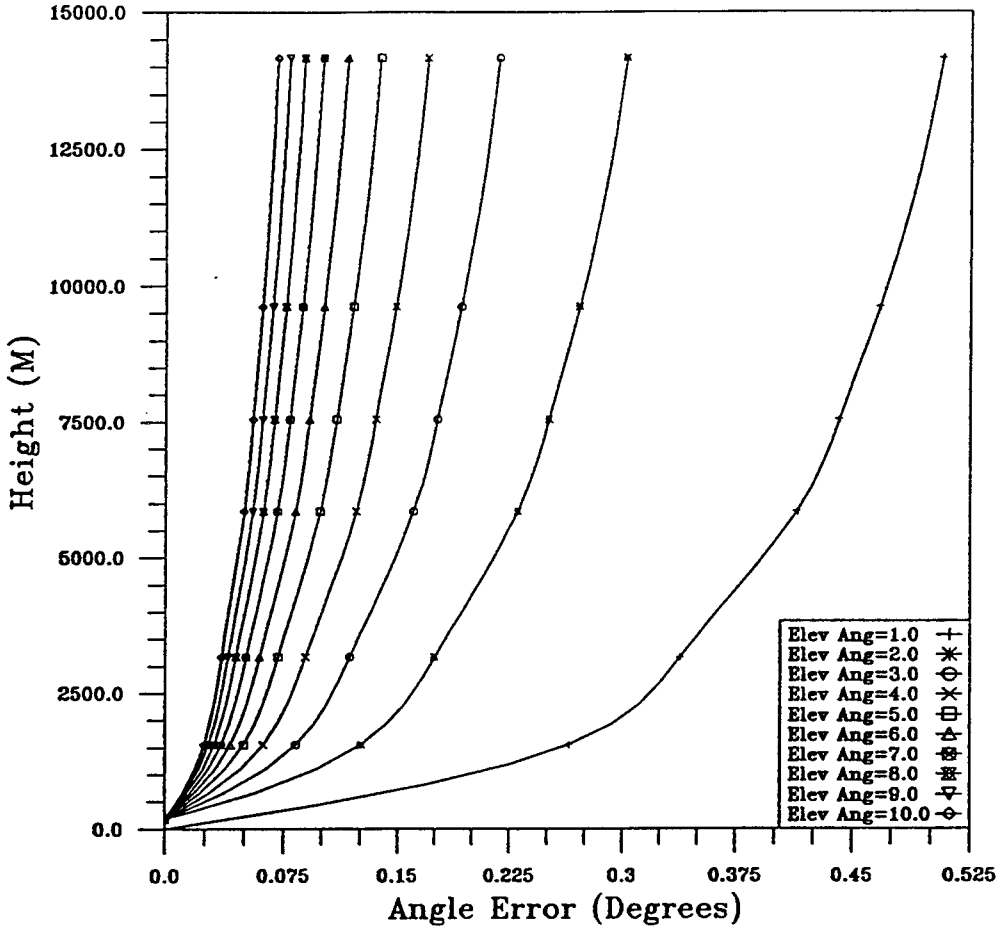

Height VS Angle Error
FNMOC
SQUARE=2274 NLAT=37.5-40 ELON=282.5-285
AUGUST DC REGION AM 1994

Figure V-4-7. Elevation Angle Error for Each One Degree Interval for FNMOC Database from One to Ten Degree Elevation Angles for Bay Area of Washington DC Vicinity for AM of August during 1994.

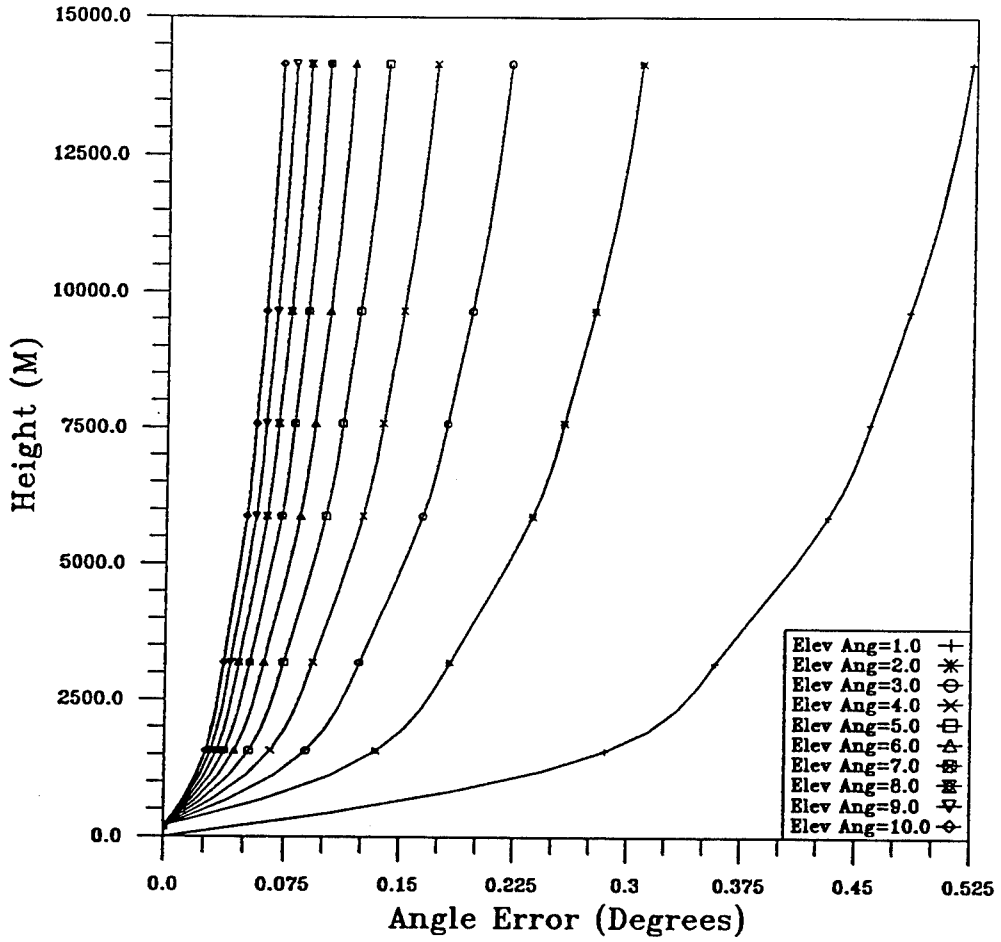

Height VS Angle Error
FNMOC
SQUARE=2274 NLAT=37.5-40 ELON=282.5-285
AUGUST DC REGION PM 1994

Figure V-4-8. Elevation Angle Error for Each One Degree Interval for FNMOC Database from One to Ten Degree Elevation Angles for Bay Area of Washington DC Vicinity for PM of August during 1994.

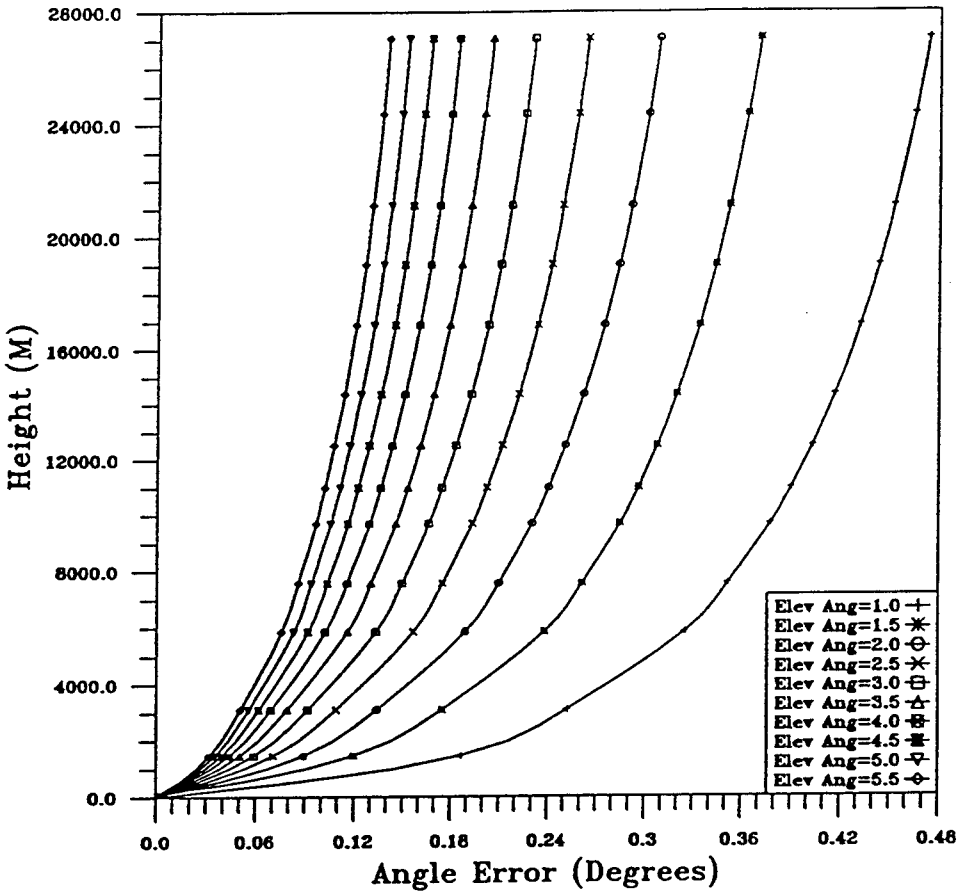

HEIGHT VS ANGLE ERROR
DC AUGUST
ECMWF Data
SQR=2273 NLAT=37.5-40.0 ELON=280.0-282.5
10-Year Average

Figure V-4-9. Elevation Angle Error for Each Half Degree Interval for ECMWF Database from One to 5.5 Degree Elevation Angles for In-land Area of Washington DC Vicinity During 1980-1991.

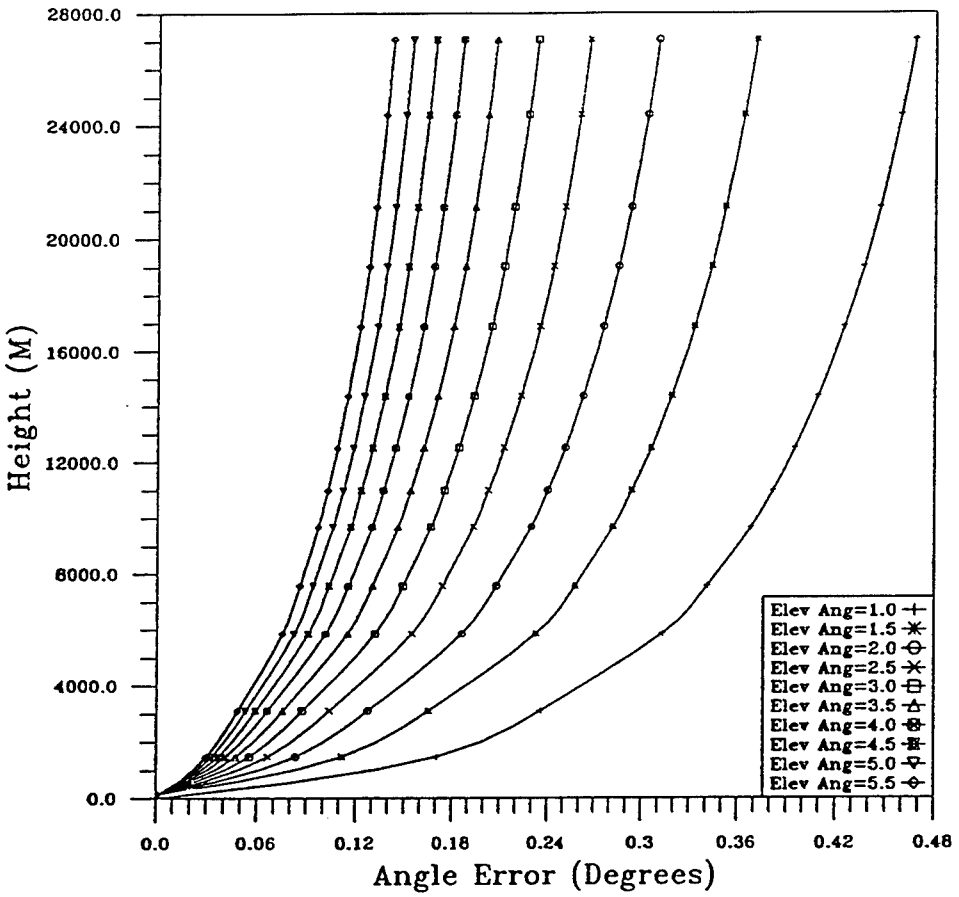

HEIGHT VS ANGLE ERROR
DC AUGUST
ECMWF Data
SQR=2274 NLAT=37.5-40.0 ELON=282.5-285.0
10-Year Average

Figure V-4-10. Elevation Angle Error for Each Half Degree Interval for ECMWF Database from One to 5.5 Degree Elevation Angles for Bay Area of Washington DC Vicinity During 1980-1991.

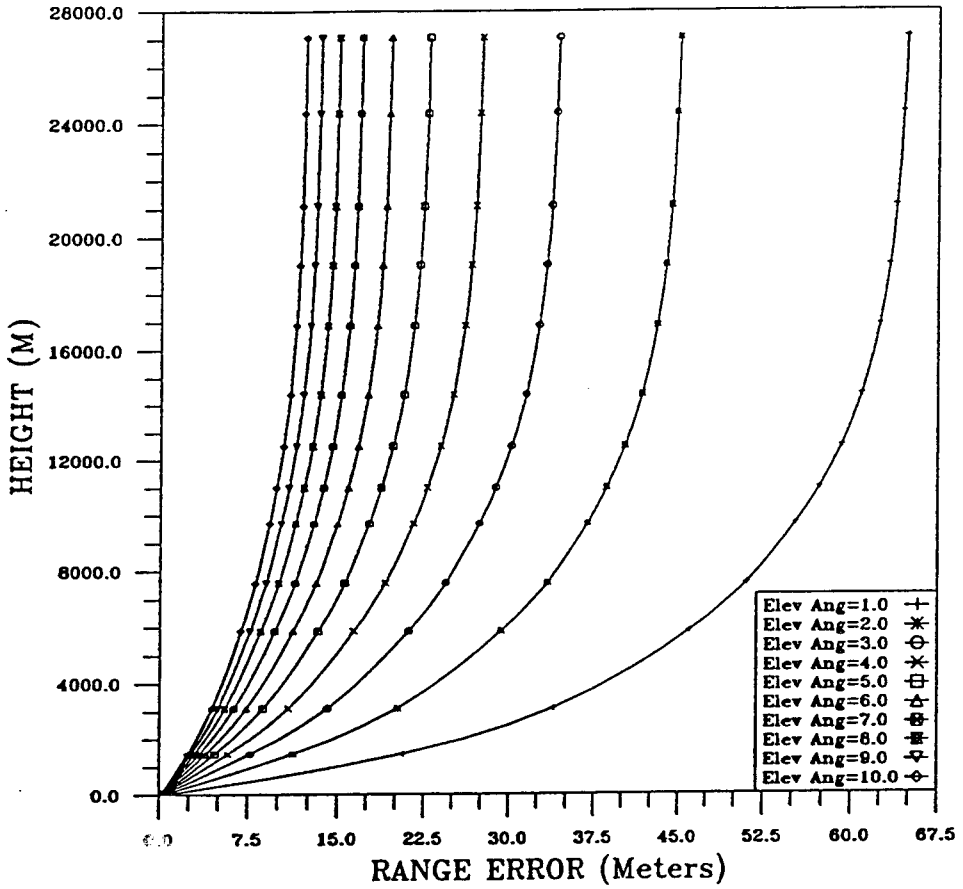

HEIGHT VS RANGE ERROR
DC AUGUST
ECMWF Data
SQR=2273 NLAT=37.5-40.0 ELON=280.0-282.5
10-Year Average

Figure V-5-1. Range Error for Each One Degree Interval for ECMWF Database from One to Ten Degree Elevation Angles for In-land Area of Washington DC Vicinity During 1980-1991.

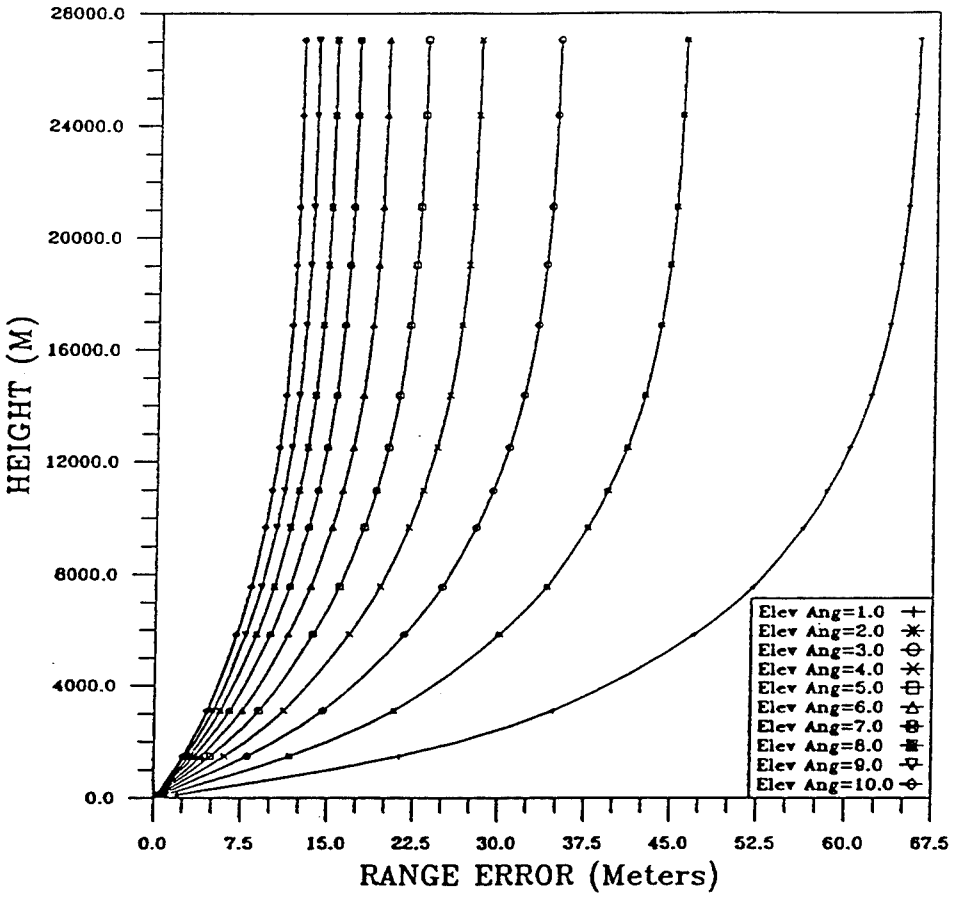

HEIGHT VS RANGE ERROR
DC AUGUST
ECMWF Data
SQR=2274 NLAT=37.5-40.0 ELON=282.5-285.0
10-Year Average

Figure V-5-2. Range Error for Each One Degree Interval for ECMWF Database from One to Ten Degree Elevation Angles for Bay Area of Washington DC Vicinity During 1980-1991.

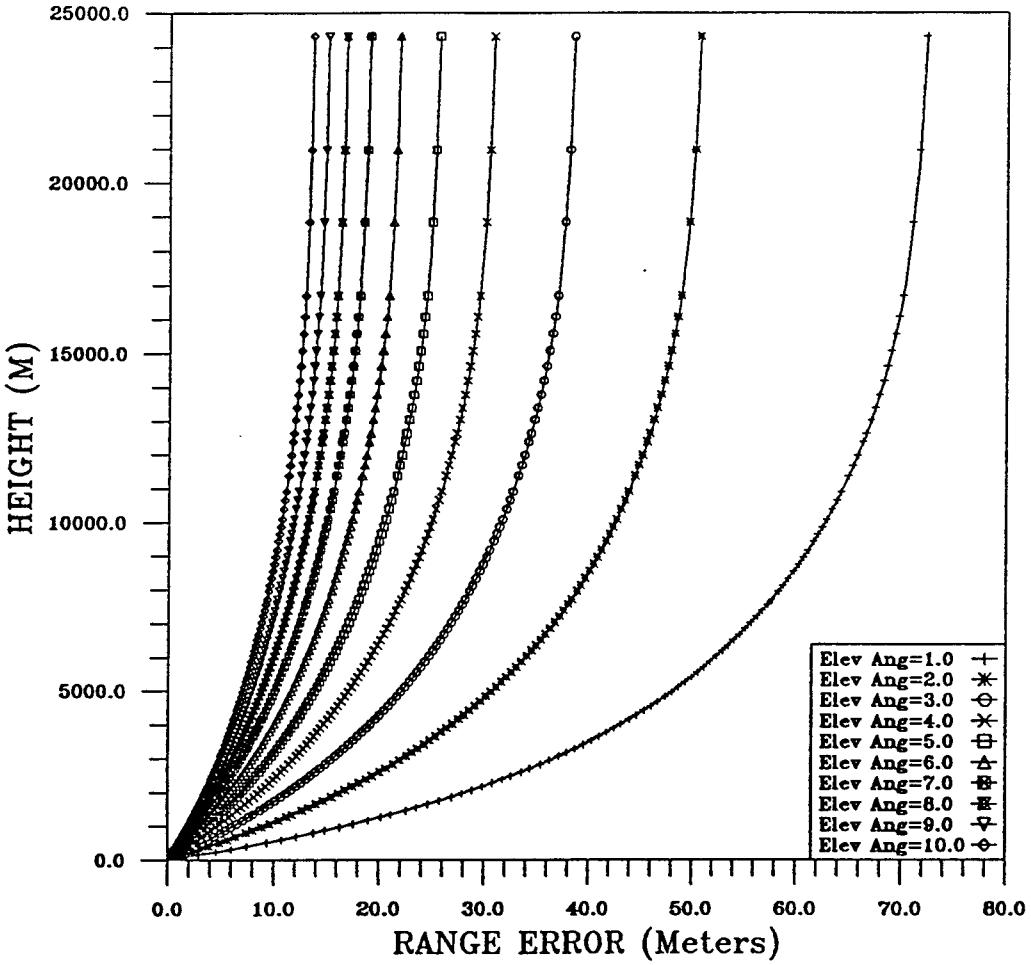

Figure V-5-3. Range Error for Each One Degree Interval for NCDC Database from One to Ten Degree Elevation Angles for AM of August for Bay Area of Washington DC Vicinity During 1980-1993.

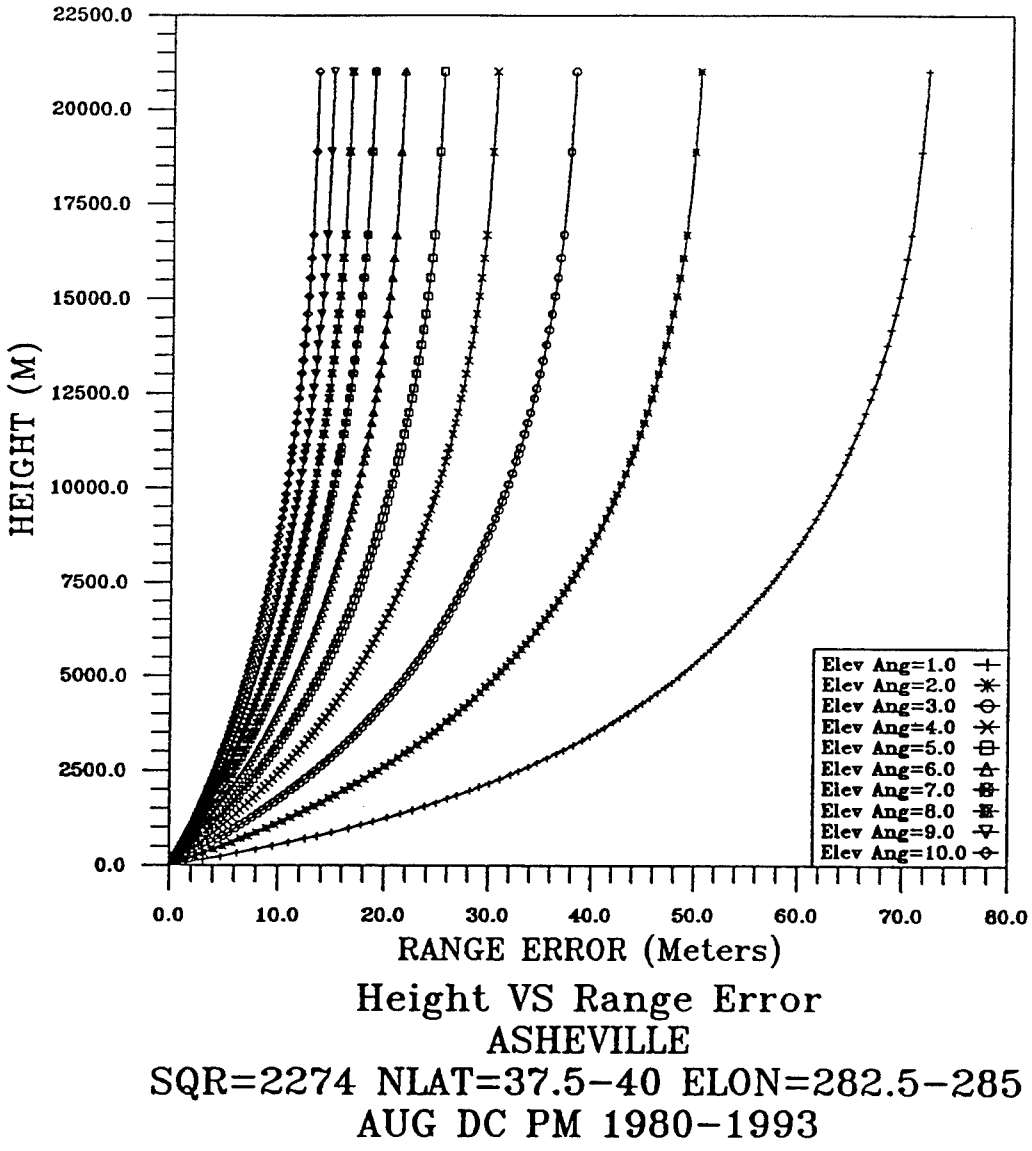

Figure V-5-4. Range Error for Each One Degree Interval for NCDC Database from One to Ten Degree Elevation Angles for PM of August for Bay Area of Washington DC Vicinity During 1980-1993.

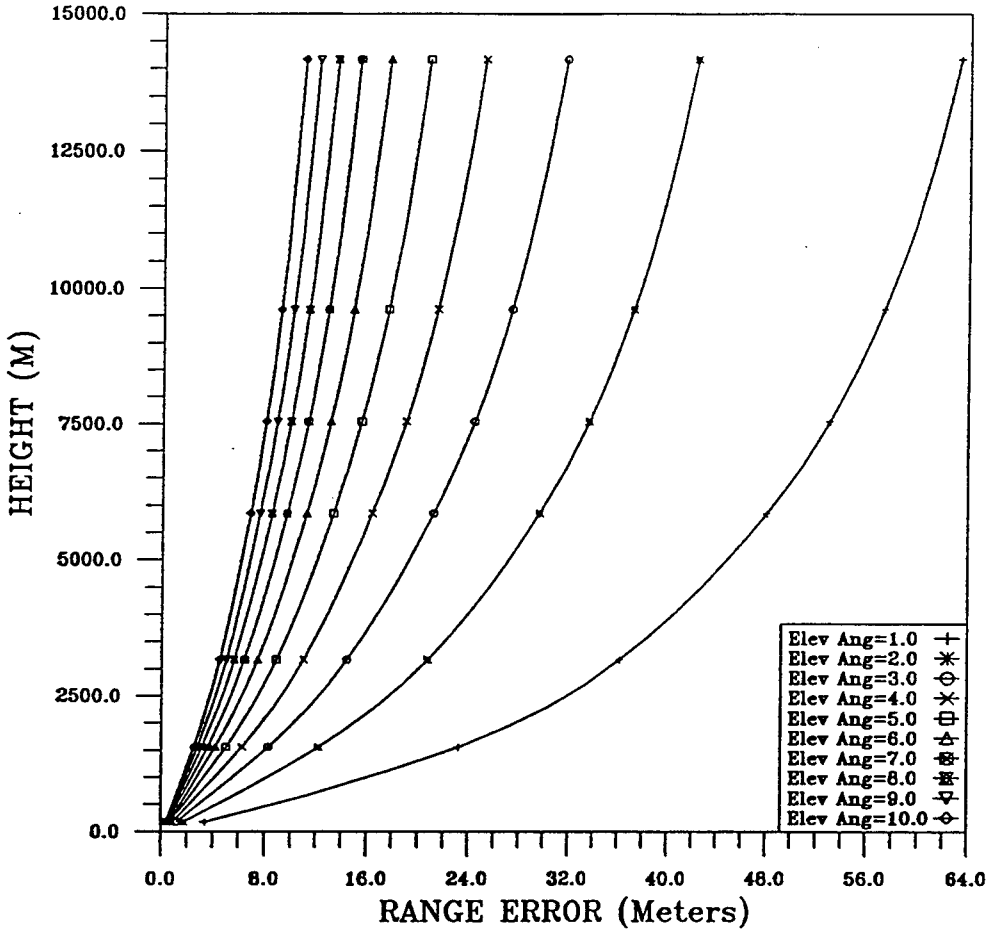

Height VS Range Error
FNMOC
SQUARE=2273 NLAT=37.5-40 ELON=280-282.5
AUGUST DC LAND REGION AM 1994

Figure V-5-5. Range Error for Each One Degree Interval for FNMOC Database from One to Ten Degree Elevation Angles for AM of August for In-land Area of Washington DC Vicinity During 1994.

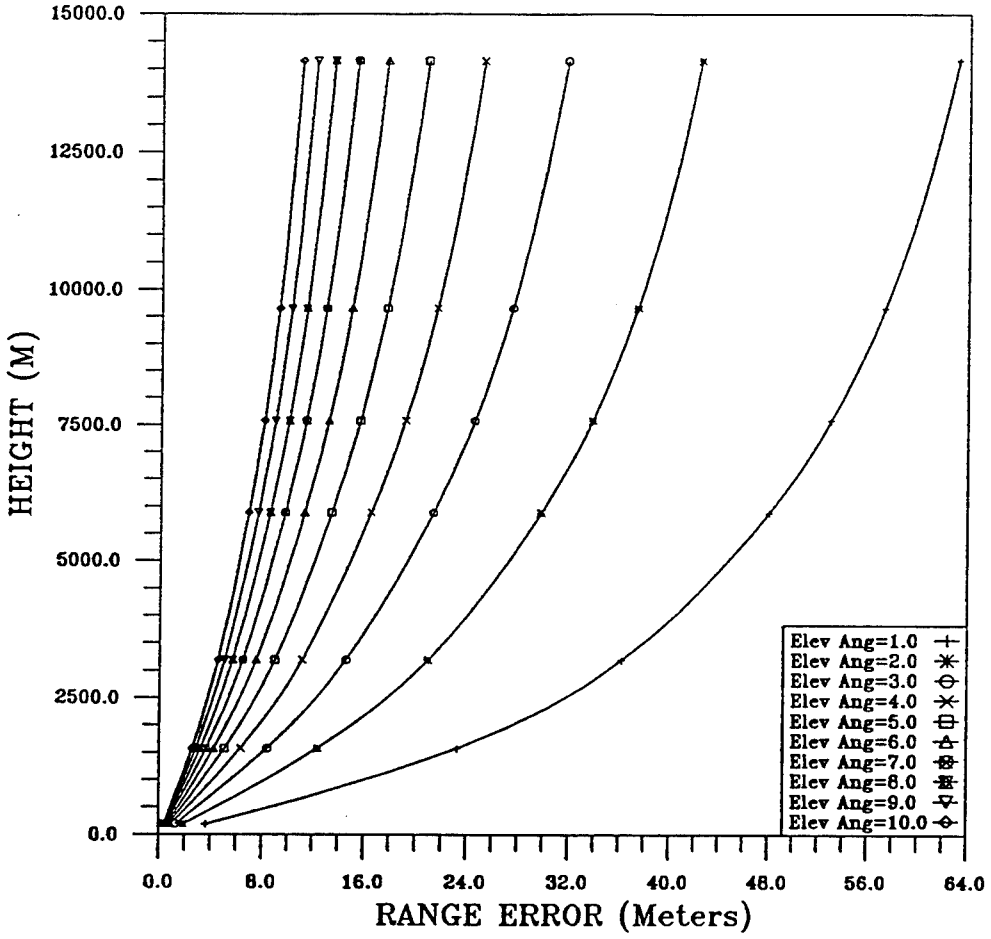

Height VS Range Error
FNMOC
SQUARE=2273 NLAT=37.5-40 ELON=280-282.5
AUGUST DC LAND REGION PM 1994

Figure V-5-6. Range Error for Each One Degree Interval for FNMOC Database from One to Ten Degree Elevation Angles for PM of August for In-land Area of Washington DC Vicinity During 1994.

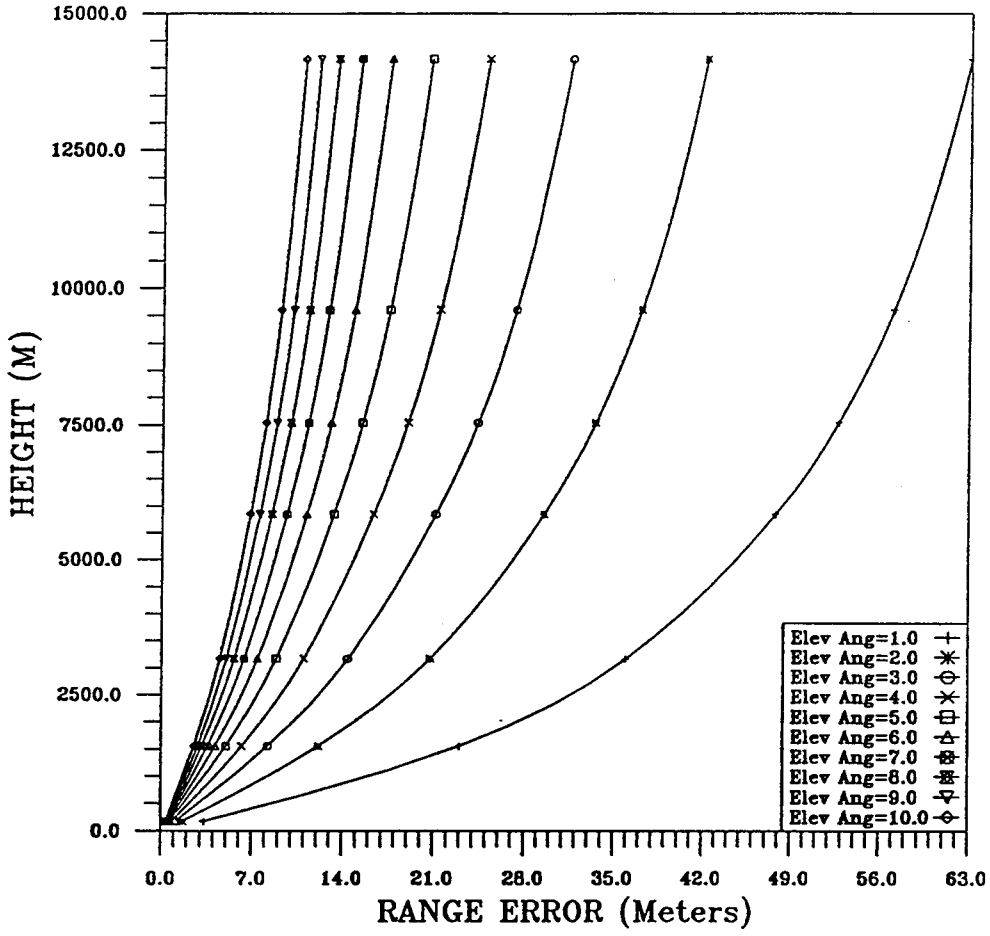

Height VS Range Error
FNMOC
SQUARE=2274 NLAT=37.5-40 ELON=282.5-285
AUGUST DC LAND REGION AM 1994

Figure V-5-7. Range Error for Each One Degree Interval for FNMOC Database from One to Ten Degree Elevation Angles for AM of August for Bay Area of Washington DC Vicinity During 1994.

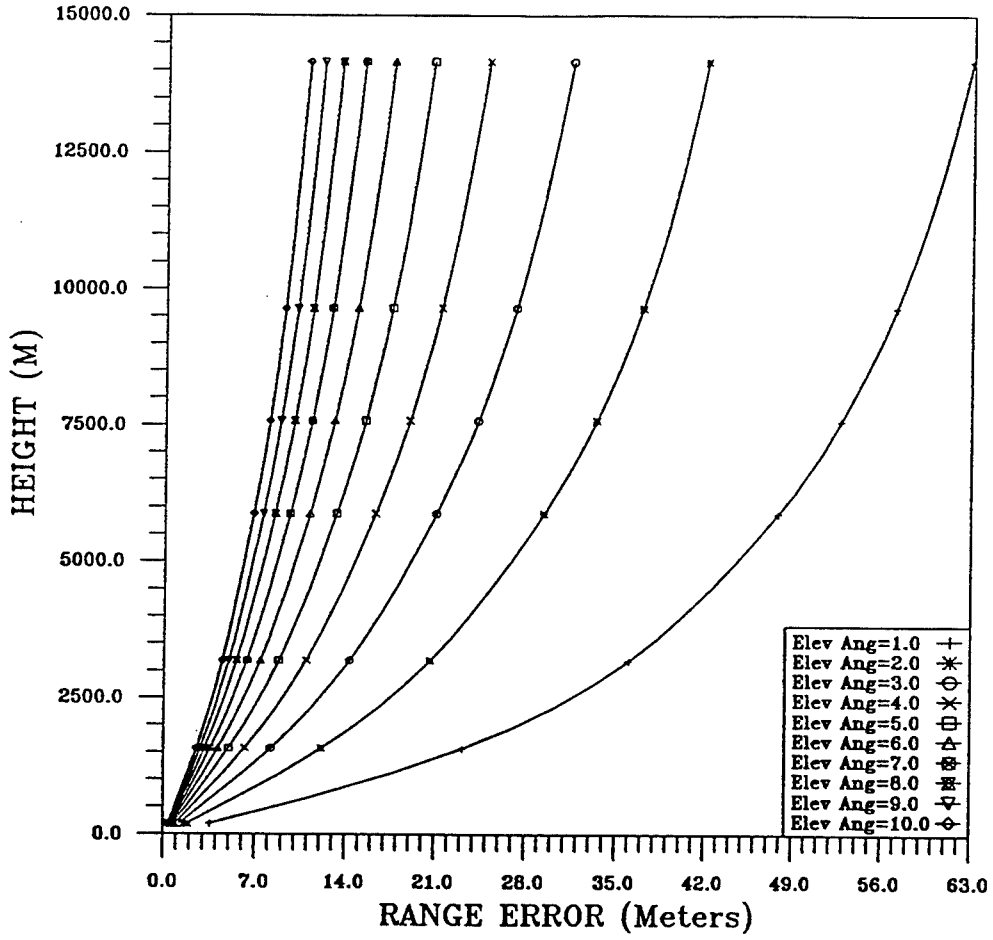

Height VS Range Error
FNMOC
SQUARE=2274 NLAT=37.5–40 ELON=282.5–285
AUGUST DC LAND REGION PM 1994

Figure V-5-8. Range Error for Each One Degree Interval for FNMOC Database from One to Ten Degree Elevation Angles for PM of August for Bay Area of Washington DC Vicinity During 1994.

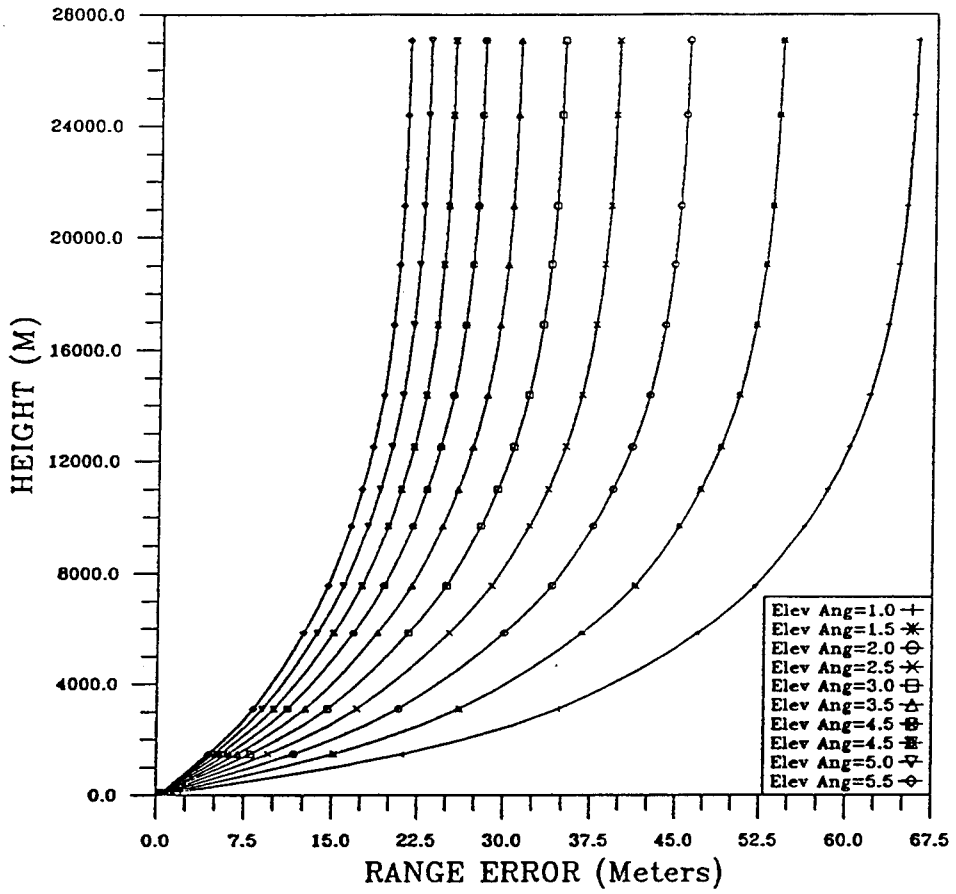

HEIGHT VS RANGE ERROR
DC AUGUST
ECMWF Data
SQR=2274 NLAT=37.5-40.0 ELON=282.5-285.0
10-Year Average

Figure V-5-9. Range Error for Each Half Degree Interval for ECMWF Database from One to 5.5 Degree Elevation Angles for Bay Area of Washington DC Vicinity During August 1980-1991.

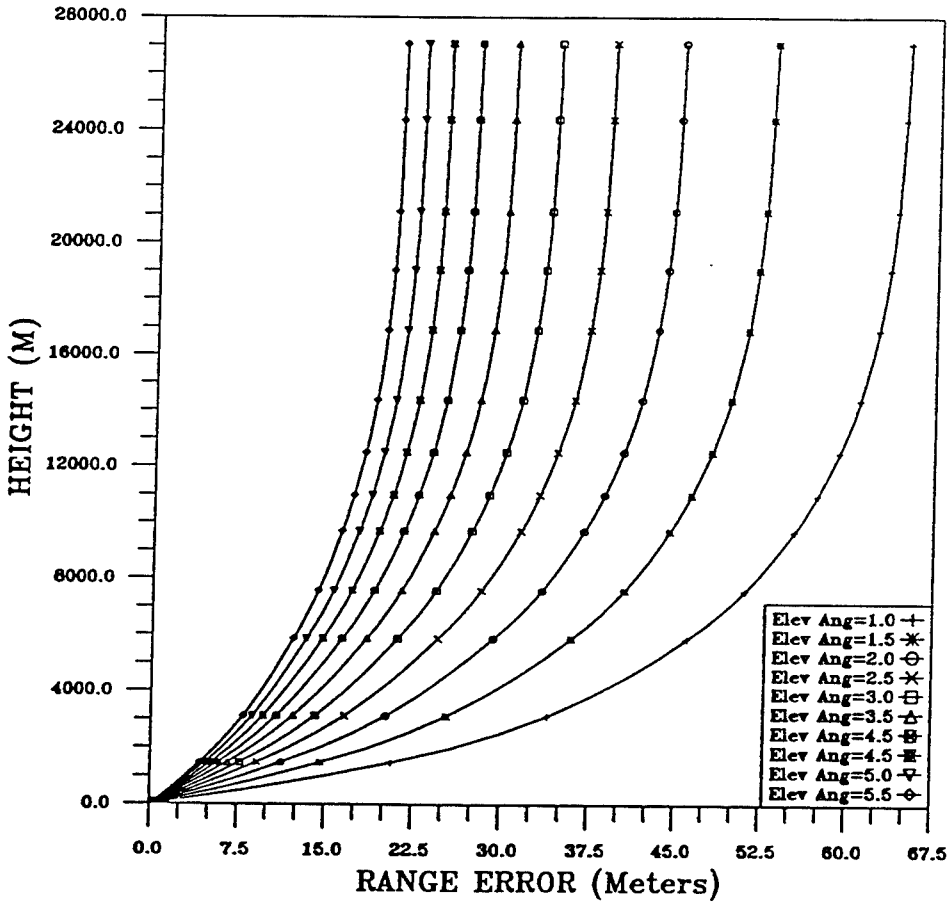

HEIGHT VS RANGE ERROR
DC AUGUST
ECMWF Data
SQR=2273 NLAT=37.5-40.0 ELON=280.0-282.5
10-Year Average

Figure V-5-10. Range Error for Each Half Degree Interval for ECMWF Database from One to 5.5 Degree Elevation Angles for In-land Area of Washington DC Vicinity During August 1980-1991.

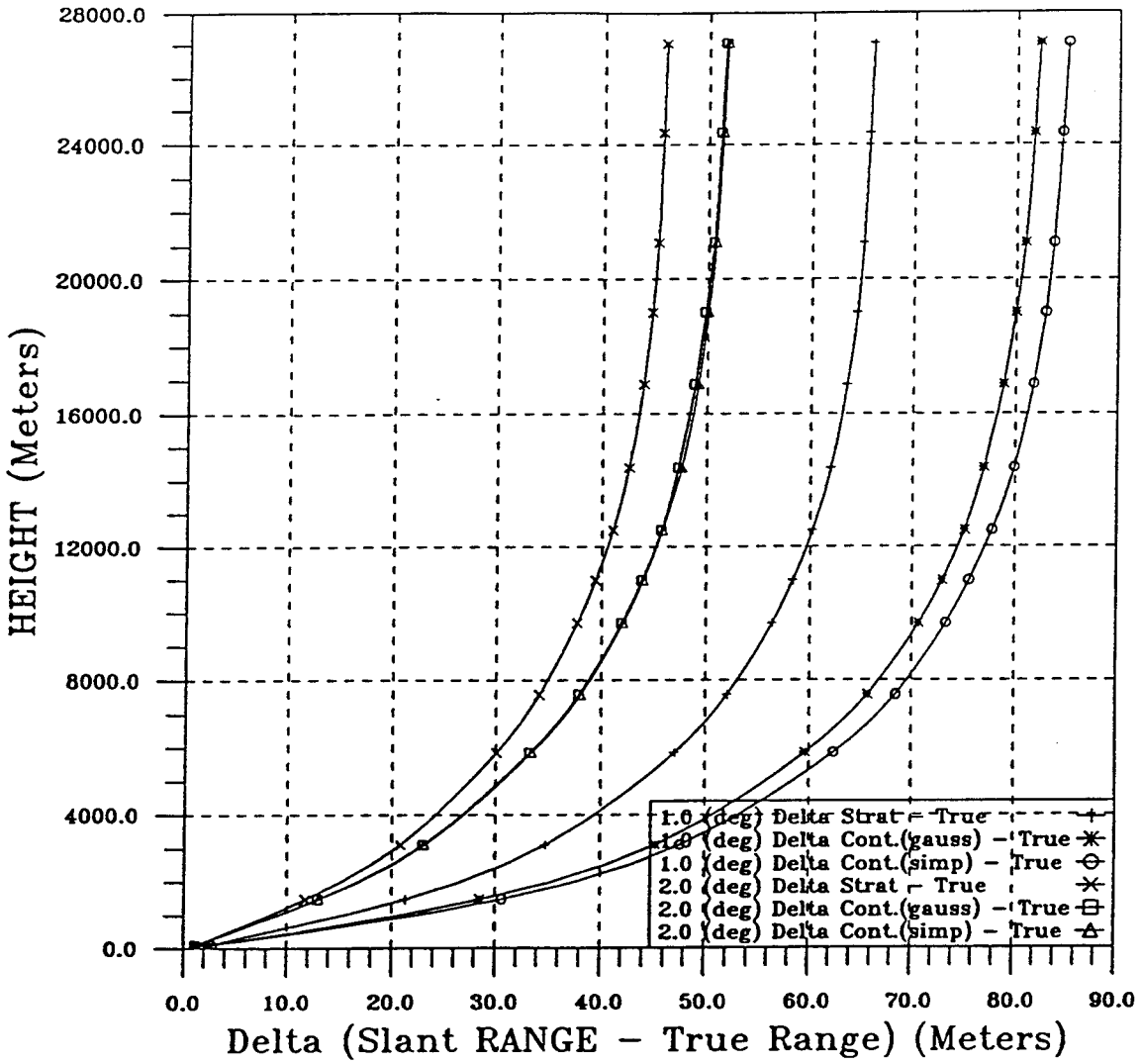

HEIGHT VS DELTA (SLANT RANGE-TRUE RANGE)
1.0 and 2.0 Degree(s)
DC AUGUST
ECMWF Data
SQR=2274 NLAT=37.5-40.0 ELON=282.5-285.0
10-Year Average

Figure V-6-1. Slant Range Error from ECMWF Database for One and two Degree Elevation Angles with Three Different Numerical Approximation Methods for Bay Area of Washington DC Vicinity During August 1980-1991.

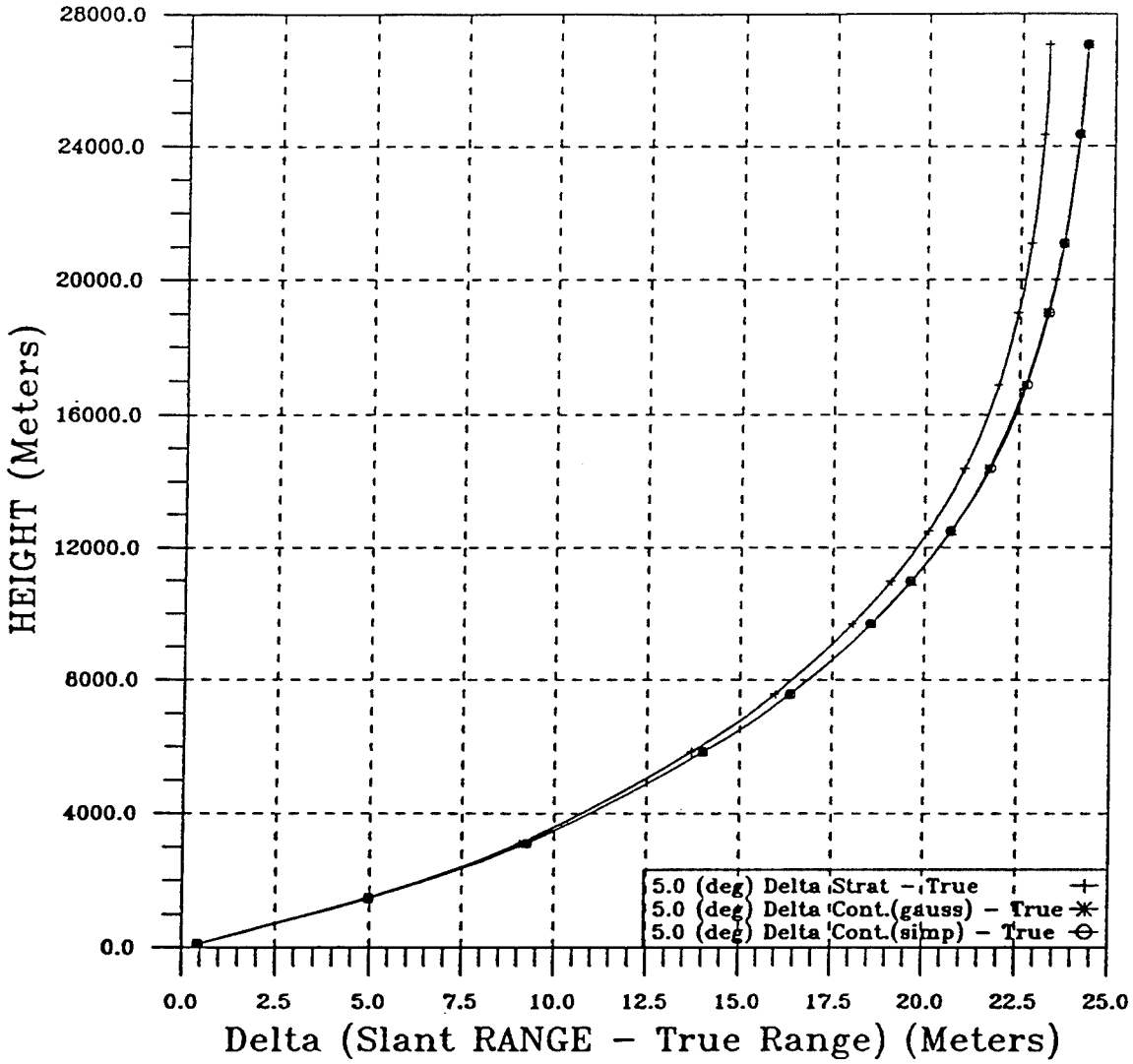

HEIGHT VS DELTA (SLANT RANGE–TRUE RANGE)
5.0 Degree(s)
DC AUGUST
ECMWF Data
SQR=2274 NLAT=37.5–40.0 ELON=282.5–285.0
10–Year Average

Figure V-6-2. Slant Range Error from ECMWF Database for Five Degree Elevation Angles with Three Different Numerical Approximation Methods for Bay Area of Washington DC Vicinity During August 1980-1991.

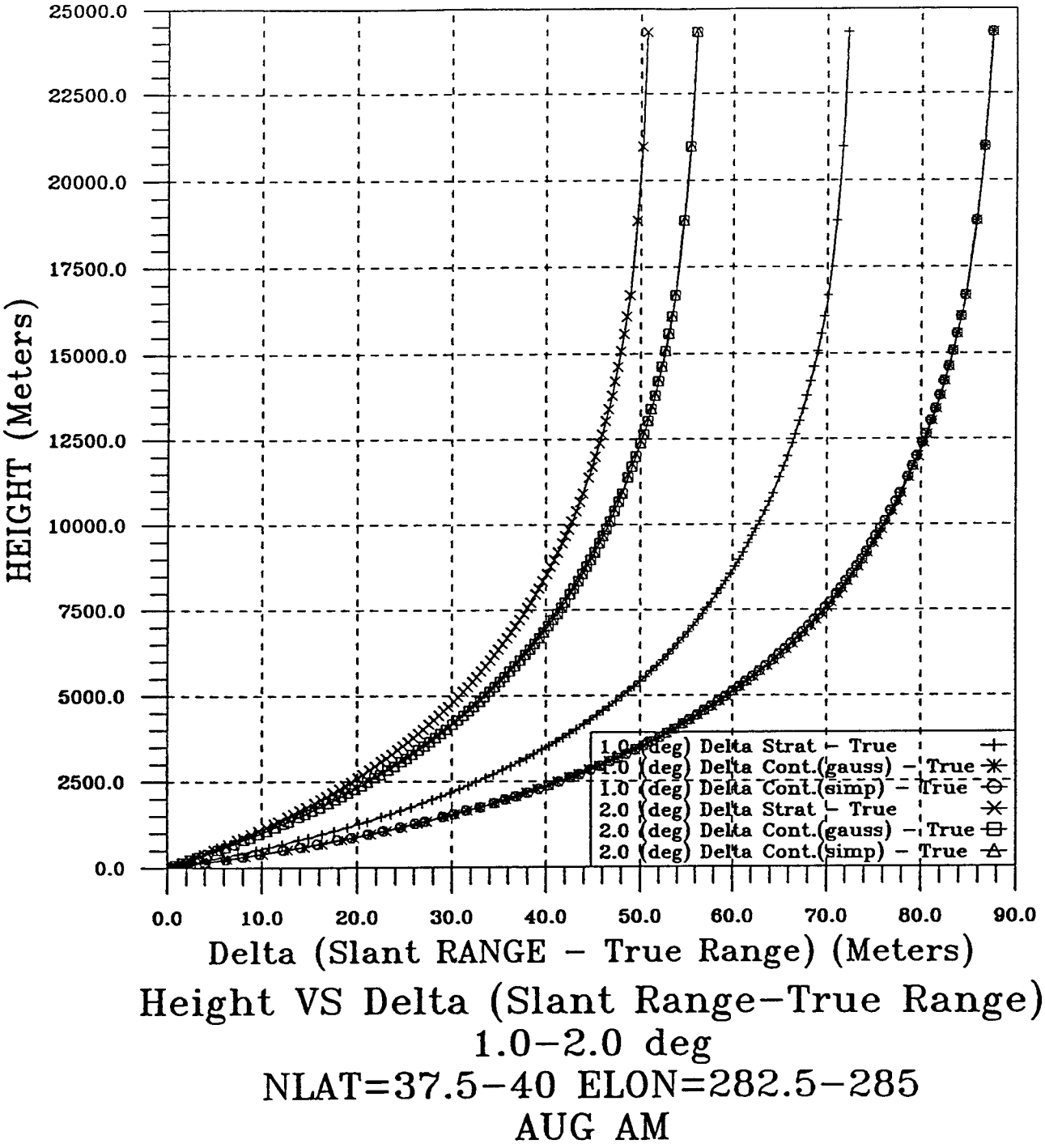

Figure V-6-3. Slant Range Error from NCDC Database for one and Two Degree Elevation Angles with Three Different Numerical Approximation Methods for Bay Area of Washington DC Vicinity During August 1980-1993.

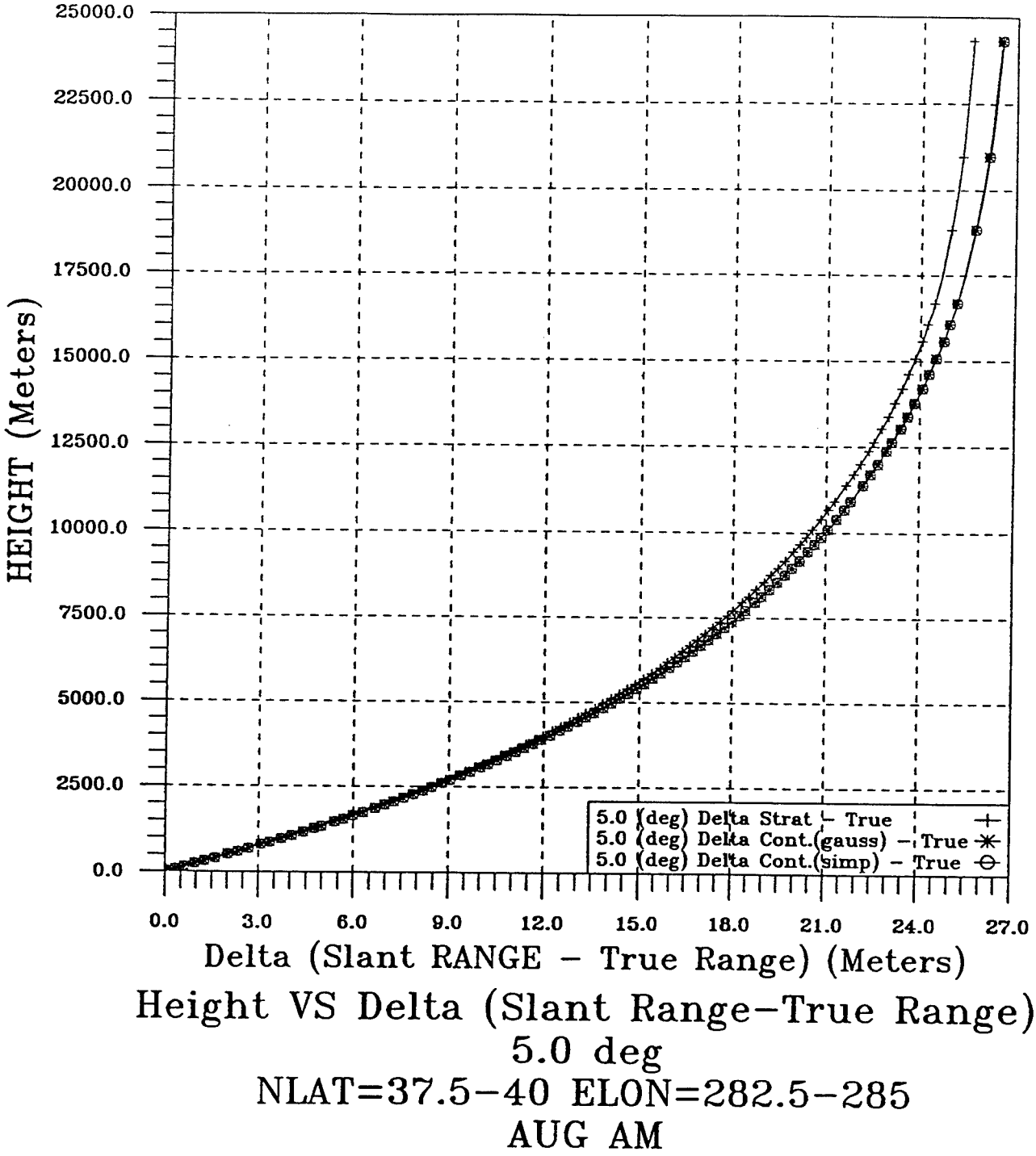

Figure V-6-4. Slant Range Error from NCDC Database for Five Degree Elevation Angles with Three Different Numerical Approximation Methods for Bay Area of Washington DC Vicinity During August 1980-1993.

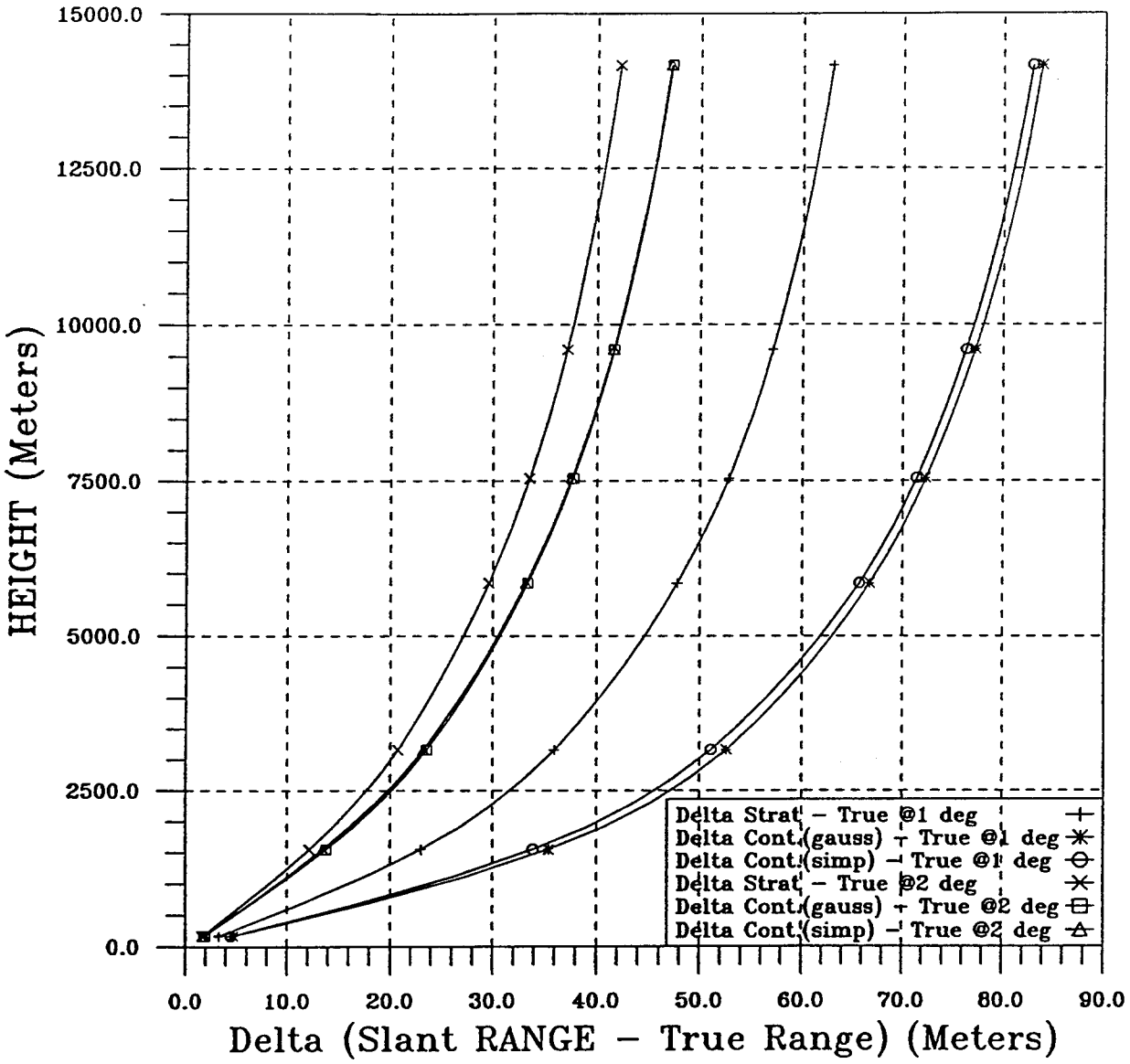

Height VS Delta (Slant Range-True Range)
1 degree and 2 degrees
SQUARE = 2274 NLAT=37.5-40 ELON=282.5-285
AUGUST DC AM 1994

Figure V-6-5. Slant Range Error from FNMOC Database for One and Two Degree Elevation Angles with Three Different Numerical Approximation Methods for Bay Area of Washington DC Vicinity During AM of August 1994.

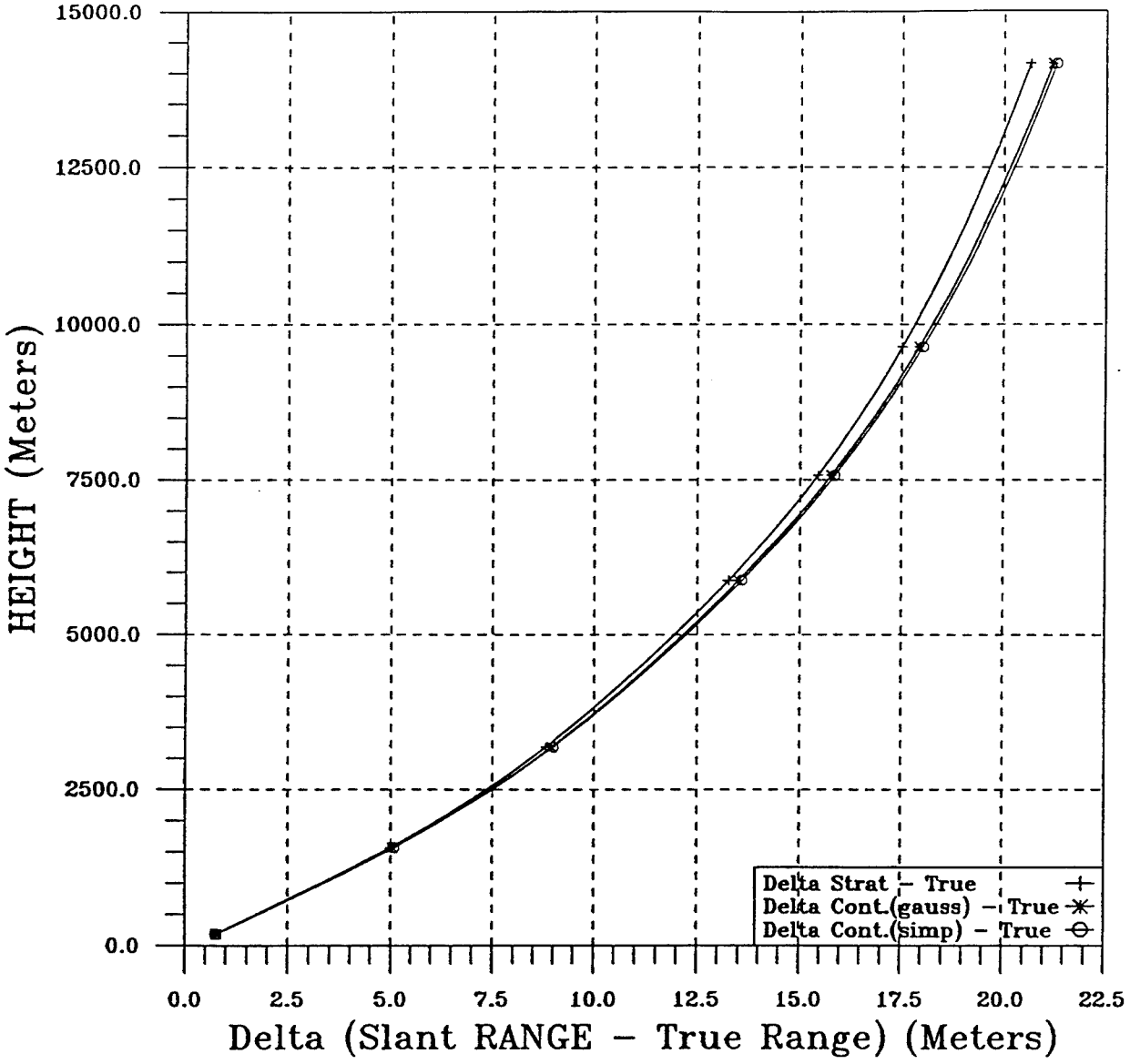

Height VS Delta (Slant Range–True Range)
5 degrees
SQUARE = 2274 NLAT=37.5–40 ELON=282.5–285
AUGUST DC PM 1994

Figure V-6-6. Slant Range Error from FNMOC Database for Five Degree Elevation Angle with Three Different Numerical Approximation Methods for Bay Area of Washington DC Vicinity During PM of August 1994.

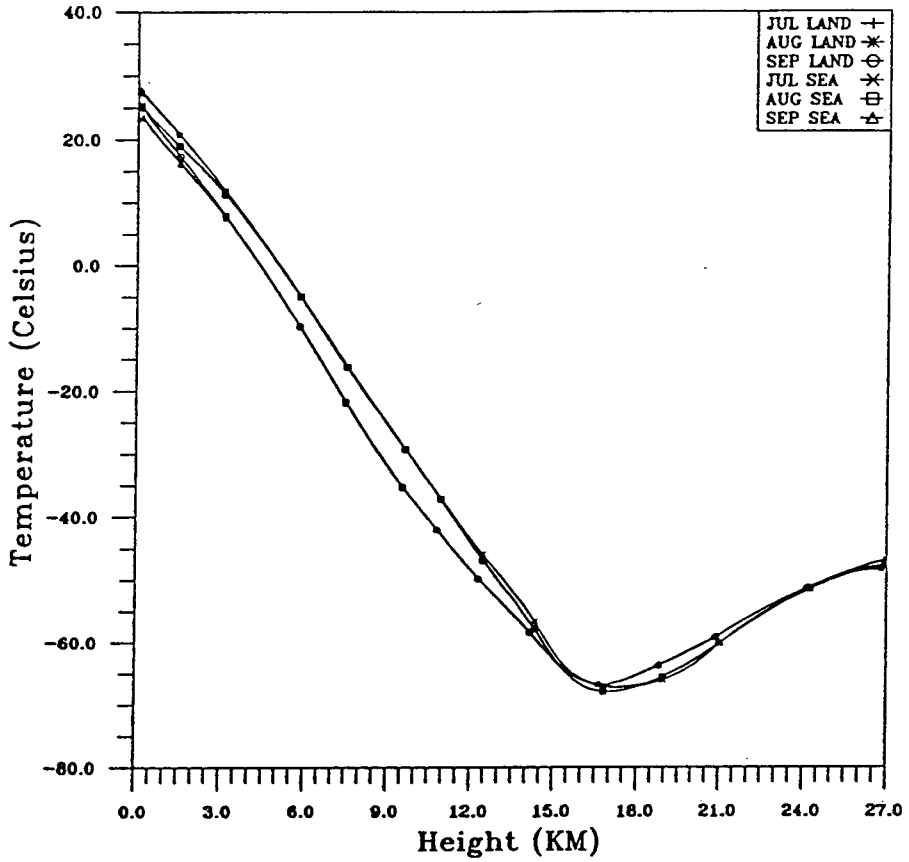

TEMPERATURE (C) VS HEIGHT (KM)
DC JULY, AUGUST, SEPTEMBER
ECMWF Data
LAND AREA NLAT=35.0-42.5 ELON=277.5-285.0
SEA AREA NLAT=35.0-42.5 ELON=280.0-287.5
10-Year Average

Figure V-7-1. Lapse Rate for Washington DC Vicinity for Average Temperature Variations of July, August, and September for both Land-based and Sea-based Area with Grid #s of 2416-2419, 2272-2275, 2128-2131 from Table 1 during July, August, and September 1980-1991 from ECMWF Database.

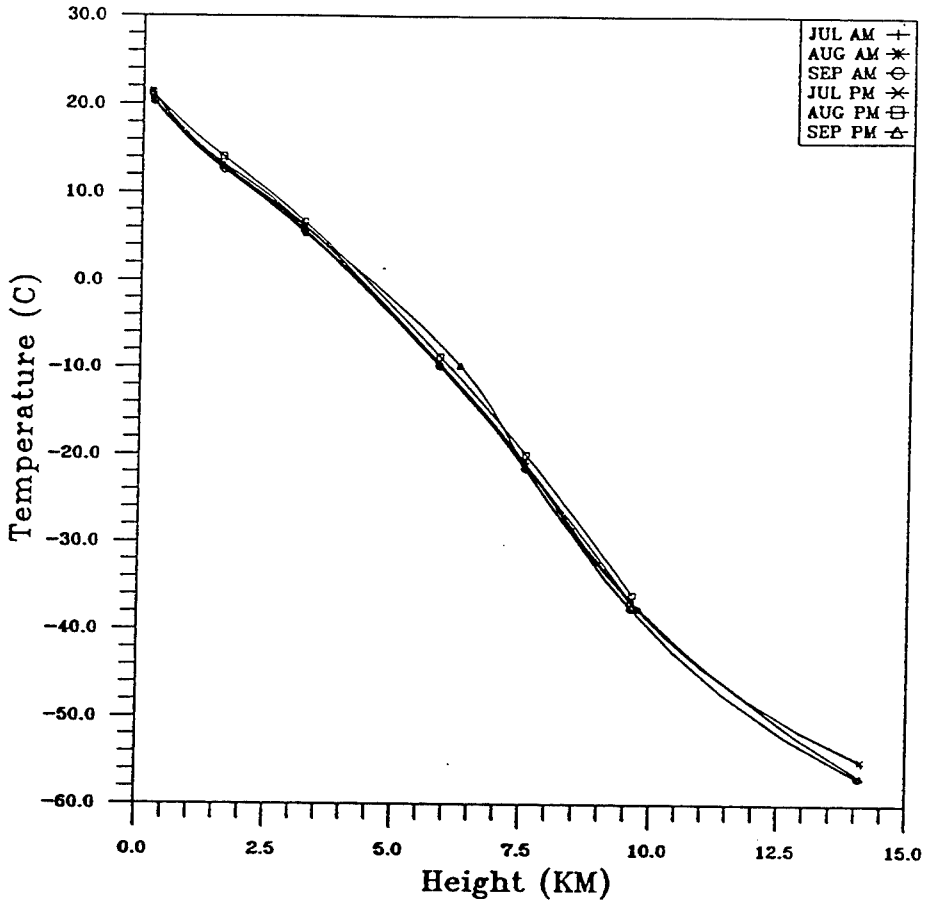

TEMPERATURE VS HEIGHT
DC LAND-BASED REGION
FNMOC
NLAT=35-42.5 ELON=277.5-285
JULY, AUGUST, SEPTEMBER 1994 (AM & PM)

Figure V-7-2. Lapse Rate for Washington DC Vicinity for Average Temperature Variations for AM & PM of July, August, and September for Land-based Area with Grid #s of 2416-2418, 2272-2274, 2128-2130 from Table 1 during 1994 from FNMOC Database.

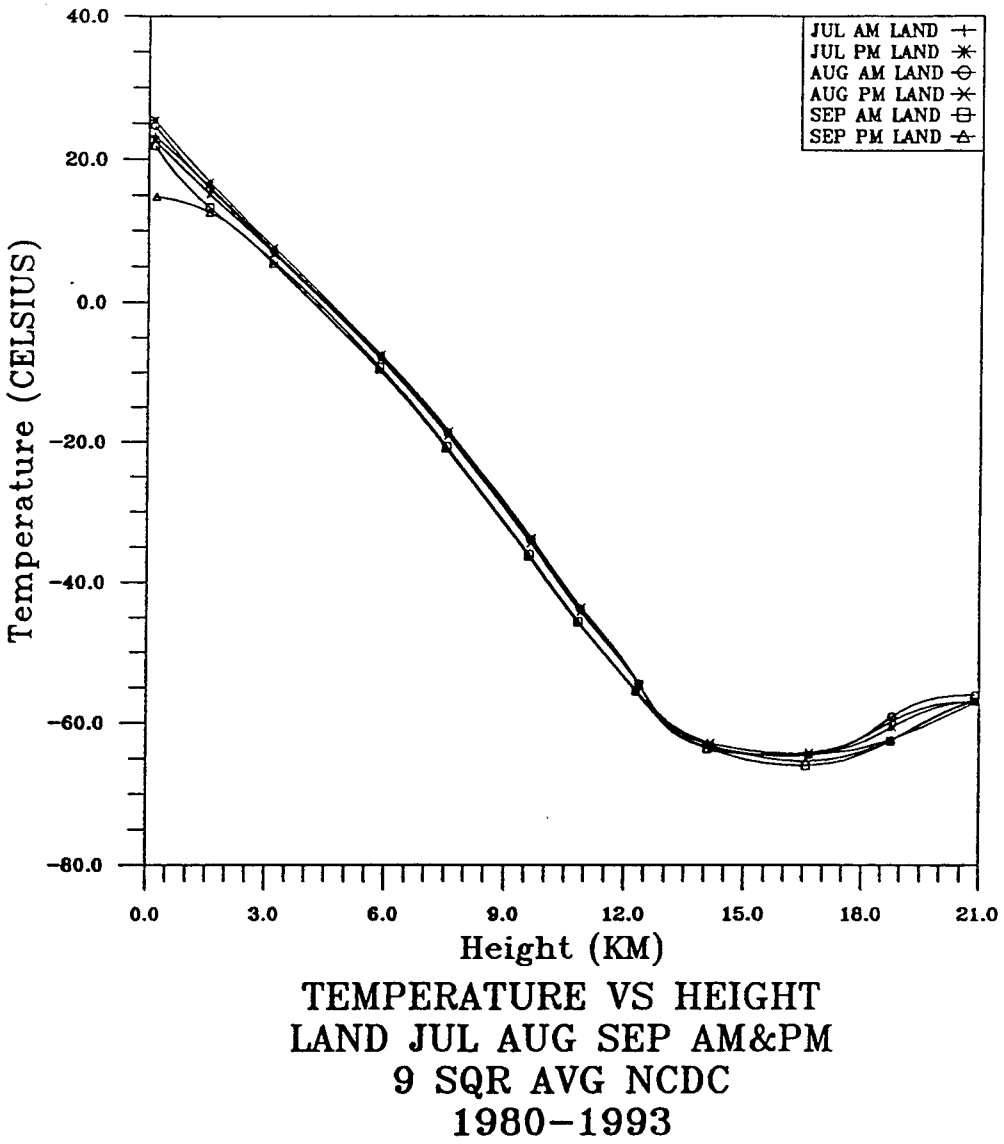

Figure V-7-3. Lapse Rate for Washington DC Vicinity for Average Temperature Variations of July, August, and September for Land-based Area with Grid #s of 2416-2418, 2272-2274, 2128-2130 from Table 1 during AM & PM of 1980-1993 from NCDC Database.

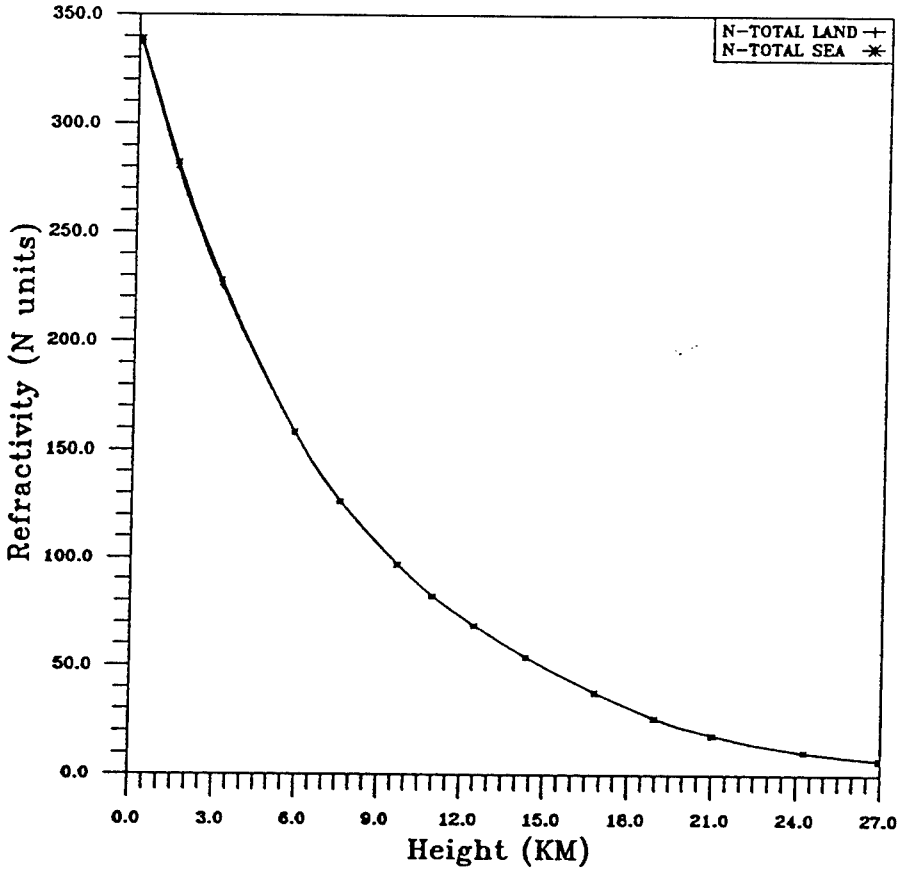

REFRACTIVITY (N) VS HEIGHT (KM)
DC AUGUST
ECMWF Data
LAND AREA NLAT=35.0-42.5 ELON=277.5-285.0
SEA AREA NLAT=35.0-42.5 ELON=280.0-287.5
10-Year Average

Figure V-7-4. Average Refractivity Variations in Washington DC Vicinity for both Land-based and Sea-based with Grid#s 2416-2419, 2272-2275, 2128-2131 in Table 1 for August 1980-1991 from ECMWF Database.

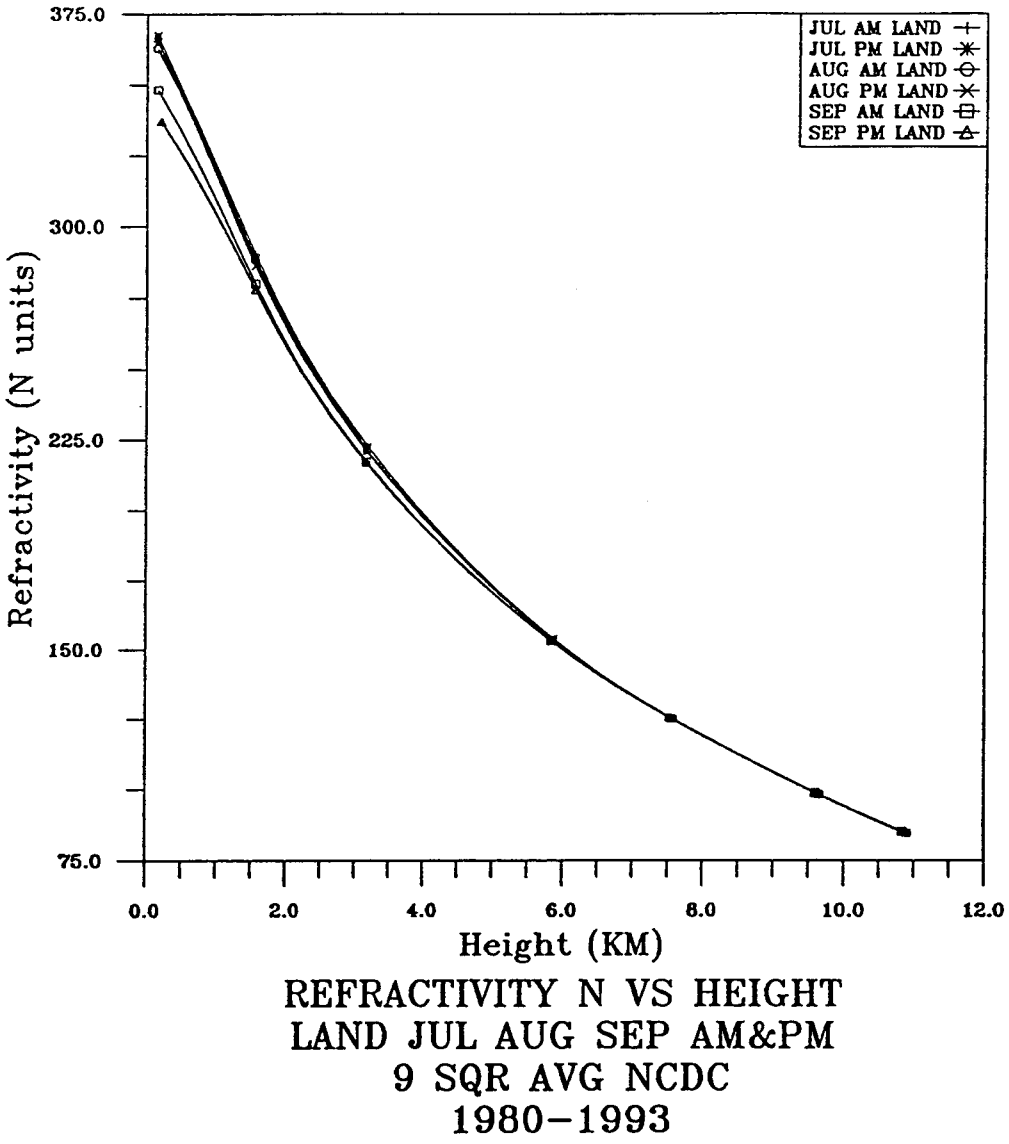

Figure V-7-5. Average Refractivity Variations in Washington DC Vicinity for Land-based with Grid#s 2416-2418, 2272-2274, 2128-2130 in Table 1 for AM &PM of July, August, and September 1980-1993 from NCDC Database.

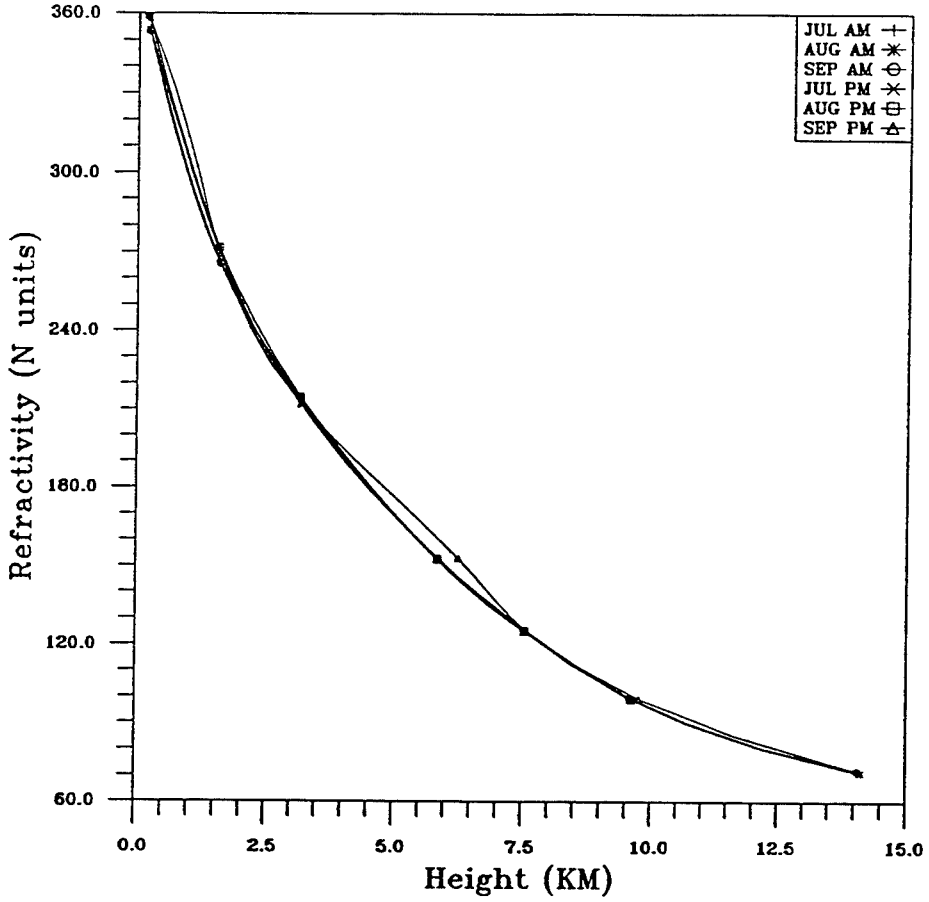

REFRACTIVITY N VS HEIGHT
DC LAND-BASED REGION
FNMOC
NLAT=35-42.5 ELON=277.5-285
JULY, AUGUST, SEPTEMBER 1994 (AM & PM)

Figure V-7-6. Average Refractivity Variations in Washington DC Vicinity for Land-based with Grid#s 2416-2418, 2272-2274, 2128-2130 in Table 1 for AM &PM of July, August, and September 1994 from FNMOC Database.

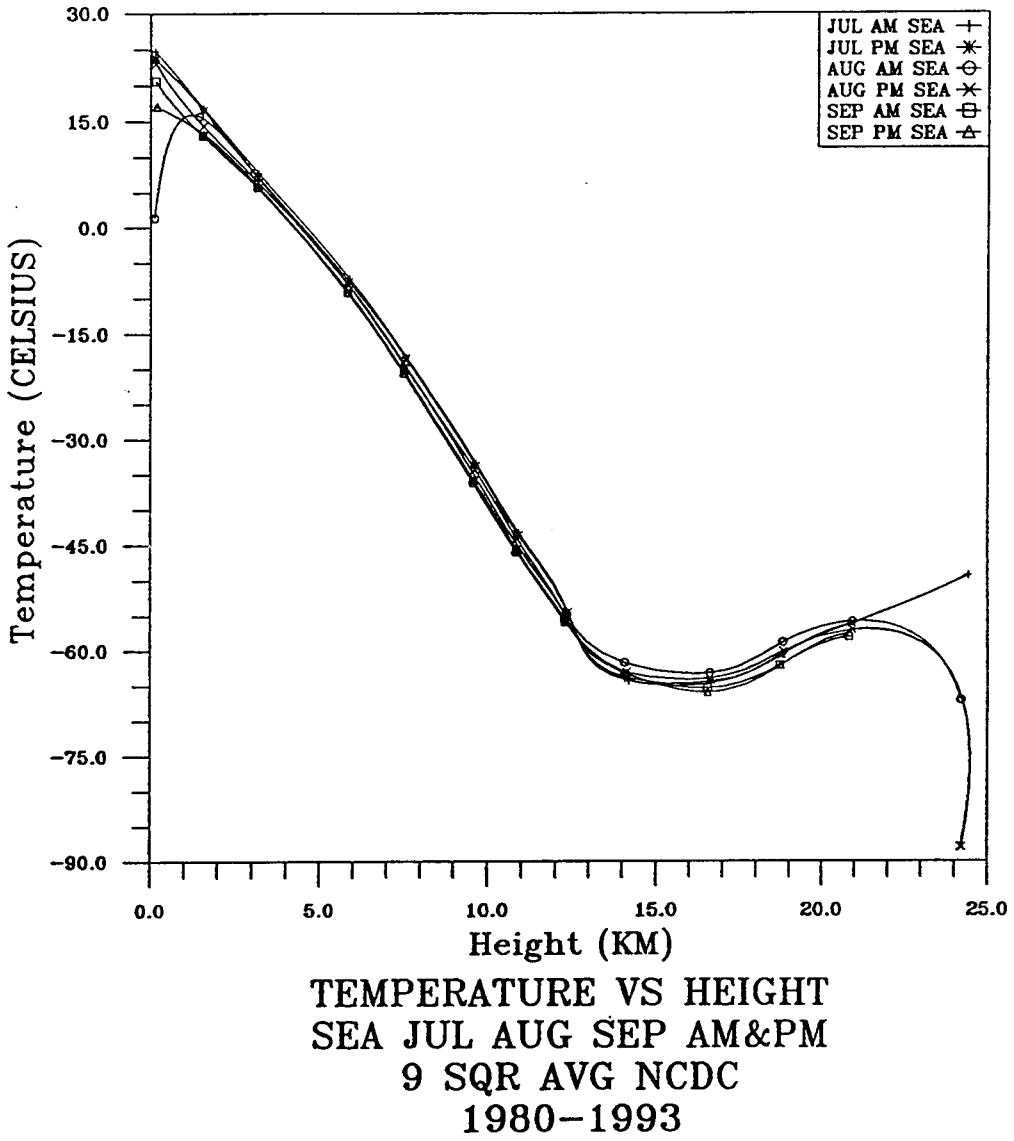

Figure V-8-1. Lapse Rate in Washington DC Vicinity for Sea-based with Grid#s 2417-2419, 2273-2275, 2129-2131 in Table 1 for AM &PM of July, August, and September 1980-1993 from NCDC Database.

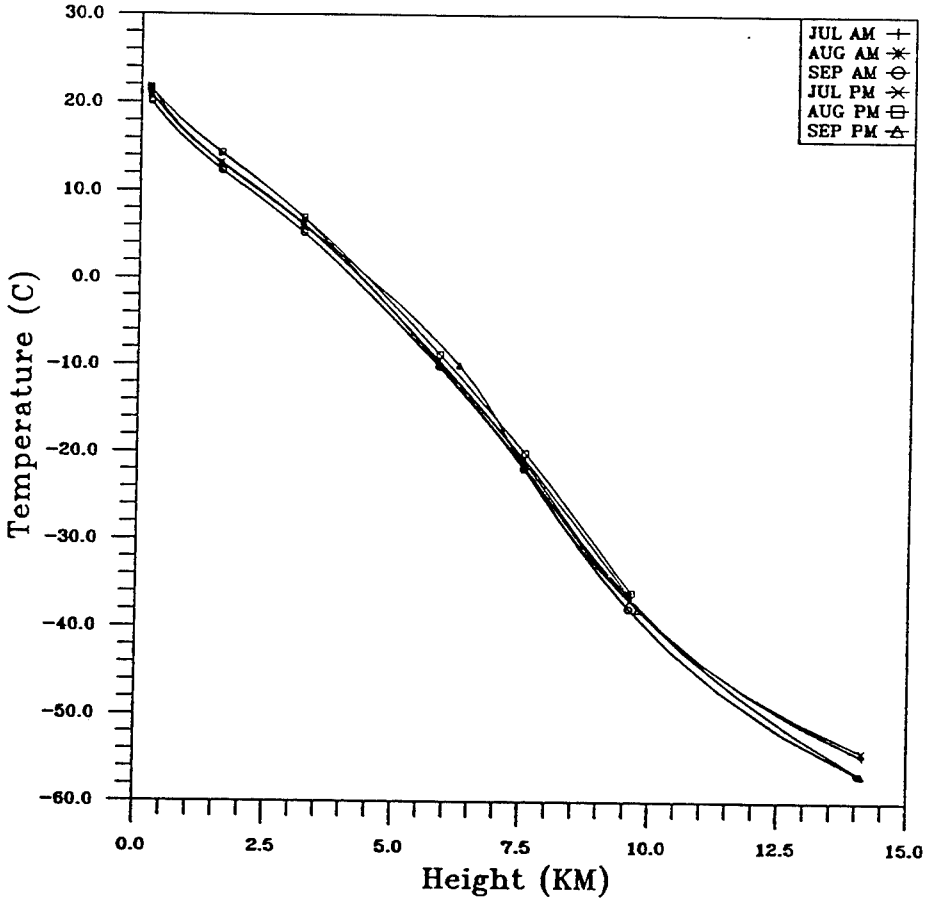

TEMPERATURE VS HEIGHT
DC COASTAL–BASED REGION
FNMOC
NLAT=35–42.5 ELON=280–287.5
JULY, AUGUST, SEPTEMBER 1994 (AM & PM)

Figure V-8-2. Lapse Rate in Washington DC Vicinity for Sea-based with Grid#s 2417-2419, 2273-2275, 2129-2131 in Table 1 for AM &PM of July, August, and September 1994 from FNMOC Database.

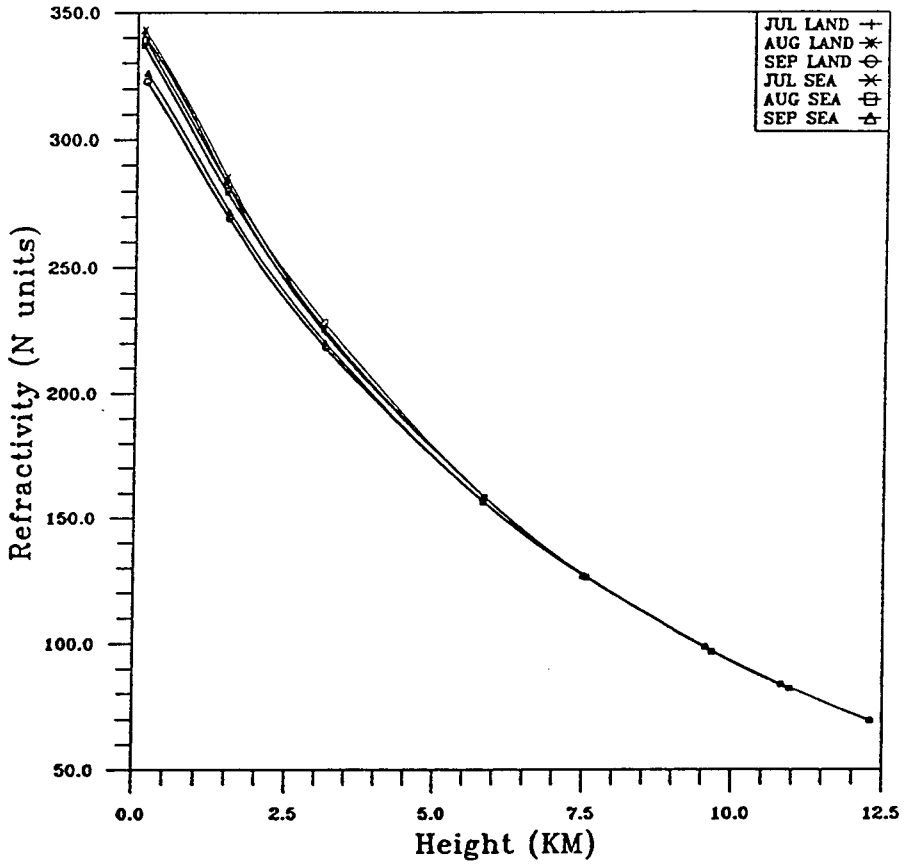

REFRACTIVITY (N) VS HEIGHT (KM)
DC JULY, AUGUST, SEPTEMBER
ECMWF Data
LAND AREA NLAT=35.0-42.5 ELON=277.5-285.0
SEA AREA NLAT=35.0-42.5 ELON=280.0-287.5
10-Year Average

Figure V-8-3. Average Refracitivity Variations in Washington DC Vicinity for Both Land-based and Sea-based with Grid#s 2416-2419, 2272-2275, 2128-2131 in Table 1 for July, August, and September 1980-1991 from ECMWF Database.

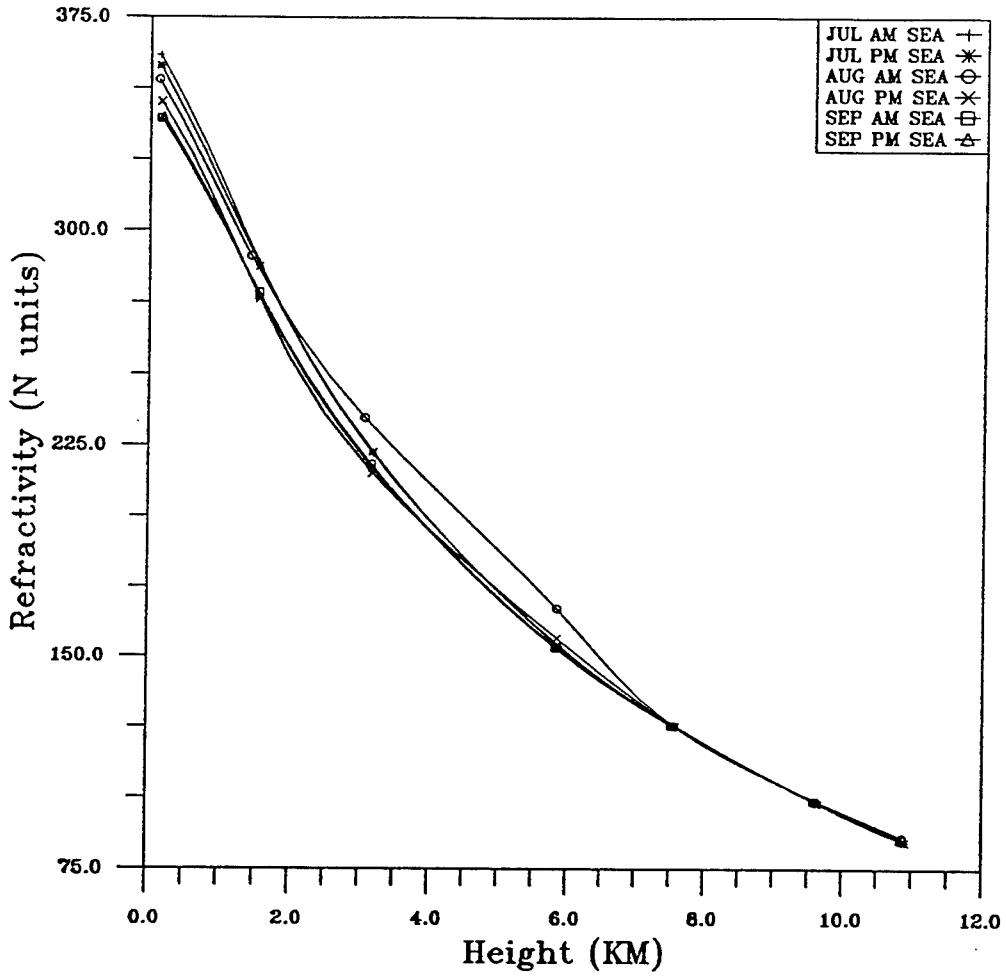

Figure V-8-4. Average Refracitivity Variations in Washington DC Vicinity for Both Land-based and Sea-based with Grid#s 2417-2419, 2273-2275, 2129-2131 in Table 1 for AM &PM of July, August, and September 1980-1993 from NCDC Database.

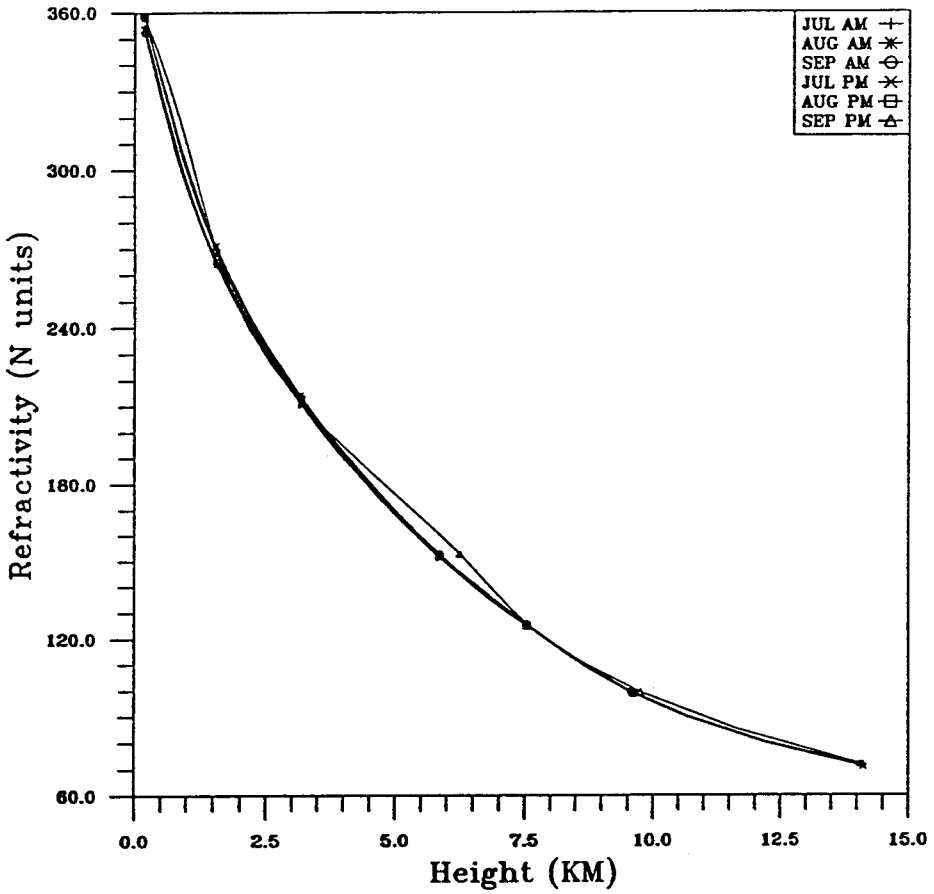

REFRACTIVITY N VS HEIGHT
DC COASTAL–BASED REGION
FNMOC
NLAT=35–42.5 ELON=280–287.5
JULY, AUGUST, SEPTEMBER 1994 (AM & PM)

Figure V-8-5. Average Refracitivity Variations in Washington DC Vicinity for Both Land-based and Sea-based with Grid#s 2417-2419, 2273-2275, 2129-2131 in Table 1 for AM &PM of July, August, and September 1994 from FNMOC Database.

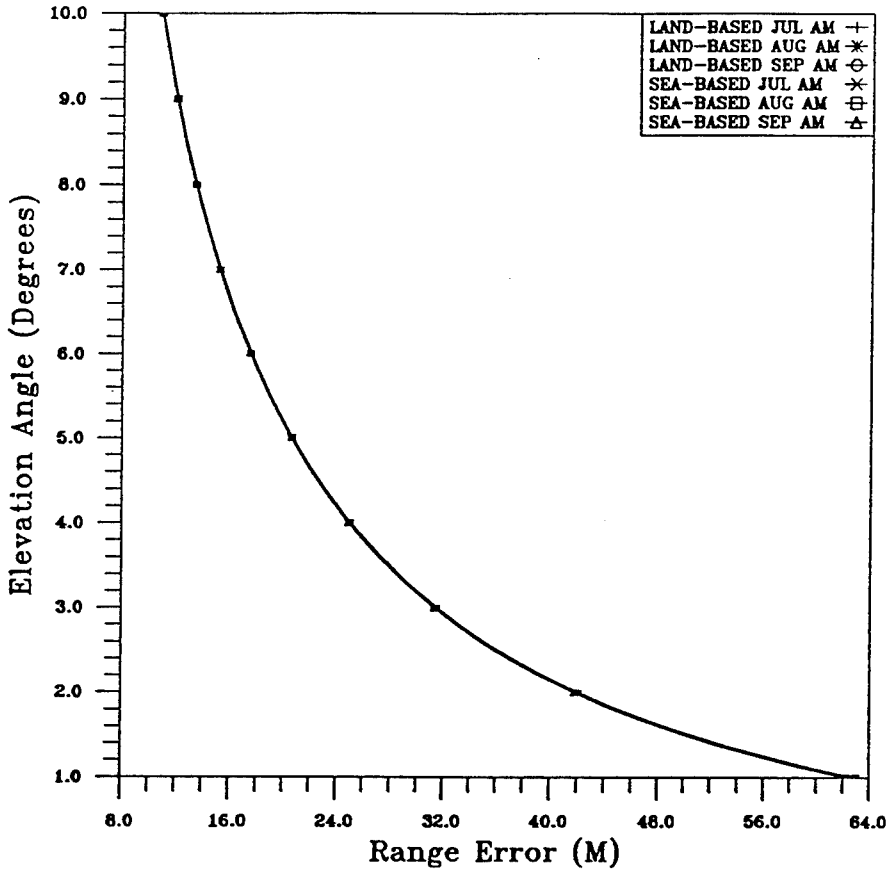

Elevation Angle VS Range Error
FNMOC
DC LAND-BASED REGION AND SEA-BASED REGION
LAND-BASED NLAT=35-42.5 ELON=277.5-285
SEA-BASED NLAT=35-42.5 ELON=280-287.5
JULY, AUGUST, SEPTEMBER AM 1994

Figure V-8-6. Range Error Variations based on Elevation Angle for FNMOC Database for both Land-based and Sea-based Area of Washington DC Vicinity for AM of July, August, and September 1994.

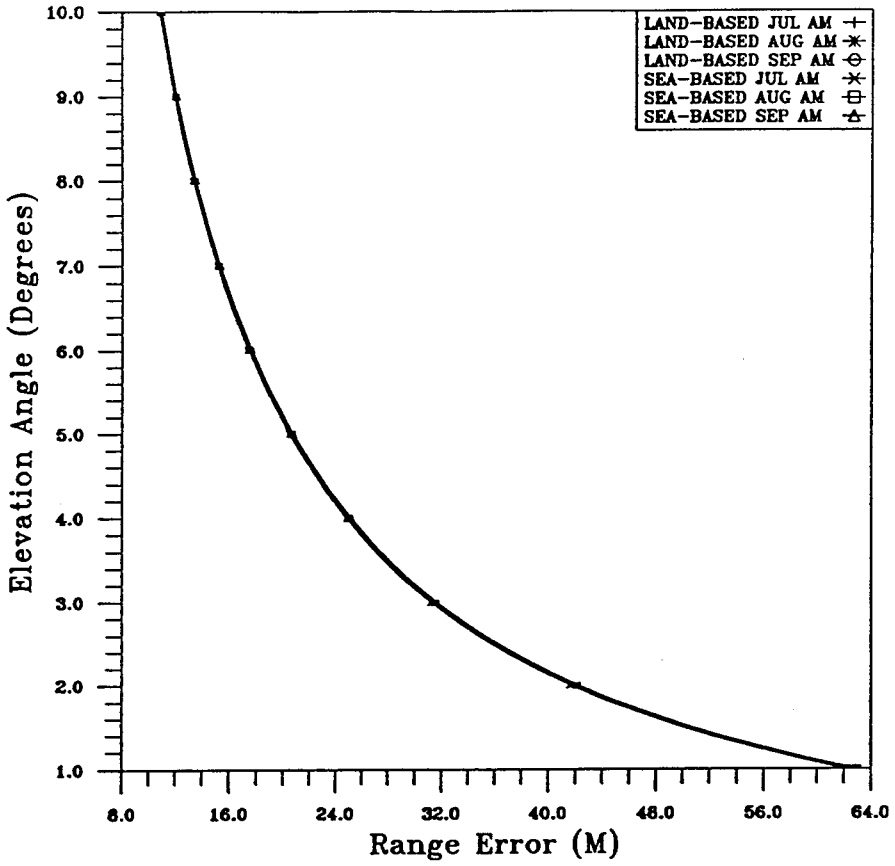

Elevation Angle VS Range Error
FNMOC
DC LAND-BASED REGION AND SEA-BASED REGION
LAND-BASED NLAT=35-42.5 ELON=277.5-285
SEA-BASED NLAT=35-42.5 ELON=280-287.5
JULY, AUGUST, SEPTEMBER PM 1994

Figure V-8-7. Range Error Variations based on Elevation Angle from One to Ten Degree for FNMOC Database for both Land-based and Sea-based Area of Washington DC Vicinity for PM of July, August, and September 1994.

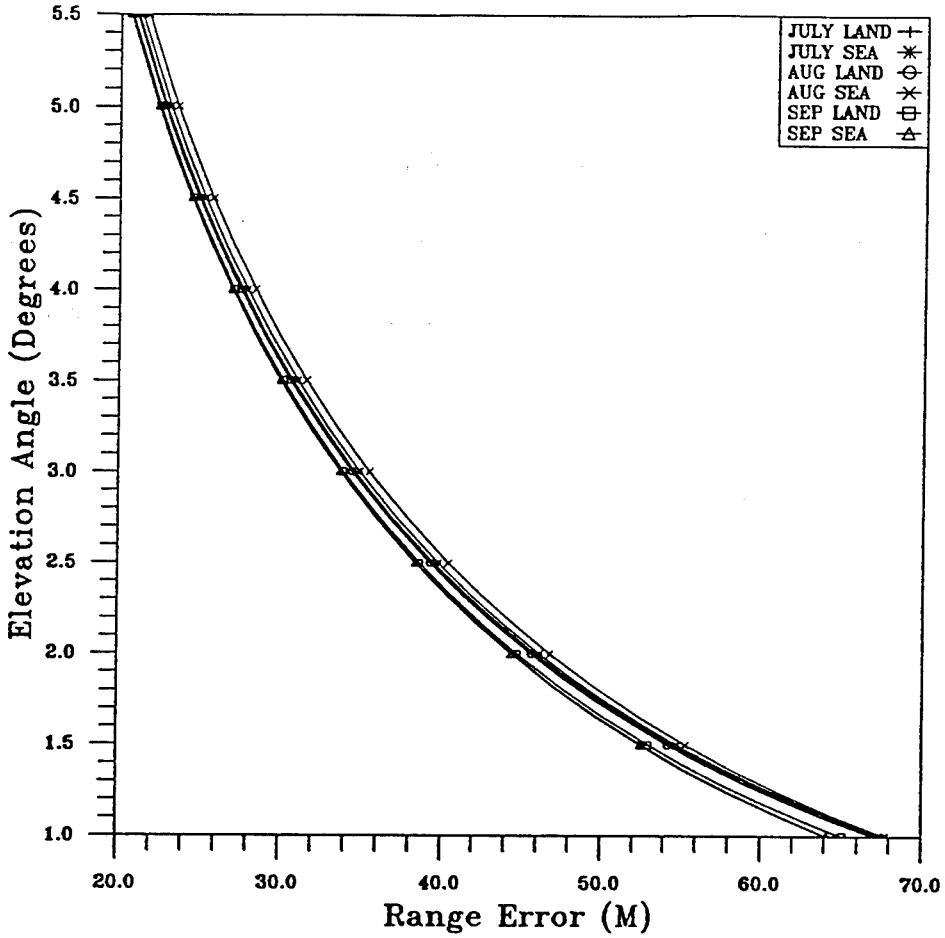

Figure V-8-8. Range Error Variations based on Elevation Angle from one to 5.5^0 for NCDC Database for both Land-based and Sea-based Area of Washington DC Vicinity for AM of July, August, and September 1980-1993.

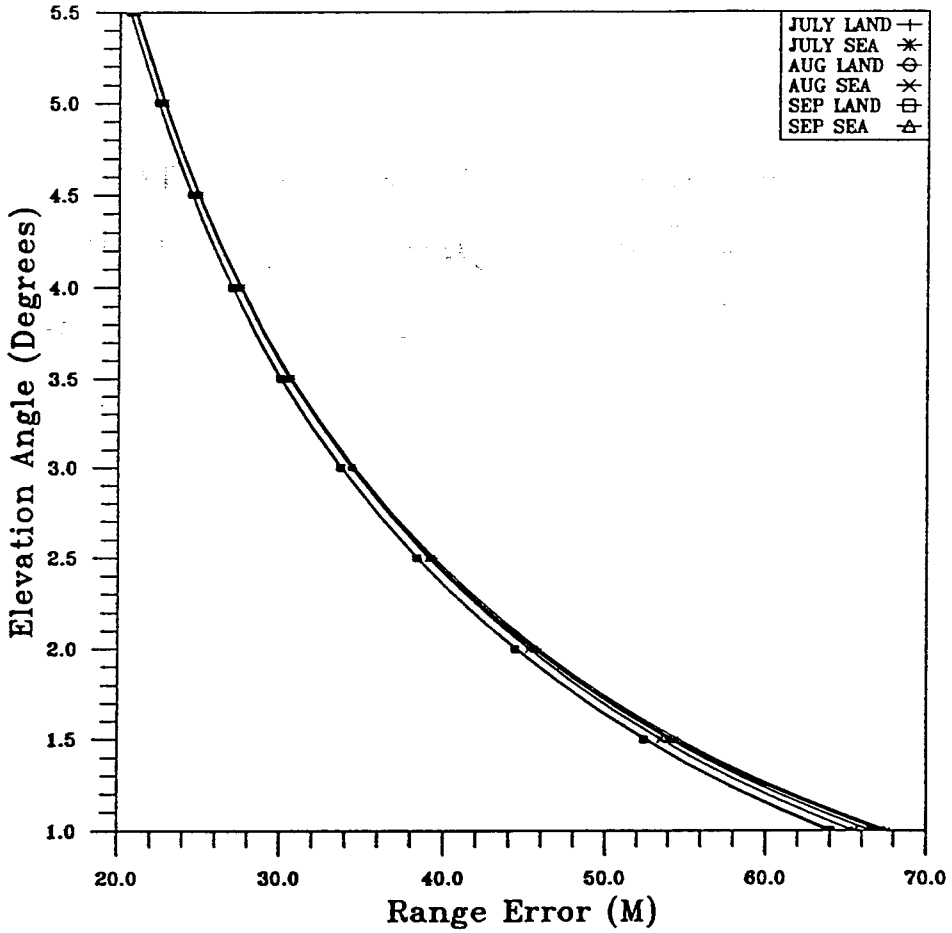

Figure V-8-9. Range Error Variations based on Elevation Angle from one to 5.5^0 for NCDC Database for both Land-based and Sea-based Area of Washington DC Vicinity for PM of July, August, and September 1980-1993.

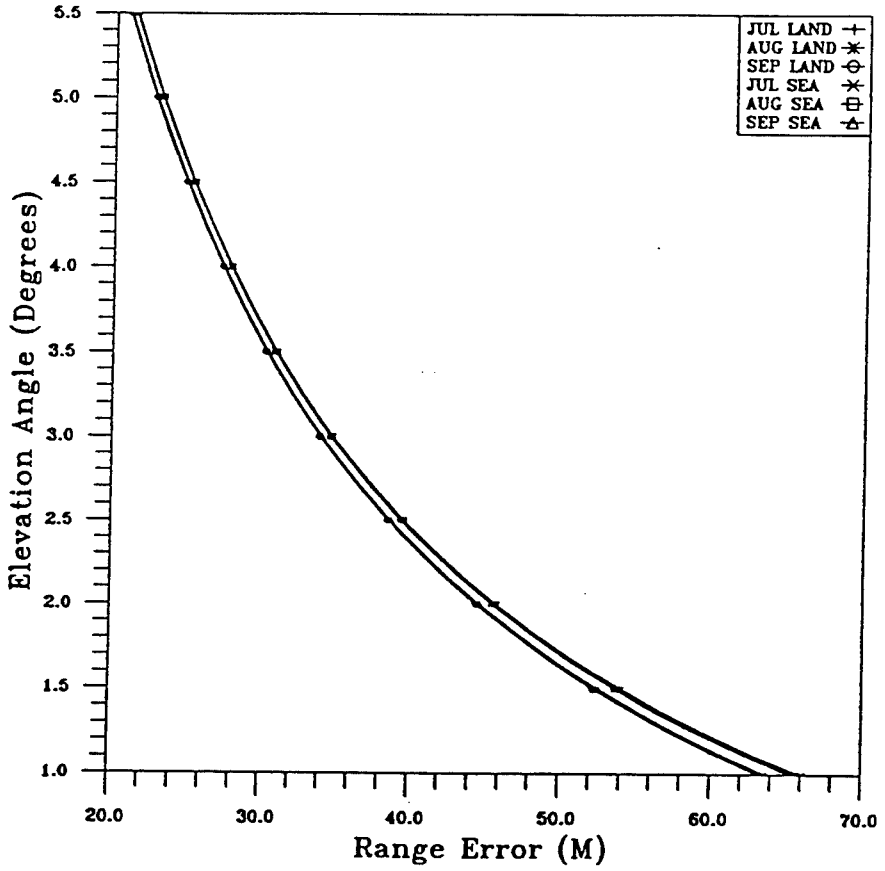

ELEVATION ANGLE VS RANGE ERROR
DC JULY, AUGUST, SEPTEMBER
ECMWF Data
LAND AREA NLAT=35.0-42.5 ELON=277.5-285.0
SEA AREA NLAT=35.0-42.5 ELON=280.0-287.5
10-Year Average

Figure V-8-10. Range Error Variations based on Elevation Angle from one to 5.5^0 for ECMWF Database for both Land-based and Sea-based Area of Washington DC Vicinity for July, August, and September 1980-1991.